Theses and Dissertations   Thesis and Dissertation Collection

1976-03

Transonic thermal blooming

Carey, Edwin Fenton, Jr.

Naval Postgraduate School, Monterey, California

http://hdl.handle.net/10945/6689

NAVAL POSTGRADUATE SCHOOL
Monterey, California

THESIS

TRANSONIC THERMAL BLOOMING

by

Edwin Fenton Carey, Jr.

March 1976

Thesis Advisor: A. E. Fuhs

REPORT DOCUMENTATION PAGE		READ INSTRUCTIONS BEFORE COMPLETING FORM
1. REPORT NUMBER	**2. GOVT ACCESSION NO.**	**3. RECIPIENT'S CATALOG NUMBER**
4. TITLE *(and Subtitle)* Transonic Thermal Blooming		**5. TYPE OF REPORT & PERIOD COVERED** Ph.D. Thesis March 1976
		6. PERFORMING ORG. REPORT NUMBER
7. AUTHOR(s) Edwin Fenton Carey, Jr.		**8. CONTRACT OR GRANT NUMBER(s)**
9. PERFORMING ORGANIZATION NAME AND ADDRESS Naval Postgraduate School Monterey, California 93940		**10. PROGRAM ELEMENT, PROJECT, TASK AREA & WORK UNIT NUMBERS**
11. CONTROLLING OFFICE NAME AND ADDRESS Naval Postgraduate School Monterey, California 93940		**12. REPORT DATE** March 1976
		13. NUMBER OF PAGES 122
14. MONITORING AGENCY NAME & ADDRESS*(if different from Controlling Office)*		**15. SECURITY CLASS. *(of this report)*** Unclassified
		15a. DECLASSIFICATION/DOWNGRADING SCHEDULE

16. DISTRIBUTION STATEMENT *(of this Report)*

Approved for public release; distribution unlimited.

17. DISTRIBUTION STATEMENT *(of the abstract entered in Block 20, if different from Report)*

18. SUPPLEMENTARY NOTES

19. KEY WORDS *(Continue on reverse side if necessary and identify by block number)*

Transonic Thermal Blooming   High Energy Laser
Subsonic Thermal Blooming
Supersonic Thermal Blooming
Atmospheric Propagation of Laser Beam
Sonic Flow with Heat Addition

20. ABSTRACT *(Continue on reverse side if necessary and identify by block number)*

According to the linearized solutions for thermal blooming, the density perturbations become infinite (i.e. "catastrophic" defocusing) as the Mach number approaches unity. However, the nonlinearities in the transonic equations cutoff the trend to infinity, and the values of the flow perturbation quantities are finite. The nonlinear equations with heat addition are transformed into simple linear algebraic equations through the

DD $_{1\ JAN\ 73}^{FORM}$ **1473**   EDITION OF 1 NOV 65 IS OBSOLETE
(Page 1)   S/N 0102-014-6601 |

(20.   CONTINUED)

specification of the streamline geometry in the heat release region. At a Mach number of unity, streamtube area variation was found to be directly proportional to the change in total temperature. A steady, two-dimensional mixed flow solution has been found for the transonic thermal blooming problem. The solution for the density perturbations within a laser beam at a Mach number of precisely unity is given. For a Gaussian beam with an intensity of 3.333×10^7 Watts/m^2 and an atmospheric absorption of 8.0×10^{-7} cm^{-1} the maximum fractional density perturbation is 1.028×10^{-6}. The transonic thermal blooming problem does not pose as serious a problem as previously anticipated.

Transonic Thermal Blooming

by

Edwin Fenton Carey, Jr.
Lieutenant Commander, United States Navy
B.M.A.E., University of Delaware, 1967
M.M.A.E., University of Delaware, 1970

Submitted in partial fulfillment of the
requirements for the degree of

DOCTOR OF PHILOSOPHY

from the

NAVAL POSTGRADUATE SCHOOL
March 1976

Author _____

Approved by:

O. Biblarz
Assoc. Prof. of Aeronautics

E. C. Crittenden
Distinguished Prof. of Physics
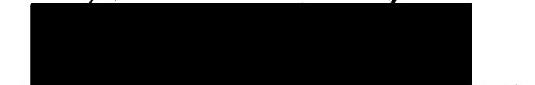
D. W. Netzer
Assoc. Prof. of Aeronautics

K. Davidson
Assoc. Prof. of Meteorology

A. E. Fuhs
Distinguished Prof. of Mechanical Engineering
Chairman, Mechanical Engineering Department
Thesis Advisor

Approved by _____
Chairman, Department of Aeronautics

Approved by _____
Academic Dean

3

ABSTRACT

According to the linearized solutions for thermal blooming, the density perturbations become infinite (i.e. "catastrophic" defocusing) as the Mach number approaches unity. However, the nonlinearities in the transonic equations cutoff the trend to infinity, and the values of the flow perturbation quantities are finite. The nonlinear equations with heat addition are transformed into simple linear algebraic equations through the specification of the streamline geometry in the heat release region. At a Mach number of unity, streamtube area variation was found to be directly proportional to the change in total temperature. A steady, two-dimensional mixed flow solution has been found for the transonic thermal blooming problem. The solution for the density perturbations within a laser beam at a Mach number of precisely unity is given. For a Gaussian beam with an intensity of 3.333×10^7 Watts/m^2 and an atmospheric absorption of 8.0×10^{-7} cm^{-1} the maximum fractional density perturbation is 1.028×10^{-6}. The transonic thermal blooming problem does not pose as serious a problem as previously anticipated.

TABLE OF CONTENTS

LIST OF TABLES

LIST OF FIGURES

NOTATION

English

A	area, square centimeters
a	speed of sound, meters/second
b	function, dimensionless
C	line contour around integration region R
c	speed of light, meters/second
C_p	specific heat at constant pressure, Joules/kilogram mass – degree Kelvin
C_v	specific heat at constant volume, Joules/kilogram mass – degree Kelvin
f	function, dimensionless
G	Green's function, dimensionless; also specified function, dimensionless
H	Heat quantity, dimensionless
h	specific enthalpy, Joules/kilogram mass
$h(x,y)$	heat addition function, Watts/cubic centimeters
I	laser beam intensity, Watts/square centimeter; also integral function representation
$I(x)$	unit function; zero for $x < 0$ and unity for $x \geq 0$
k	Gladstone-Dale constant, cubic meters/kilogram mass
L	scaling factor, dimensionless; length, meters; and functional representation of normalized velocity, dimensionless
ℓ	characteristic length (subscript 1 for x-direction and 2 for y-direction), centimeters
M	Mach number, dimensionless
N	Number of waves, dimensionless
n	normal coordinate, centimeters; also index of refraction, dimensionless

p	static pressure, Newtons/square meter
Pr	Prandtl number, dimensionless
Q	heat source, Watts/cubic centimeter
q	heat source, Watts/square centimeter; also, strength of line heat source, Watts/centimeter
R	universal gas constant, Joules/kilogram mass - degrees Kelvin ; radius of curvature, centimeters; and region of integration
r	distance, centimeters
Re	Reynolds number, dimensionless
S	line contour around shock waves; also, distance along a characteristic, centimeters
s	specific entropy, Joules/kilogram mass - degree Kelvin ; also streamline coordinate
T	static temperature, degrees Kelvin
t	maximum streamtube thickness, centimeters
$\overline{U}$	velocity vector, meters/second
U,u	speed (x-direction), meters/second
v	speed (y-direction), meters/second
w	laser beam spot size, centimeters; also speed, meters/second
x	coordinate, centimeters
y	coordinate, centimeters
Z	streamtube shape, centimeters

Greek

α	atmospheric absorption, 1/centimeters
β	variable, dimensionless; $(1 - M^2)^{1/2}$ for subsonic flow, dimensionless; and $(M^2 - 1)^{1/2}$ for supersonic flow, dimensionless
γ	ratio of specific heats, dimensionless

Δ	small change, dimensionless
δ	slope, dimensionless; also delta (impulse) function
ε	dimensionless small quantity, $0 < \varepsilon \ll 1$
η	absolute viscosity, kilogram mass/meter-second; also coordinate ($\bar{y}$-direction), centimeters
θ	flow angle, radians
κ	thermal conductivity, Watts/centimeter - degree Kelvin
λ	wavelength, centimeters
μ	Mach angle defined by arcsin(1/M)
ν	inverse radius of curvature, 1/centimeter
ξ	coordinate ($\bar{x}$-direction), centimeters; also transonic similarity parameter, dimensionless
ρ	density, kilogram mass/cubic meter
Σ	summation
σ	standard deviation of Gaussian beam, centimeters
τ	thickness ratio, dimensionless; also, vibrational relaxation time, seconds
Φ	viscous dissipation function, Watts/cubic centimeter
φ	velocity potential, dimensionless
ψ	viscous force vector, Newtons/cubic meter
Ω	angular velocity, radians/second

Superscripts

( )'	prime, dimensionless quantity
($\bar{}$)	bar, normalized quantity; also average value of a quantity
($\tilde{}$)	tilde, perturbation quantity

11

Subscripts

a,b	indicate values of a quantity in front of and behind a shock wave
i	x-direction or streamline index – first subscript – ($i = 1$ denotes freestream conditions)
j	y-direction or normal index – second subscript – ($j = 1$ denotes centerline conditions)
L	linear value
0	total or stagnation condition; also, peak value of an intensity distribution
w	wall or surface value
∞	freestream condition
1,2,	first, second, etc. perturbation quantities

Miscellaneous

∇	Del operator, 1/centimeters
∇^2	Laplace operator, 1/square centimeters

ACKNOWLEDGEMENT

I. INTRODUCTION

The optical quality of a propagating laser beam is degraded when there are density gradients in the medium. A laser beam propagating through an absorbing medium creates local changes in the density which affect the index of refraction of the medium. Therefore, the density gradients will refract the light into regions of higher index of refraction (higher density) causing defocusing of the beam. This process, which is known as thermal blooming, has been studied by many authors [Refs. 1, 2, and 3] to determine its effect on a laser beam propagating through various media.

When a laser beam is slued, a complicated coupled process of thermal expansion and fluid flow (relative winds) takes place. Depending on the rate of sluing, the beam will experience subsonic, transonic, and supersonic winds at various radial distances from the laser source. The subsonic and supersonic thermal blooming problems have been solved [Refs. 4 - 8]. A computer program (DIDER) has been developed and experimentally verified [Ref. 9] for beam interaction with supersonic flows internal to a Gas Dynamic Laser.

A solution for the transonic regime, and, in particular, the case when the freestream Mach number is precisely unity, has been of considerable interest because the addition of heat can lead to extremely strong density gradients. As

with the theoretical investigation of transonic flows over airfoils and wedges, the linear small perturbation flow equations valid for subsonic flow (elliptic equations) and supersonic flow (hyperbolic equations) are no longer complete in the transonic regime.

Many authors [Refs. 10 - 15] have studied various methods of solving the transonic flow equations without heat addition. The assumptions based on known transonic behavior about air-foils and wedges are used to simplify the governing equations and, further, to obtain approximate numerical solutions. Often, the assumptions greatly restrict the types of transonic flows that can be solved. For example, in the parabolic method [Ref. 16], the transonic flow equation is transformed into a parabolic differential equation. Since the solutions to parabolic differential equations are well established in the literature, this method may be used when the acceleration or deceleration is approximately constant in the region of interest (i.e. across the cord of many airfoils); however, this method is not valid in the region of the stagnation point or where the flow acceleration changes sign.

With heat addition, the basic flow equations for transonic flow become more complicated. Zierep [Ref. 17] has solved the case when the Mach number is precisely unity; but, in solving the equation, he has reduced the problem to that of one dimension. Others [Refs. 18 and 19] have solved the nonsteady transonic equation with heat addition; however, the results are valid only for a short time after beam turn

on (i.e. no steady state solution). Even for the short time solutions, extrapolation techniques between the property values at the critical points on the subsonic side and the supersonic side are employed to obtain the values across the transonic regime. Experimental investigations are being conducted [Ref. 20] to determine the influence of transonic sluing on thermal blooming. These experiments indicate that a steady two-dimensional solution is possible. Further experimentation will provide better guidelines for a theoretical analysis of the problem.

In this thesis, transonic thermal blooming in steady two-dimensional invisid flow is formulated and solved for a Gaussian heat release distribution. In particular, it examines the problem when the freestream Mach number is precisely unity. This is accomplished by using a method developed by Broadbent [Refs. 21 - 25] in which the streamlines throughout the flow are adjusted in such a manner that the heat addition necessary to achieve these streamlines equals the required heat distribution and boundary conditions. The method is exact since specifying the streamlines reduces the nonlinear coupled momentum equations in natural (streamline) coordinates to simple algebraic linear difference equations that can be "marched" through the entire flow field. Boundary conditions are the freestream properties upstream of the heat release region and those on a bounding streamtube sufficiently removed from the heat release region that the flow is considered isentropic. The boundary conditions

on the bounding streamtube are calculated by methods similar to those employed in determining the velocity and pressure distributions over airfoils of known shape. Since stagnation points do not exist on the bounding streamtube flow, a modification to the method presented by Sprieter and Alksne [Ref. 10] for airfoils and wedges was developed.

In Section II, the theory used in analyzing the transonic thermal blooming problem is presented and includes a description of the assumptions made during the mathematical analysis, a summary of the pertinent equations derived in the Appendices, and a discussion of the method of solution. In Section III, the numerical results for the Mach 1.0 flow with a Gaussian heat release distribution are presented. Lastly, Section IV gives a brief discussion of the conclusions and of the other methods that show promise in solving the transonic thermal blooming problem.

II. THEORY

A laser beam that is slued through the atmosphere at a constant rate of Ω radians per second will experience regions of subsonic, transonic, and supersonic flow in planes perpendicular to its axis at various radial positions along the beam, Fig. 1. The region to be investigated in this paper is the transonic region in which mixed subsonic and supersonic flow exists, as in contrast to purely subsonic flow or supersonic flow, and, in particular, the case when the Mach number is precisely unity; that is, at a radial position given by Eq. (1).

$$r_{M_\infty = 1.0} = r^* = \frac{\sqrt{\gamma R T_\infty}}{\Omega} \qquad (1)$$

For this analysis, the laser beam is initially of a given axial symmetric Gaussian intensity sluing into an isotropic, quiescent medium of constant density ρ (kgm m^{-3}). Viscosity, and thermal conduction are neglected. Justification for this assumption is given in Appendix A. The heating effect of the laser beam on the medium is approximated by a molecular relaxation process which is rapid enough that the absorbed energy is instantaneously transformed into heat. The energy distribution is of the form given in Eq. (2).

$$Q = I\alpha = I_0 \alpha \, \exp\left(- \frac{(x^2+y^2)}{2\sigma^2}\right) \qquad (2)$$
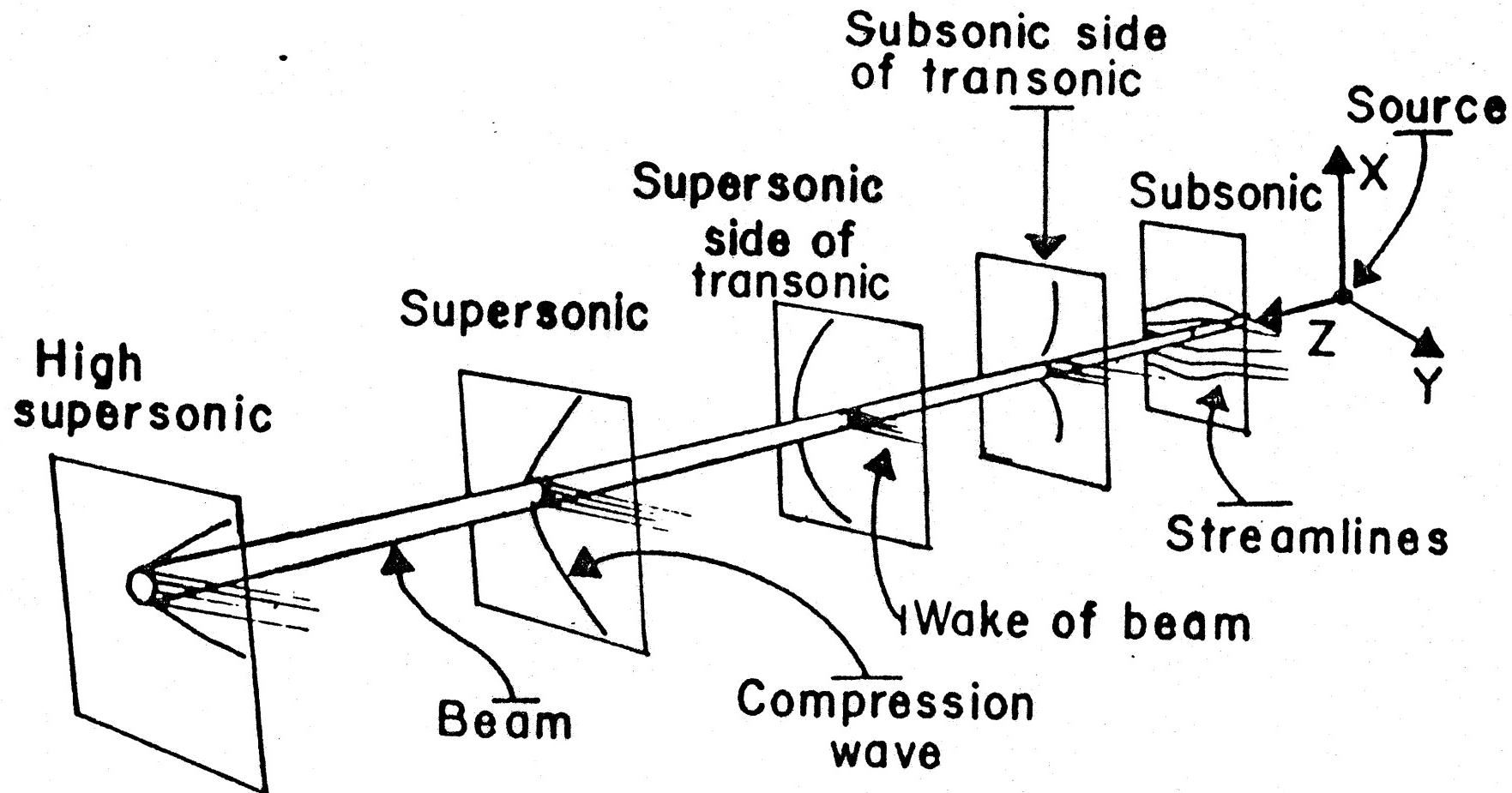
18

FIGURE 1. Flow Regimes Along a Sluing Laser Beam

where Q (Watts cm^{-3}) is the time rate of heat absorbed per volume; I_0 (Watts m^{-2}) is the beam maximum intensity; α (cm^{-1}) is the absorption coefficient; and the exponential of the Gaussian with standard deviation σ (cm), which is related to the spot size of the beam by $w = \sqrt{2}\,\sigma$, is centered at the origin of the x-y coordinate system transverse to the beam axis at r*.

The theory employed for this investigation separates the steady transonic flow with heat addition into two entirely different flow regimes, Fig. 2. The internal, heat addition region can be treated exactly by the Broadbent method [Ref. 18], in which the nonlinear equations of motion and the energy equation are solved numerically in natural coordinates. Then, a mesh of streamlines and normals is constructed throughout the flow field, Fig. 3., which reduces the momentum equations to simple algebraic equations solvable for the flow properties. Finally, the mesh of streamlines is adjusted until the properties calculated from the linearized momentum equations satisfy the energy equation and boundary conditions. Boundary conditions are obtained from the external, isentropic flow region by approximating the transonic solution over a bounding streamtube to the internal region.

The governing equations in the internal region have been derived for flow with heat addition, but without viscosity, heat conduction or body forces. A small perturbation analysis
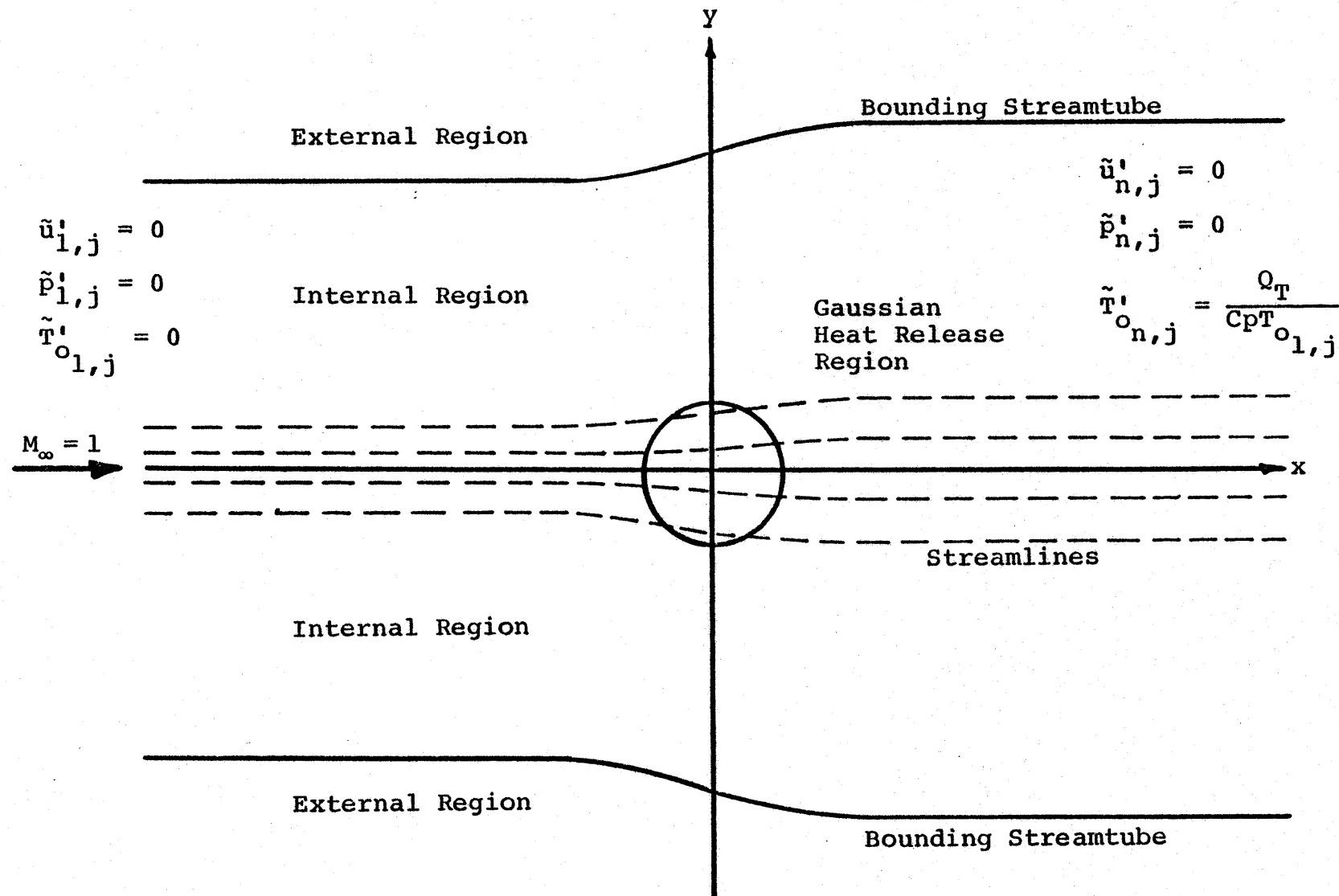
FIGURE 2.   Transonic Flow Configuration with Heat Addition
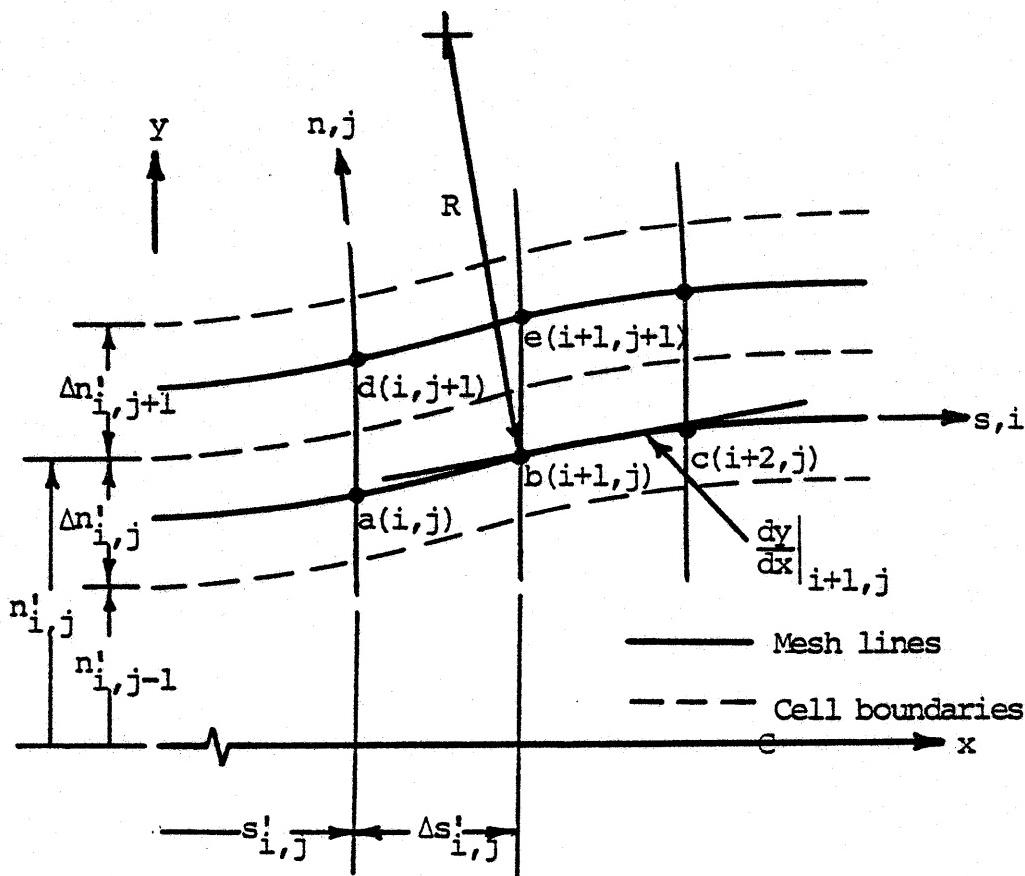
FIGURE 3. Natural Coordinate System with Flow Mesh

for transonic flow (Appendix A) shows that viscosity, heat conduction, and body forces can be neglected to first order. The small perturbation, steady two-dimensional transonic equation with head addition is written as:

$$(1-M_\infty^2)\phi_{x'x'} + \phi_{y'y'} - M_\infty^2(\gamma+1)\phi_{x'}\phi_{x'x'} = \frac{1}{CpT_\infty}\frac{\partial q(x',y')}{\partial x'}$$

(3)

where the term on the right-hand side is added for flows with heat addition; $q(x',y')$ (Joules kgm^{-1}) is the heating function; Cp (Joules kgm^{-1} $°K^{-1}$) is the heat capacity; T_∞ (°K) is the freestream static temperature; M_∞ is the freestream Mach number; and ϕ is the nondimensional velocity potential. Therefore, in vector notation, the steady state equations [Ref. 26] are:

$$\nabla \cdot (\rho\overline{U}) = 0$$

(4)

$$\rho\overline{U}\cdot\nabla\overline{U} + \nabla p = 0$$

(5)

$$\rho\overline{U}\cdot\nabla(h + \frac{1}{2}\overline{U}\cdot\overline{U}) = Q = I\alpha$$

(6)

$$p = \rho RT$$

(7)

where $\overline{U}$ (m sec^{-1}) is the velocity; p (newtons m^{-2}) is the static pressure; h (Joules kgm^{-1}) is the enthalpy; and R (Joules kgm^{-1} °K) is the universal gas constant. Using a two-dimensional natural coordinate system [Ref. 26], shown in Fig. 3, the governing equations were derived from

the above equations. The momentum equations are represented
in the following convenient numerical form (Appendix B).

$$\tilde{u}'_{i+1,j+1} - \tilde{u}'_{i,j+1} + \frac{\overline{\Delta n}'_{(i,i+1),j}}{\gamma M_\infty^2}(\tilde{p}'_{i+1,j+1} - \tilde{p}'_{i,j+1}) = 0 \tag{8a}$$

$$\tilde{p}'_{i+1,j+1} - \tilde{p}'_{i,j+1} + \frac{\gamma M_\infty^2}{2}(u'_{i+1,j+1}\nu'_{i+1,j+1} + u'_{i+1,j}\nu'_{i+1,j}) = 0 \tag{8b}$$

where $\Delta n'_{i,j}$ is the streamtube width at the i,jth station;
γ is the ratio of specific heats; $\nu'_{i,j}$ is the inverse curva-
ture defined as $\Delta n'_{i,j}/R$; and the prime (') denotes dimension-
less quantities with respect to the freestream values. The
quantities with a bar and parenthesized subscripts represent
average values between the indicated stations (i.e. $\overline{\Delta n}'_{(i,i+1),j}$
is the average streamtube width between station i,j and i+1,j),
and the properties with the tilde (~) denote perturbation
values from freestream conditions (i.e. $\tilde{u}_{i,j} = (u_{i,j} - u_{1,j})$).
The natural coordinates s and n are tangent and normal to
the streamlines, respectively. Eqs. (8a) and (8b) represent
two nonlinear equations since $\tilde{u}'$, $\tilde{p}'$, $\Delta n'$ and ν' are dependent
variables. However, specifying the streamlines of the flow,
these equations become linear equations solvable for
$\tilde{u}'_{i+1,j+1}$ and $\tilde{p}'_{i+1,j+1}$ at point e in terms of $\tilde{u}'_{i+1,j}$, $\tilde{p}'_{i+1,j}$
at point d and $\tilde{u}'_{i,j+1}$, $\tilde{p}'_{i,j+1}$ at point b, Fig. 3.

The remaining flow properties $\tilde{\rho}'_{i+1,j+1}$ and $\tilde{T}'_{i+1,j+1}$ can
be calculated from the continuity equation, Eq. (9), and

24

equation of state, Eq. (10), derived in Appendix B. However, the new properties at the point e (i+1,j+1) may not satisfy the energy equation, Eq. (11). If it is not satisfied, an iteration process is performed by varying the streamline distribution and recalculating the properties until coincidence exists throughout the entire flow field. Hence, the solution of the problem is reduced to finding the streamline distribution that satisfies Eqs. (8) through (12) with the boundary conditions determined from the external region.

$$\rho'_{i+1,j+1} u'_{i+1,j+1} n'_{i+1,j+1} = 1 \tag{9}$$

$$p'_{i+1,j+1} = \rho'_{i+1,j+1} R T'_{i+1,j+1} \tag{10}$$

$$\tilde{T}'_{i+1,j+1} - \tilde{T}'_{i,j+1} + \frac{1}{2} M_\infty^2 (\gamma+1) (u'^2_{i+1,j+1} - u'^2_{i,j+1}) = \tag{11}$$

$$\frac{(\overline{I\alpha\Delta n'})}{Q_\infty} (i,i+1),j \ \Delta s'_{i,j+1}$$

where

$$Q_\infty = \frac{\rho_\infty u_\infty C p T_\infty (1+\frac{1}{2}(\gamma-1) M_\infty^2)}{\Delta n_{1,j}} = \frac{p_\infty u_\infty (1+\frac{1}{2}(\gamma-1) M_\infty^2) \gamma}{(\gamma-1) \Delta n_{1,j}} \tag{12}$$

Insight into the behavior of the streamlines at the sonic speed was obtained from the solution of the linearized small perturbation equation with heat addition [Refs. 4 - 8]. A computer program (BLOOM) was devised (Appendix G)

which gave solutions for a flow very slightly below the sonic speed ($M_\infty = 0.999$), Figs. 4 and 6, and very slightly above the sonic speed ($M_\infty = 1.001$), Figs. 5 and 7. Computation of the nonlinear term in Eq. (3) from the linear results indicate that the linear equations are valid to $M_\infty = 0.9999$ subsonically and $M_\infty = 1.0001$ supersonically. From the linear solutions, a trend of the streamline shape is obtained in the near sonic regime, even if not at sonic conditions. Nature usually exhibits a strong propensity to accomplish changes in a rather smooth fashion (even a shock wave is a smooth change in conditions if viewed microscopically enough); thus, a knowledge of flow conditions in the near sonic range gives a good clue to the sonic flow behavior. In Figs. 4 through 7, the Gaussian heat distribution is centered at the origin on the centerline, and the relative airflow is from left to right.

From the appropriate density calculations and plots, discussed later in the thesis, it can be seen that the wake term becomes less significant compared with the source term, which is directly associated with the horizontal velocity perturbation, as sonic velocity is approached from either direction (i.e. $M < 1$ and $M > 1$). Figs. 4 and 5 show the horizontal (longitudinal) velocity perturbation at Mach numbers of 0.999 and 1.001, respectively. Figs. 6 and 7 show the vertical (transverse) velocity perturbation at these same Mach numbers. Note that, subsonically, the horizontal
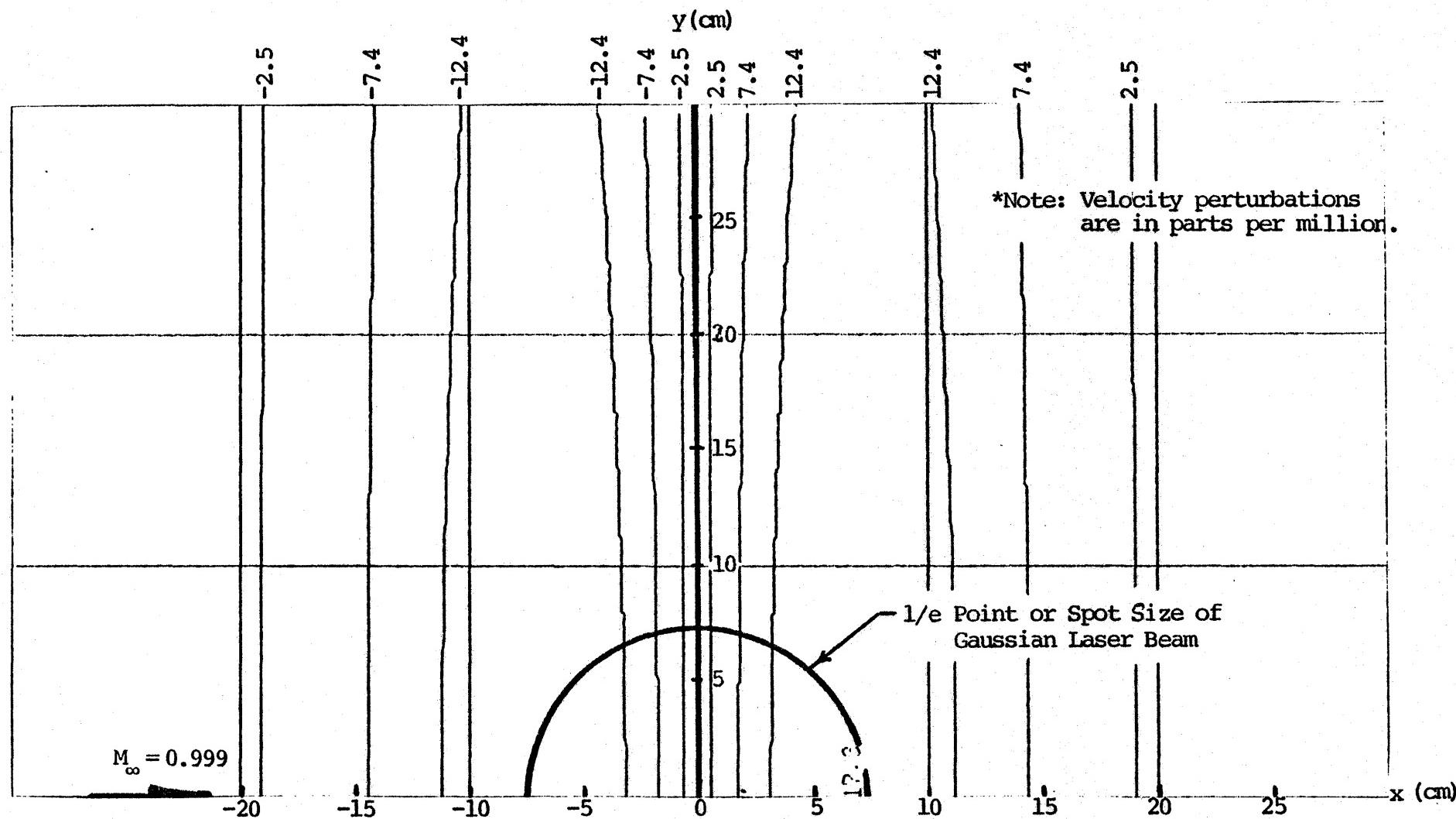
FIGURE 4. Velocity Perturbation (ũ') in Flow Direction for $M_\infty = 0.999$
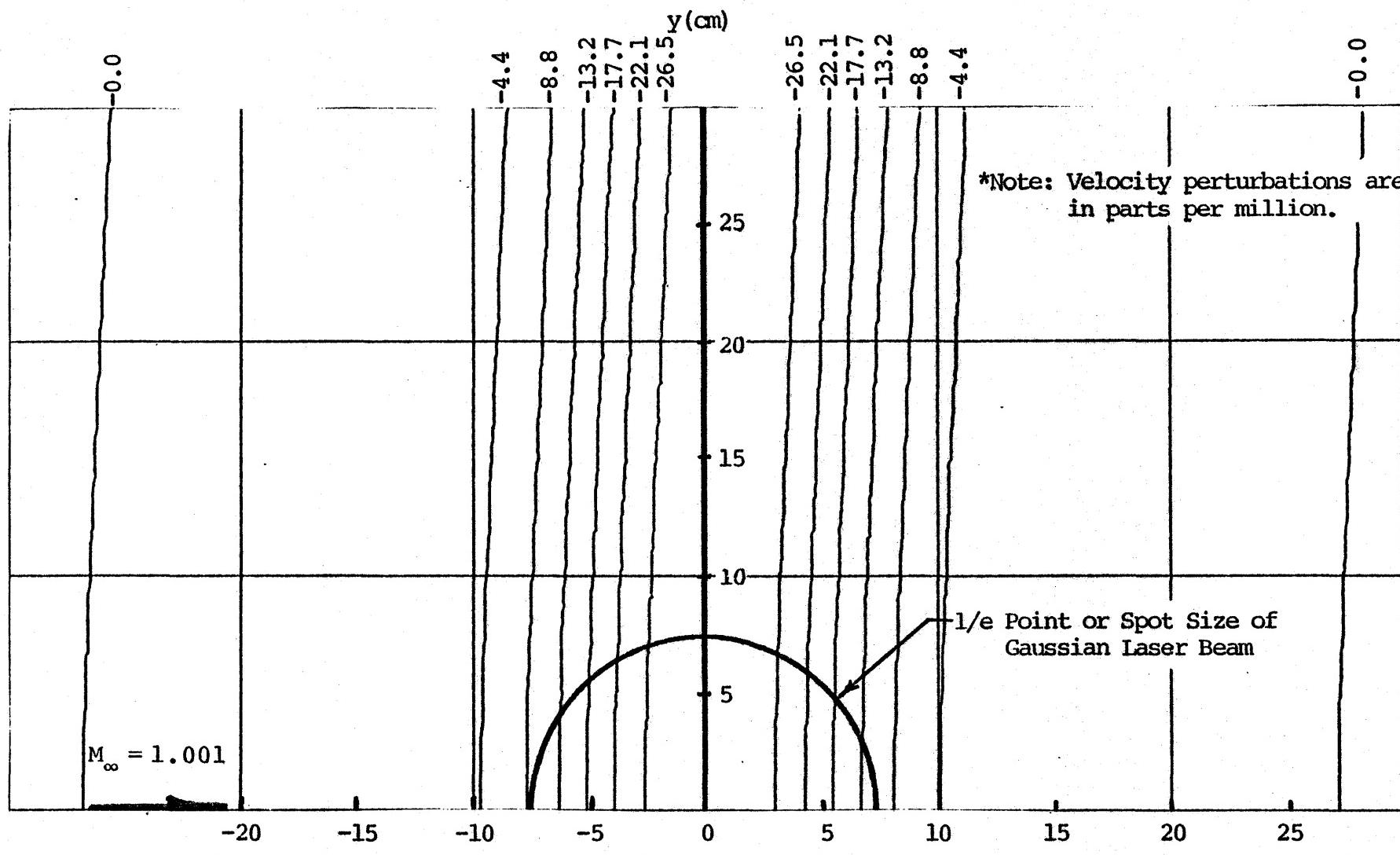
FIGURE 5. Velocity Perturbation (ũ') in Flow Direction for $M_\infty = 1.001$
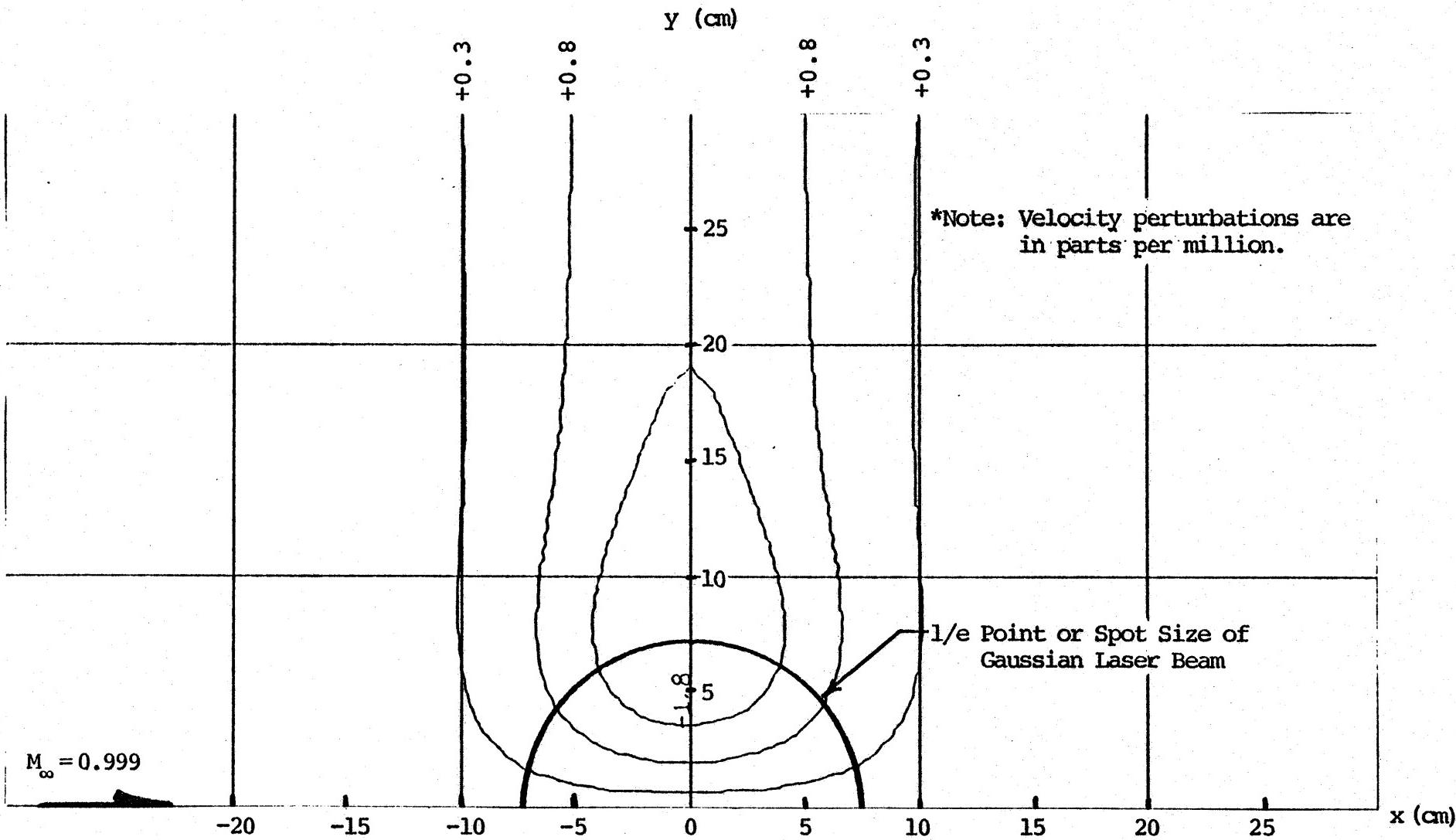
FIGURE 6. Lateral Velocity ($\tilde{v}'$) Perturbation for $M_\infty = 0.999$
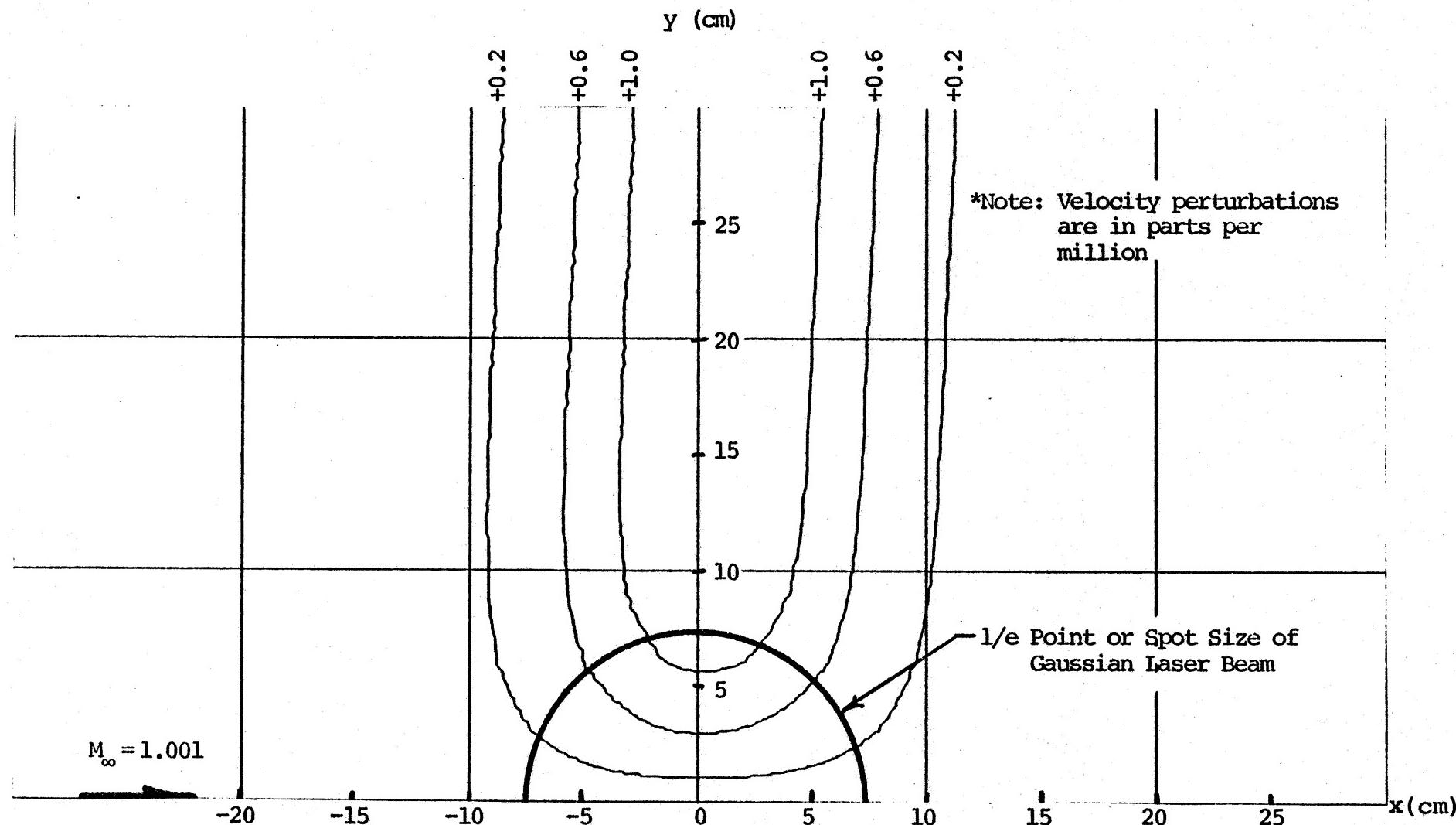
FIGURE 7. Lateral Velocity ($\tilde{v}'$) Perturbation for $M_\infty = 1.001$

perturbation, Fig. 4, decreases to a negative valley
slightly upstream of the laser beam center and then changes
rapidly to an equal positive peak slightly farther downstream
of the beam center. The perturbation contours are of very
small curvature near the beam center; the supersonic per-
turbations, Fig. 5, show a negative valley near the beam
center with a return to freestream conditions downstream of
the center. In the supersonic case, the contours are nearly
normal to the flow throughout, in keeping with the character
of supersonic flow; whereas, in the subsonic case, the con-
tours are closed, in keeping with subsonic flow behavior.
The patterns of disturbance, however, appear to be consistent
as the sonic speed is crossed.

The vertical or transverse velocity perturbation, Figs.
6 and 7, show similar behavior in the two speed regimes.
As expected, the subsonic flow perturbation profiles are
closed while those for supersonic flow are open to infinity.
In both cases, the perturbations exhibit an odd symmetry
about the main flow centerline. For the subsonic case, the
perturbations are greater than zero to the left of the rela-
tive flow and less than zero to the right. This is a direct
indication of the spreading of the streamlines as the heat
release region is approached by the air flow. Downstream
of the laser beam, the streamlines again become parallel
with the undisturbed flow direction. The supersonic case
shows the same patterns except that the spreading effect on
the streamlines is felt infinitely far in the transverse

direction, roughly along the characteristic lines from the disturbances.

The effect of spreading of the streamlines as the beam is passed, which can be constructed from these plots of longitudinal and transverse velocity perturbations, is thus seen to be quite similar immediately below and immediately above the sonic speed. Fig. 2 is a sketch of the streamlines. It is expected therefore that the streamline behavior at the sonic speed will not vary radically from this pattern.

Based on the streamline distribution in Fig. 2, the following relationship between area change (streamtube width variation) and change in total temperature (heat input) was chosen, Eq. (13).

$$\frac{dA}{A} = \frac{dn}{n} = \frac{1}{2}(\gamma+1)(1+\beta)\frac{dT_o}{T_o} \qquad (13)$$

where T_o is the local total temperature of the flow and β is a variable. One dimensional influence coefficients with area change and heat addition [Ref. 27], Eq. (14), were used to determine the required β at precisely Mach 1.0.

$$\frac{dM^2}{dx} = \frac{G(x)}{(1-M^2)} \qquad (14)$$

where

$$G(x) = M^2(1+\frac{1}{2}(\gamma-1)M^2)(-2\frac{d\ln(n)}{dx} + (1+\gamma M^2)\frac{d\ln(T_o)}{dx})$$

In order for Eq. (14) to remain finite and to be defined at Mach 1.0, $G(x)$ must tend to zero in the limit as the Mach number approaches unity. If Eq. (13) is substituted into Eq. (14) and the limit taken, it is found that it must be zero at precisely Mach 1.0 (Appendix C). Hence, the stream-tube area change is related to the heat input by Eq. (15).

$$\frac{dn'_{i,j}}{n'_{i,j}} = \frac{1}{2}(\gamma+1) \; \frac{dT'_{o_{i,j}}}{T'_{o_{1,j}}} \tag{15}$$

where the maximum difference between $n'_{i,j}$ and $n'_{1,j}$, and $T'_{o_{i,j}}$ and $T'_{o_{1,j}}$ is of the order of 10^{-6} and, hence, the freestream values can be used in the denominator. Using this approximation for the streamtubes, an explicit formulation of the streamtube shape, at any position $s'_{i,j}$ along a streamtube, was obtained (Appendix C).

$$n'_{i,1} = \frac{1}{2}(\Delta \tilde{n}'_{i,1}+1); \quad i \geq 1 \tag{16a}$$

$$n'_{i,j} = \frac{1}{2}\Delta n'_{i,1} + \sum_{\ell=1}^{j-1} \Delta \tilde{n}'_{i,1+1} + (j - \frac{1}{2}); \quad i \geq 1, \; j \geq 2 \tag{16b}$$

where for a Gaussian heat input at Mach 1.0 (Appendix C),

$$\Delta \tilde{n}'_{i,j} = \frac{(\gamma+1)\sqrt{2}\sigma' I_o \alpha}{2Q_\infty} \exp\left(-\frac{(j-1)^2}{2\sigma'^2}\right) \left[1+\mathrm{erf}\left(\frac{s'_i}{\sqrt{2}\sigma'}\right)\right] \; ; \; i \geq 1, \; j \geq 1 \tag{16c}$$

33

Once the streamtube shape is known, the slope (dy/dx), Eq. (17), and the radius of curvature (R), Eq. (18), can be calculated at every mesh point throughout the flow.

$$\frac{dy}{dx}\bigg|_{i,j} \equiv \delta_{i,j} = \frac{n'_{i+1,j} - \frac{1}{2}\Delta n'_{i+1,j} - n'_{i,j} + \frac{1}{2}\Delta n'_{i,j}}{\Delta s'_{i,j}}; \quad \substack{i \geq 1, \\ j \geq 1}$$

(17)

$$v'_{i,j} = \frac{\Delta n_{i,j}}{R} = \frac{\delta_{i,j} - \delta_{i-1,j}}{\Delta s'_{i,j}(1+\delta^2_{i,j})^{3/2}} \cong \frac{\delta_{i,j} - \delta_{i-1,j}}{\Delta s'_{i,j}}; \quad \substack{i \geq 1 \\ j \geq 1}$$

(18)

Therefore, the proportionality between the streamtube shape and heat release distribution gives not only an explicit formulation for the streamtubes and, hence, linearization of the nonlinear momentum equations but also simultaneous agreement between those properties calculated from the momentum equations and the energy equation. The problem, in the case of precisely $M_\infty = 1.0$ flow, becomes one of determining the correct boundary conditions.

The boundary conditions that are used are those corresponding to freestream conditions $(\tilde{u}'_{1,j} = \tilde{p}'_{1,j} = \tilde{\rho}'_{1,j} = \tilde{T}'_{1,j} = 0)$, which are far enough upstream that the properties are not affected by the perturbation caused by the heat release region, and the pressure $(p'_{i,j*})$ and/or velocity $(u'_{i,j*})$ on the j*th streamtube which is considered far enough removed from the heat release region that the flow can be considered isentropic. Eqs. (16b) and (16c) can be used to determine

the streamtube shape and displacement where $j = j*$. However, a more convenient form is derived in Appendix C for a Gaussian heat release distribution at $M_\infty = 1.0$ which can be written as:

$$n'_{i,j*} - n'_{1,j*} = \frac{(\gamma+1) I_o \alpha \sigma'^2 \pi}{4Q} \left[1 + erf(\frac{s'_i}{\sqrt{2}\sigma'}) \right] \quad ; \quad i \geq 1, \ j \geq 4.5$$

(19)

and the slope of the bounding streamtube:

$$\frac{dn'_{i,j*}}{ds'_{i,j*}} = \frac{(\gamma+1) I_o \alpha \sqrt{2\pi}\sigma'}{4Q} \exp - \frac{s'^2_i}{2\sigma'^2} = \frac{t'}{\sqrt{2\pi}\sigma'} \exp - \frac{t'}{2\sigma'^2}$$

(20)

where t' is the maximum growth in the streamtube.

Since the mass flow is constant in a streamtube, the bounding streamtube can be considered as a solid wall similar to the surface of a wedge with a cusp extending forward to the freestream conditions upstream at infinity, Fig. 2. By hypothesis, this flow is isentropic and can be treated by methods similar to those used in analyzing transonic airfoil and wedge flows. In particular, an approximate solution is obtained through an iteration process on the integral equation derived by Green's functions for small disturbance transonic flow similar to that performed by Sprieter and Alksne [Ref. 10 and 11] for thin airfoils and wedges but modified for the streamtube configuration which has no stagnation points. The absence of stagnation points

in the case of the flow around the bounding streamtube enhances the accuracy of the approximate numerical techniques because the stagnation point represents a singularity in the problem and places added constraints on the method and accuracy of the solution in the region of the stagnation point. In this method, the quadratic, nonlinear nature of the governing equations is retained which precludes shock-free supercritical flows in the transonic regime.

The integral equation for transonic flow is derived by a Green's function analysis on the small perturbation transonic equation without heat addition, Eq. (3) without the right-hand side, resulting in Eq. (21).

$$\bar{u}_W(\bar{x},0) = \bar{u}_{L_W}(\bar{x},0) + \frac{1}{2}\bar{u}_W^2(\bar{x},0) - \frac{1}{2}I \tag{21}$$

where

$$\bar{u}_W(\bar{x},0) = \frac{M_\infty^2(\gamma+1)\tilde{u}'(x,0)}{\beta^2} = \frac{M^2 - M_\infty^2}{\beta^2} \tag{22}$$

$$\bar{u}_{L_W}(\bar{x},0) = \frac{1}{\pi} \int_{-\infty}^{\infty} \frac{d\bar{z}}{d\bar{\xi}} \frac{d\bar{\xi}}{(\bar{x}-\xi)} \tag{23}$$

$$I = \int_{-\infty}^{\infty} \frac{u_W^2(\bar{x},0)}{b} E(\frac{\bar{\xi} - \bar{x}}{b}) \, d\bar{\xi}, \tag{24}$$

$$E(\frac{\bar{\xi} - \bar{x}}{b}) = -\frac{b}{2\pi} \int_0^{\infty} \frac{\partial^2}{\partial \xi^2} \ln \frac{r_1}{r_2} \, d\bar{\eta} \tag{24}$$

36

and the normalized variables are defined in Appendix D. Eq. (21) is a function only of $\bar{x}$, the normalized coordinate along the wall surface, and $\bar{\tau}$, the normalized amplitude of the wall slope, given by:

$$\frac{d\bar{z}}{d\bar{x}} = \bar{\tau} \exp - \frac{\bar{x}^2}{2\bar{\sigma}^2} \tag{25a}$$

where

$$\bar{\tau} = \frac{M_\infty^2 (\gamma+1)\tau}{\beta^3} = \frac{M_\infty^2 (\gamma^2-1) I_o \alpha \sqrt{2\pi}\, \sigma}{\beta^3 p_\infty u_\infty \gamma} \tag{25b}$$

The iteration technique (Appendix D) is performed for various subsonic freestream Mach numbers starting at the initial supercritical flow and proceeding toward the Mach 1.0 flow. Each solution obtained by the iteration technique gives a unique $\bar{\tau}$, which determines the freestream Mach number and its corresponding normalized velocity distribution $\bar{u}_w(\bar{x},0)$ along the surface. If $(\bar{u}_w-1)$ versus $\bar{\tau}^{2/3}$ is plotted for each position along the surface, it is found that as the freestream Mach number tends toward unity the slope becomes constant. This corresponds to the phenomenon of the Mach number freeze [Ref. 26] wherein the local Mach number is invariant with changes in the freestream Mach number when the latter is near unity or, more precisely,

$$\left.\frac{dM}{dM_\infty}\right|_{M_\infty=1} = 0 \tag{26}$$

37

Vincenti and Wagoner [Ref. 28], Liepmann and Bryson [Refs. 29 and 30], and others have shown that the corresponding approximate relation yielded by the small-disturbance transonic theory is given by:

$$\frac{d\xi}{d\xi_\infty}\bigg|_{\xi_\infty=0} = 0 \qquad (27)$$

where

$$\xi = -\frac{(1-M^2)}{(M_\infty^2(\gamma+1)\tau)^{2/3}} = \frac{(\bar{u}-1)}{\tau^{2/3}} \qquad (28)$$

The freeze of Mach number extends over a finite range near Mach 1.0 where it is constant. Hence, ξ, the slope of the $(\bar{u}-1)$ versus $\bar{\tau}$ curve at each location $\bar{x}$, is constant near the sonic condition, and the local Mach number at each position can be calculated by Eq. (28). With the local Mach number distribution known, the velocity perturbation can be calculated from Eq. (22), and the other flow properties can be determined from isentropic flow relations [Ref. 27].

The Mach 1.0 flow is completely specified. Boundary conditions are known upstream of the heat release region and on a bounding streamtube. Calculation of the entire flow field is readily calculated from the simple algebraic equations obtained by Broadbent's method, where the streamtube configuration is known precisely at Mach 1.0.

III. NUMERICAL RESULTS

The computed flow properties are for the Mach 1.0 thermal blooming problem with the characteristics listed in Table I.

Gaussian Beam	
Peak Intensity (I_o)	3.333×10^7 Watts/m^2
Standard Deviation (σ)	5 cm.
Atmospheric Absorption (α)	8.0×10^{-7} cm^{-1}
Atmospheric Freestream Conditions	
Temperature (T_∞)	288.0 °K
Pressure (p_∞)	1.013×10^5 Newtons/m^2
Density (ρ_∞)	1.2246 kgm/m^3
Velocity $(u_\infty = a^*)$	340.0 m/sec
Streamtube Width $(\Delta n_{1,j} = \Delta n_\infty)$	1 cm.
Streamline Cell Length $(\Delta s_{i,1})$	1 cm.
Ratio of Specific Heats (γ)	1.4
Specific Heat at Constant Pressure (Cp)	1005.0 Joules/kgm°K

Table I

Freestream Flow Properties And
Laser Beam Characteristics

The first step in the procedure is to determine the boundary conditions for the heat release region. Far upstream of the heat release region, all the dimensionless perturbation quantities are zero. The other boundary conditions are calculated by Sprieter's method [Ref. 10] for the bounding streamtube, the shape of which depends upon the heat release distribution and is known, Eq. (16).

Using Sprieter's numerical iteration procedure on the transonic flow integral equation, Eq. (21), the normalized velocity distribution along the bounding streamtube was obtained for several freestream Mach numbers between the initial supercritical flow and Mach 1.0. The results are graphed in Fig. 8. From these solutions, a $(\bar{u}-1)$ versus $\bar{\tau}^{2/3}$ curve, Fig. 9, was plotted for several positions along the streamtube. The results indicate that the slope (ξ) is constant for each position and, hence, the Mach number can be considered frozen.

From the values of $\xi(\bar{x})$, the local Mach number variation at a freestream Mach number of unity was calculated from Eq. (28), since ξ is known and constant for the known physical streamtube shape, Eq. (30), from Eq. (D6).

$$\tau = \frac{t}{\sqrt{2\pi}\,\sigma} = 1.386 \times 10^{-6} \tag{30}$$

where

$$t = \frac{(\gamma-1)L\alpha\pi\sigma^2}{\gamma P_\infty u_\infty} = 1.737 \times 10^{-5} \text{ cm.}$$

40

(a) Shock Wave at $\bar{x} = 9.5$

1/e of Gaussian beam

(b) Shock Wave at $\bar{x} = 11.5$

(c) Shock Wave at $\bar{x} = 14.5$

(d) Shock Wave at $\bar{x} = 19.5$

(e) Shock Wave at $\bar{x} = 24.5$
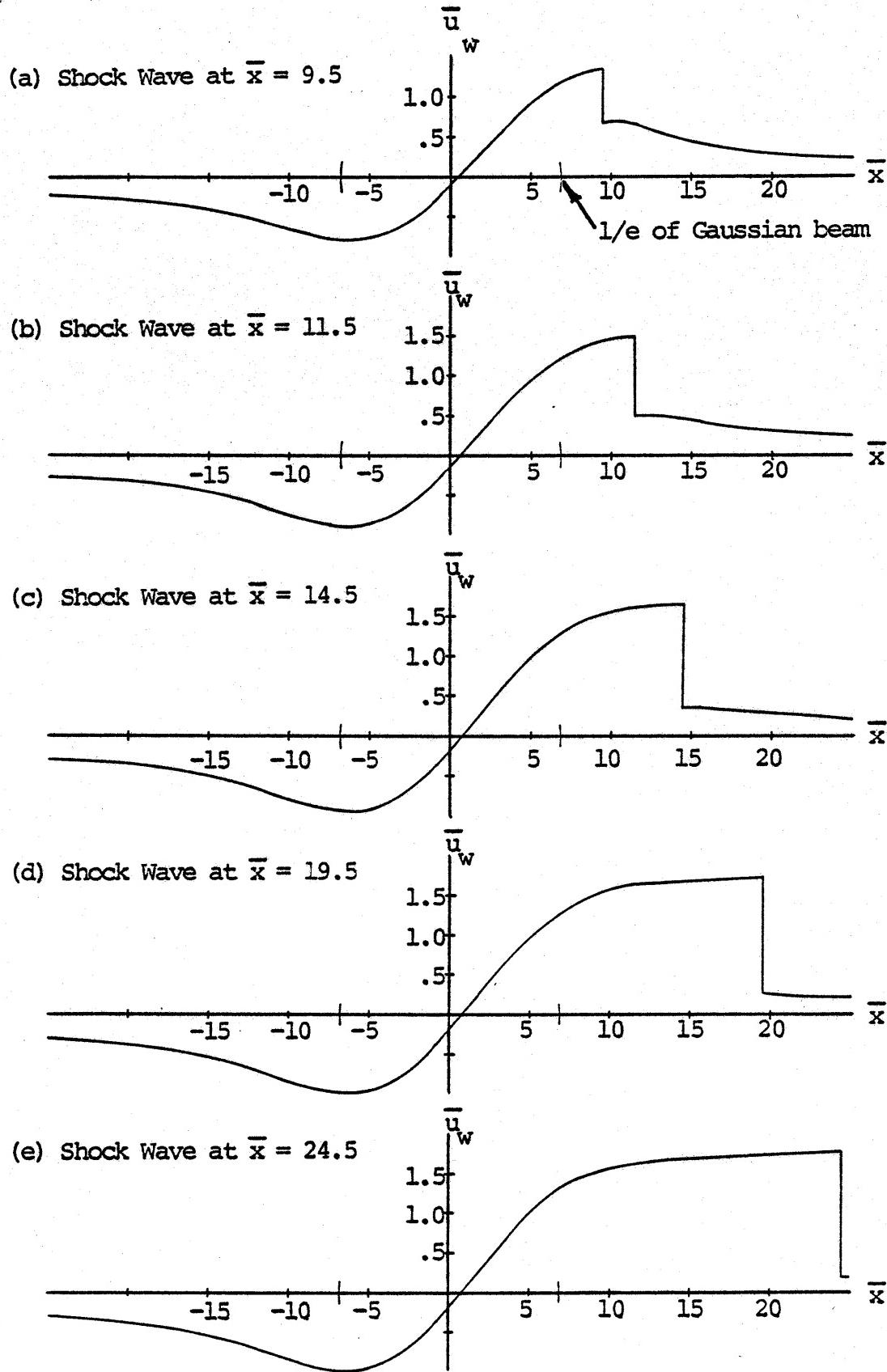
FIGURE 8. High Subsonic Supercritical Flows on
Bounding Streamtube
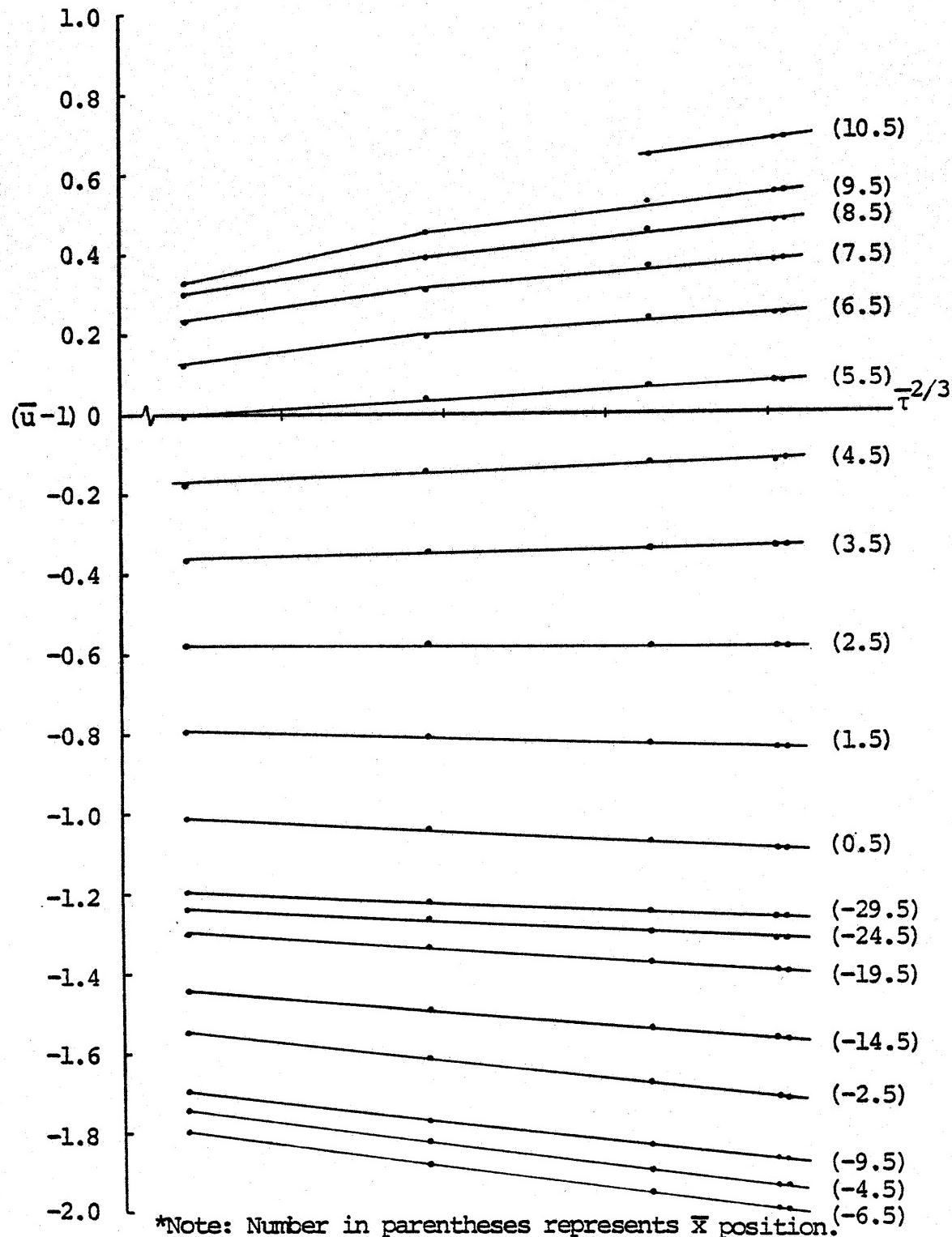
FIGURE 9.   Mach Number Freeze ξ = Constant for
Various $\bar{x}$ Positions

is the maximum growth of the bounding streamtube.

Once the local Mach number was determined, the velocity perturbation along the bounding streamtube was calculated from Eq. (22) and is plotted in Fig. 10. The remaining flow properties were calculated by the isentropic flow relations [Ref. 27].

It has been shown that the area change of the stream-tubes in the heat addition region is directly proportional to the change in total temperature; that is, $\beta = 0$ in Eq. (13). The energy equation is automatically satisfied by this selection for the area variation. Since the heat release distribution is known, all of the streamtubes are specified. From the streamtube shape, the radius of curvature of the streamlines were calculated at every point throughout the region, Eq. (18).

With the curvature known, the calculation of the flow properties in the heat region is reduced to the solution of two simple linear algebraic equations, Eqs. (8a) and (8b), the momentum equations in natural coordinates. The results of this "marching" technique are shown in Fig. 11 where the density perturbations in the upper half of the symmetric laser beam are presented. This method has the distinct advantage that it can be solved on an HP 9830 computer.

Figs. 12 and 13 show the linear supersonic and subsonic density perturbation solutions calculated from the computer program (BLOOM) developed in Appendix G. The results
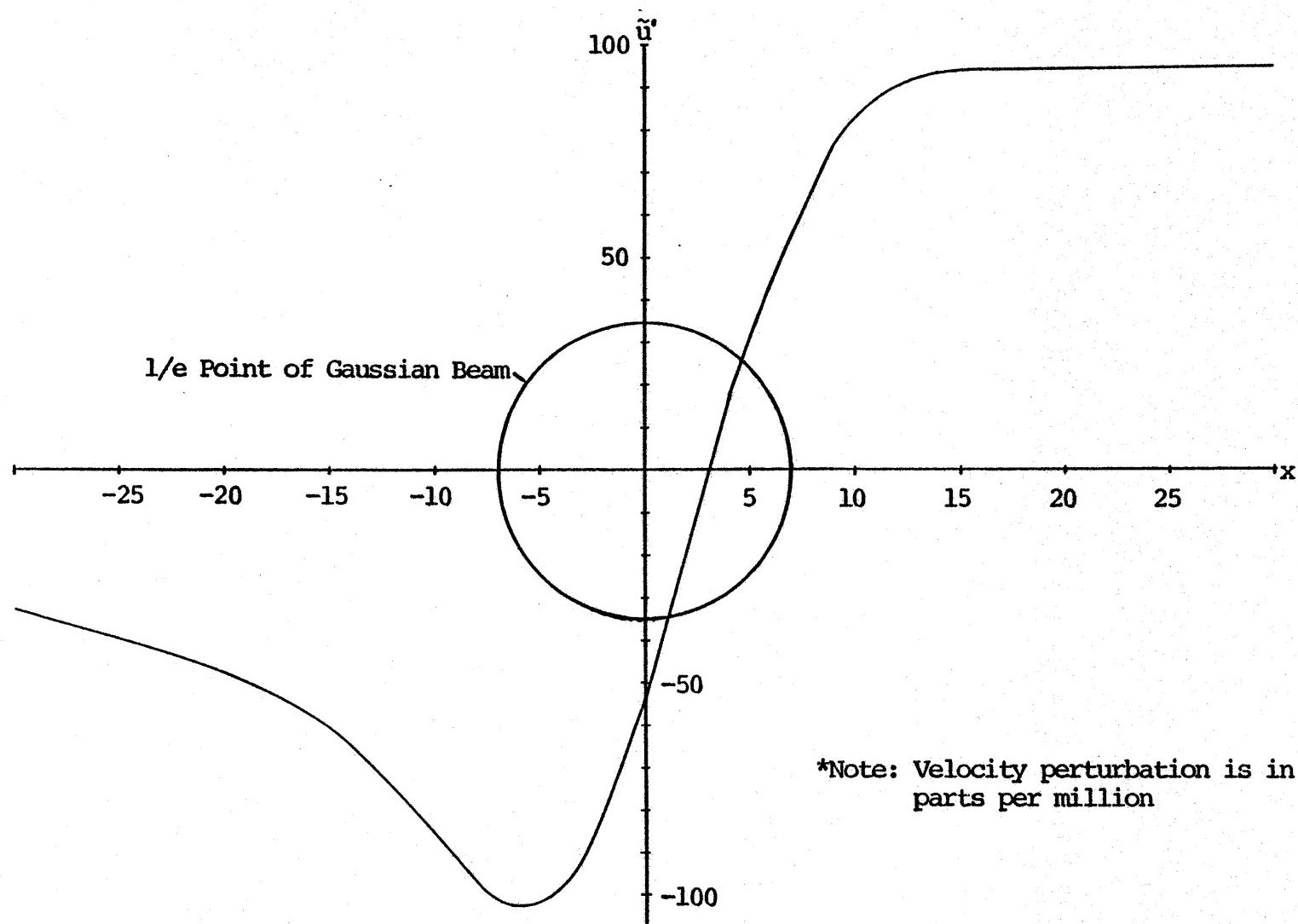
FIGURE 10. Velocity Perturbations on Bounding Streamtube at $M_\infty = 1.0$
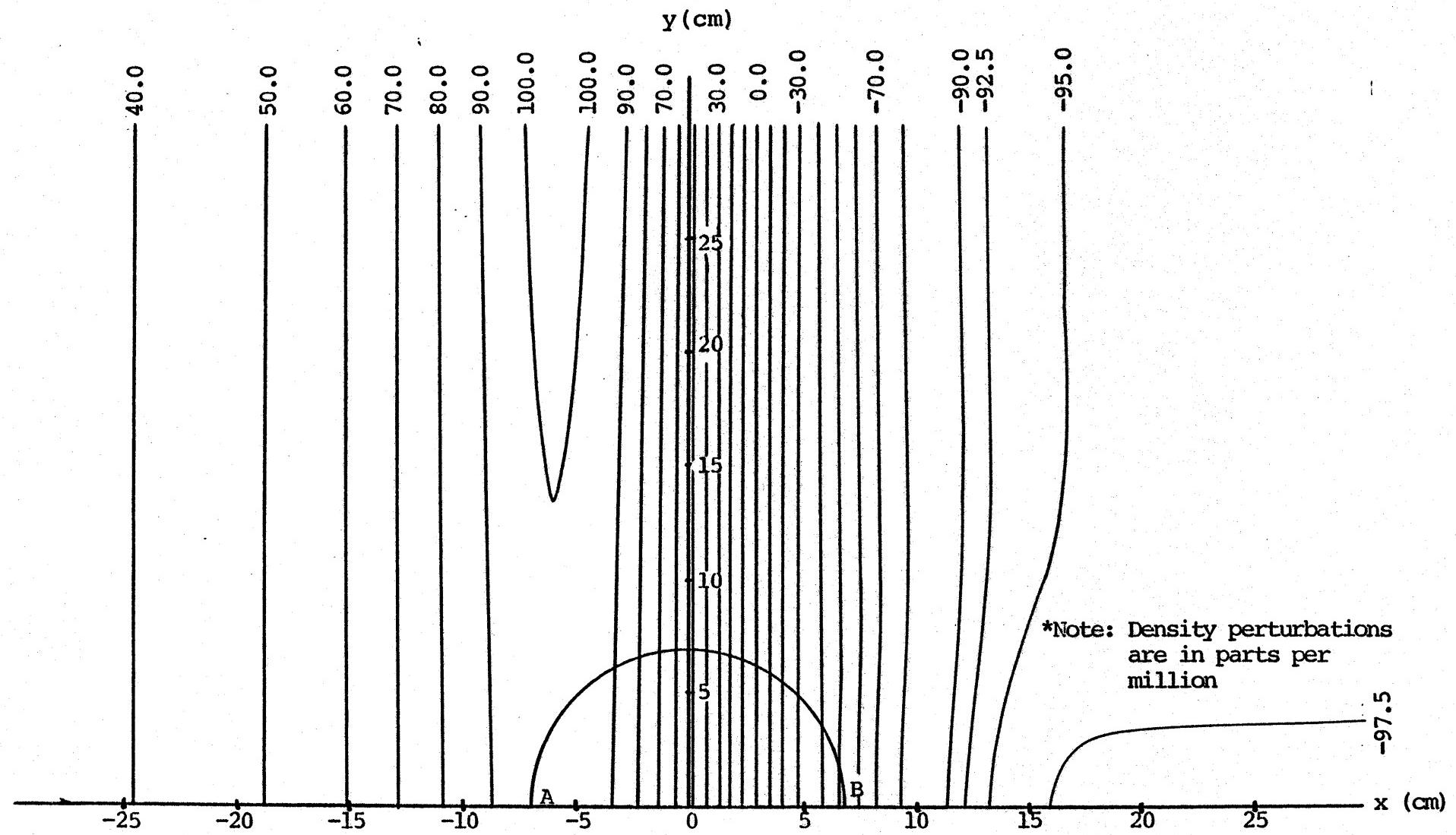
FIGURE 11.   Density Perturbation ($\tilde{\rho}'$) for $M_\infty = 1.0$
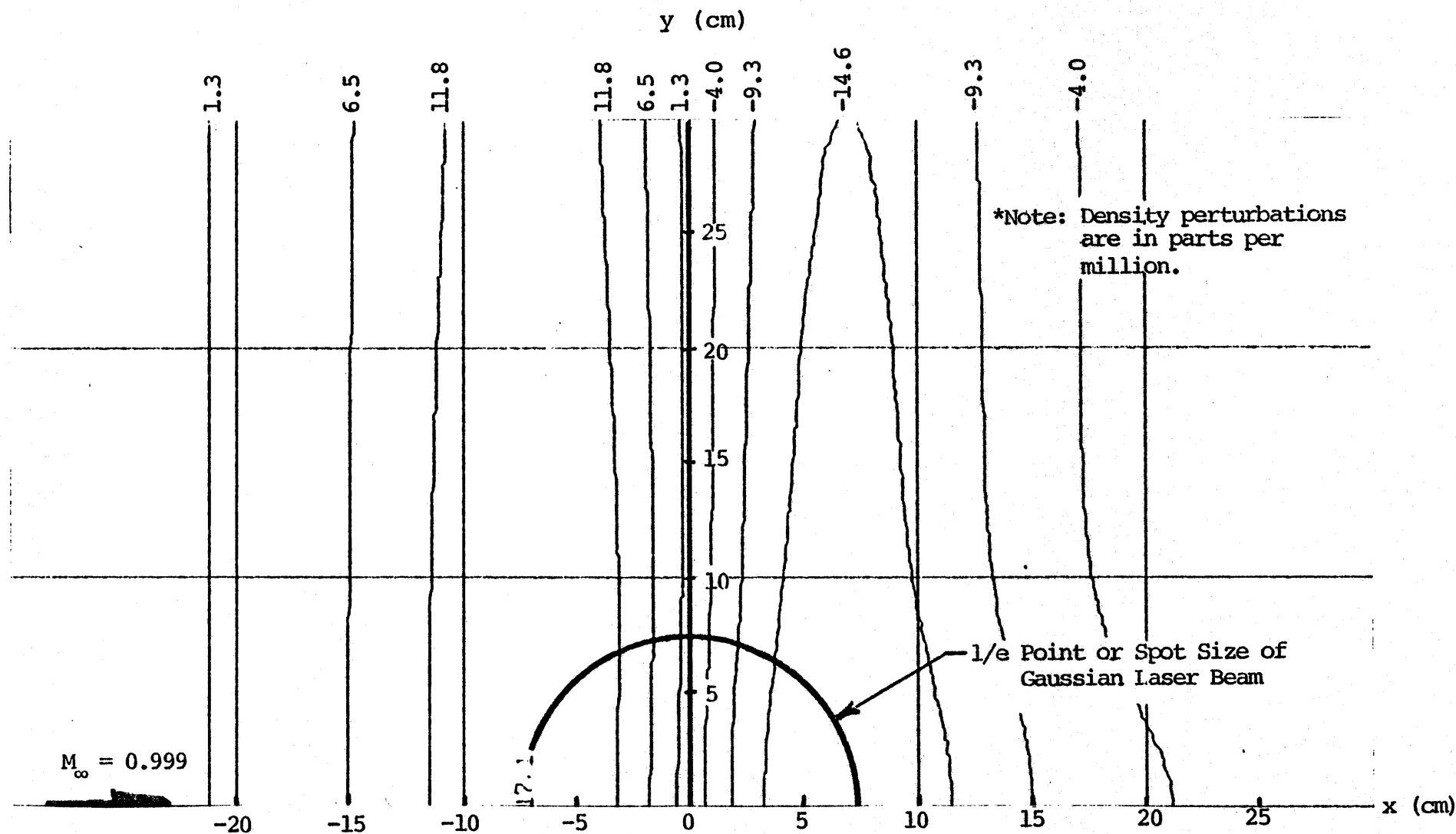
FIGURE 12. Density Perturbations ($\tilde{\rho}'$) for $M_\infty = 0.999$

46
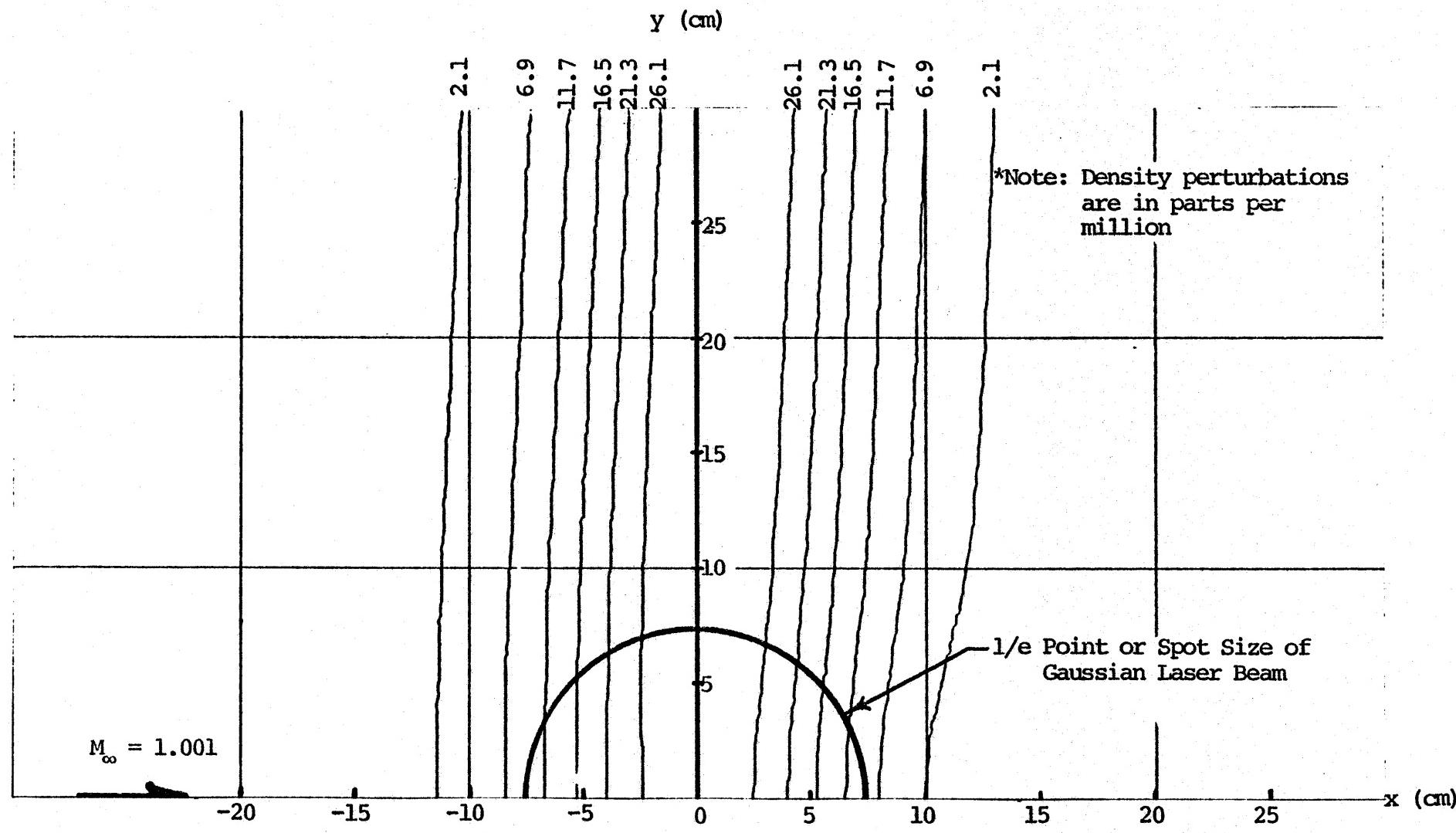
FIGURE 13. Density Perturbation ($\tilde{\rho}'$) for $M_\infty = 1.001$

47

presented in Fig. 10 at Mach 1.0 are consistent with a continuous transition through the transonic regime. Although the solution calculated is for precisely Mach 1.0, it can be logically hypothesized that the flow behavior through the transonic regime is as shown graphically in Fig. 14.

The linear supersonic and subsonic solutions, and Sprieter's high subsonic solutions are in excellent agreement with this hypothesis as well as that conjectured from the hodograph plane representation for transonic flow (Appendix E). Therefore, there is a steady, two-dimensional solution for the transonic thermal blooming problem which is finite and does not result in "catastrophic" defocusing of the laser beam.

IV. CONCLUSIONS

It has been demonstrated that there is a two-dimensional steady state solution to the transonic thermal blooming problem for a sluing laser beam with a freestream Mach number of precisely unity. According to the linearized solutions for thermal blooming, the density perturbations become infinite as a Mach number of unity is approached. Due to nonlinear effects the trend to infinity is cutoff, and the finite value of perturbation quantities has been established.

In obtaining the solution, it was found that at precisely Mach 1.0 that the streamtube area variation through the heat release region is directly proportional to the change in total temperature in that region. With the streamtube shapes known, an exact solution for the flow field can be obtained by Broadbent's method [Ref. 21] with the corresponding boundary values for Mach 1.0 isentropic flow far from the heat release region. There are no restrictions on the existence of shock waves nor on the symmetry or asymmetry of the heat release distribution, provided the bounding streamtube in the isentropic region and the boundary conditions on it can be calculated.

Furthermore, in obtaining the solution at precisely Mach 1.0, it was found that shock waves exist throughout the transonic regime, Fig. 14. As the sonic condition is approached from subsonic speeds, a shock wave forms at the

49

Shock Strength
10^{-4}

1/e point of Gaussian beam

A ———————————————— A
B ———————————————— B

Shock   Sonic Line

Distance (x)
C ———————————————— C
0

Shock

D ———————————————— D
E ———————————————— E
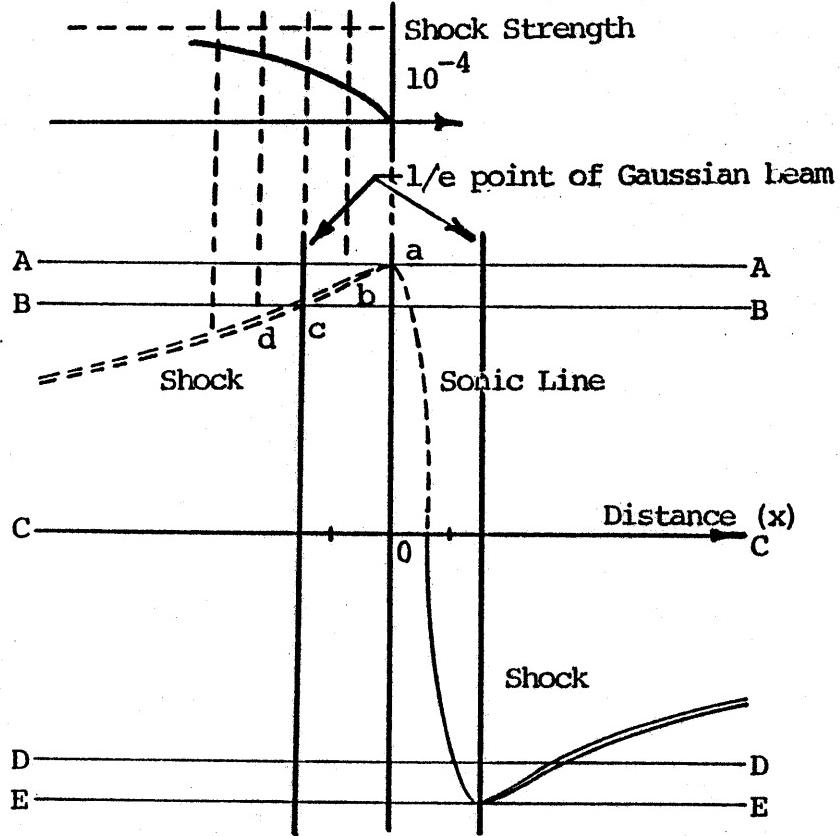
(f) Mach Number (M=1+ε) versus Position Along
Beam Centerline in the Transonic Regime.
(Dashed line represents hypothesized
Supersonic behavior.)

FIGURE 14.   Laser Beam Centerline Mach
Number Distribution in the
Transonic Regime

ε
A ———————————————— A
0.0

(a) Supersonic Flow

ε
B ———————————————— B
0.0

(b) Supersonic Supercritical Flow

Shock Wave at ∞

ε
C ———————————————— C

(c) Sonic Flow

ε 0.0
D ———————————————— D
x

(d) Subsonic Supercritical Flow

ε
E ———————————————— E
0.0

(e) Subsonic Flow

50
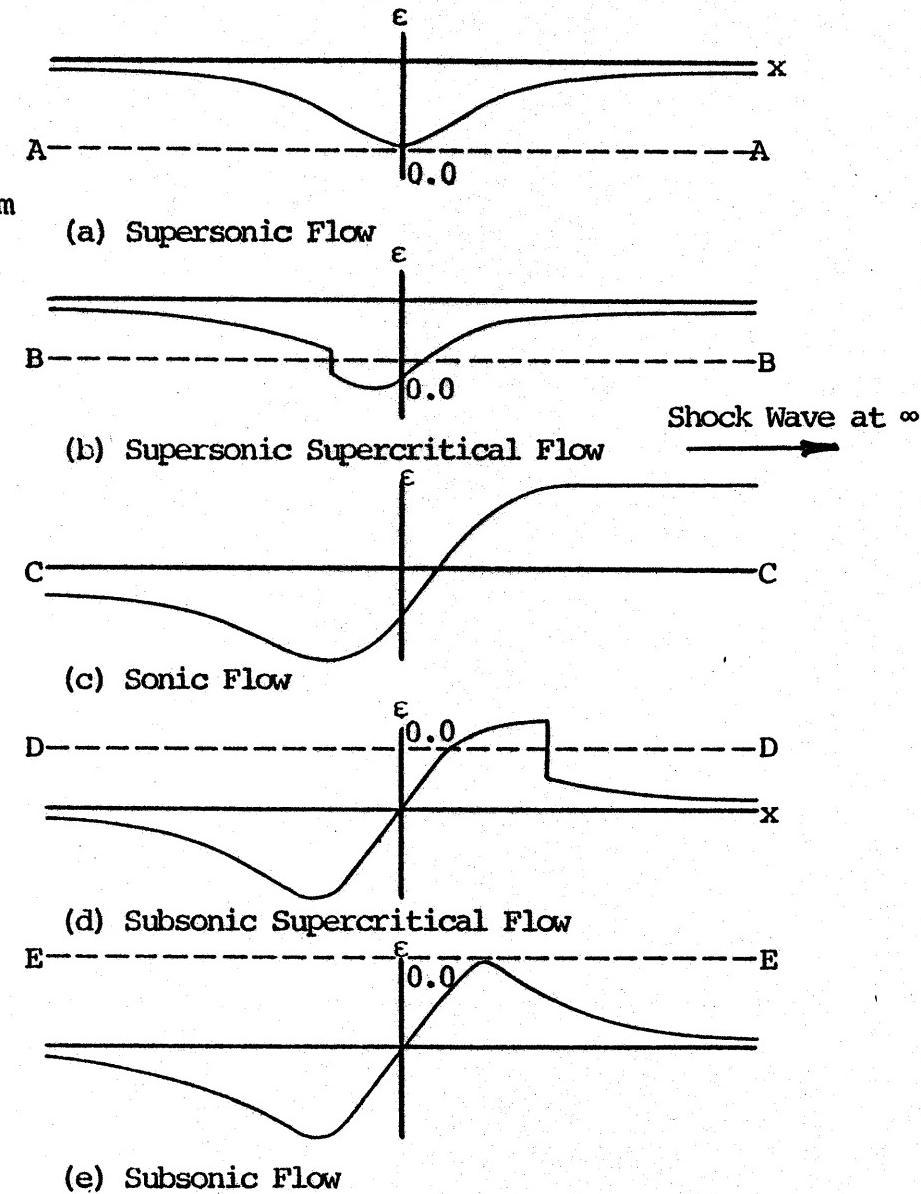
downstream 1/e (one spot size) size, of the Gaussian heat release distribution, where the local Mach number first becomes sonic, and rapidly moves downstream to infinity. If the sonic speed is approached supersonically, a shock is formed at the beam center. To be consistent with the results in the subsonic portion of the transonic regime, it has been hypothesized that the shock moves rapidly upstream to infinity. Finally, the analysis in Appendix F indicates that there is a minimum laser sluing rate that must be maintained to preclude significant phase distortion in the beam at Mach 1.0.

The results of the Mach 1.0 thermal blooming problem for a Gaussian intensity distribution are in excellent agreement with the approximate results obtained by Ellinwood and Mirels [Ref. 19]. Fig. 15a shows these results where the maximum density perturbation was calculated to be of the order of $Q^{2/3}$. Q is defined as:

$$Q = \frac{(\gamma-1) I_o \alpha r}{\gamma p a} ,$$

(31)

where r is the radius (spot size) of a circular beam of uniform heating intensity ($I_o \alpha$). This approximation, when applied to the Gaussian beam of Section III, gives a maximum density perturbation of the order of 10^{-4} which is consistent with that obtained in this paper, and shown in Fig. 15b. Although the density perturbations are very small (i.e. measured in parts per million), significant optical defocusing

51

$Q^{2/3}$

Linear Theory

Nonlinear Theory

$0(Q^{2/3})$

$\dfrac{\Delta\rho}{\rho}$

0

1.0

Mach Number, $M = \Omega r/a_\infty$
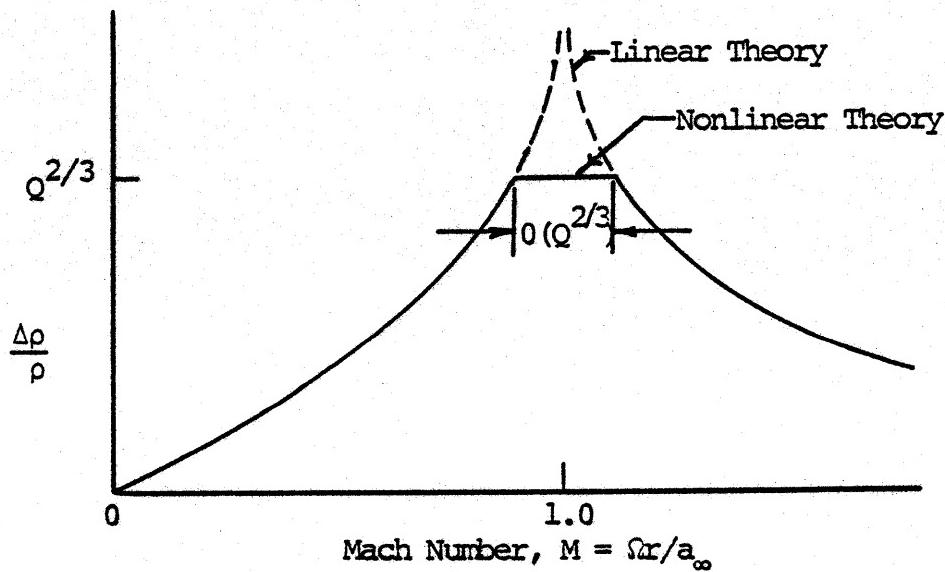
(a) Results of Ellinwood and Mirels [Ref. 16]

• Linear Theory from DIDER

◎ Nonlinear Theory
from Broadbent Solution

100.0

$\dfrac{\Delta\rho}{\rho}$

(parts per
million)

0.0

.999   1.0   1.001

Mach Number, $M = \Omega r/a_\infty$
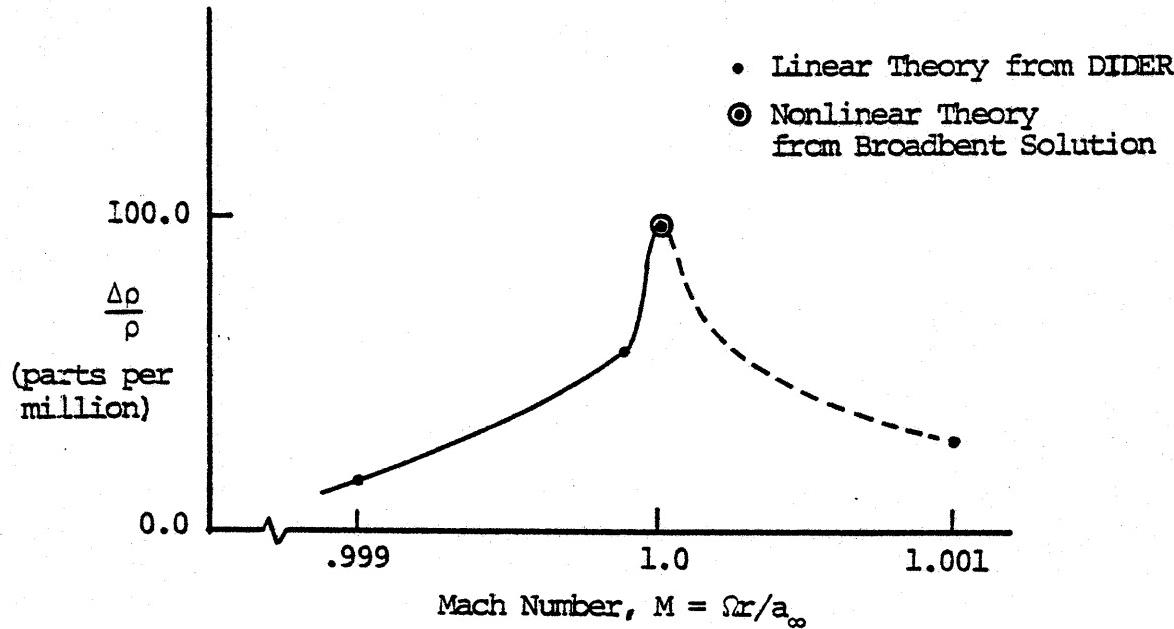
(b) Results of Linear Subsonic and Supersonic Solutions from DIDER
[Refs. 4 and 5] and of Broadbents Method at Mach 1.0

FIGURE 15.   Schematic Representation of the Steady State
Density Perturbations for a Sluing
Two-Dimensional Laser Beam

52

of the laser beam could result (Appendix F). With an increase in the beam area due to defocusing, a large decrease in the beam intensity I (Watts/m^2) will occur.

Two other methods that show promise in solving the transonic thermal blooming problem are the finite difference method developed by Murman and Cole [Ref. 12] for isentropic transonic flow which can be extended to include heat addition, and the "finite element method" of solving partial differential equations [Ref. 31] which is a powerful method for solving a wide range of engineering problems.

A Mach 1.0, steady state solution for thermal blooming in a laser beam with a given Gaussian heat release distribution has been presented in this thesis, Fig. 11. Subsequent investigations should be performed to ascertain the Mach 1.0 solutions for various Gaussian and non-Gaussian heat release distributions, beam intensities (I), atmospheric absorption coefficients (α), and freestream flow properties. In this manner, a correlation might be developed that would be useful as an engineering approximation to the density perturbations at various transonic Mach numbers, vice a simple order of magnitude linear extrapolation as presented by Ellinwood and Mirels [Ref. 19]. Although solutions are known at Mach 1.0 and in the linear subsonic and supersonic regions, from the computer program BLOOM, it would be premature to establish a criterion that could be used in estimating transonic behavior in general before additional work is completed.

APPENDIX A

DERIVATION OF STEADY TRANSONIC FLOW
FOR A CONDUCTING GAS WITH HEAT ADDITION

Eqs. (A1) through (A4) govern steady compressible flow with heat addition and constant properties [Ref. 32]. These equations include viscosity and heat conduction. The distribution of the heat addition is given by the function $Q_o f(x,y)$ and is assumed known. The gas flow is assumed uniform at infinity $(x = \pm\infty)$.

$$\nabla \cdot (\rho \overline{U}) = 0 \tag{A1}$$

$$\rho \overline{U} \cdot \nabla \overline{U} + \nabla p = \psi \tag{A2}$$

where
$$\psi \equiv \eta \nabla (\nabla \cdot \overline{U})/3 + \eta \nabla^2 U$$

$$\rho T \overline{U} \cdot \nabla s = -\Phi - \nabla \cdot q \tag{A3}$$

where
$$\Phi = \frac{2\eta}{3} (\nabla \cdot \overline{U})^2 - \eta (\nabla^2 (\overline{U} \cdot \overline{U}) - (\nabla \times \overline{U})^2 - 2\overline{U} \cdot \nabla^2 \overline{U})$$

and
$$\nabla \cdot q = -\kappa \nabla^2 T - Q_o f(x,y)$$

$$\nabla p = \rho a^2 \nabla s / Cp + a^2 \nabla \rho \tag{A4a}$$

or
$$\exp\left(\frac{s - s_o}{Cv}\right) = T/\rho^{(\gamma-1)} \tag{A4b}$$

The following dimensionless variables are defined:

$$x' = x/\ell_1 \qquad y' = y/\ell_2$$

$$\rho' = \rho/\rho_\infty \qquad T' = T/T_\infty \qquad \bar{U}' = \bar{U}/U_\infty$$

$$s' = s/Cv_\infty \qquad \eta' = \eta/\eta_\infty = 1 \qquad \kappa' = \kappa/\kappa_\infty = 1$$

where ℓ_1 and ℓ_2 are characteristic lengths in the x and y directions, respectively, and the reference values are the freestream conditions. Substituting the dimensionless variables into Eqs. (A1) through (A4) and eliminating the pressure term in the momentum equation, Eq. (A2), with the equation of state, Eq. (A4), the equations simplify to the following:

$$\rho' \nabla' \cdot \bar{U}' + \bar{U}' \cdot \nabla' \cdot \rho' = 0 \tag{A5}$$

$$\rho' \bar{U}' \cdot \nabla' \bar{U}' = - \frac{T' \nabla' \rho'}{M_\infty^2} - \frac{\rho' T' \nabla' s'}{\gamma M_\infty^2} + \frac{\nabla'(\nabla' \cdot \bar{U}')}{3 \, Re} + \frac{\nabla'^2 \bar{U}'}{Re} \tag{A6}$$

$$\rho' T' \bar{U}' \cdot \nabla' s' = \frac{\gamma(\gamma-1) M_\infty^2}{Re} \left\{ - \frac{2}{3} (\nabla' \cdot \bar{U}')^2 + \nabla'^2 (\bar{U}' \cdot \bar{U}) \right.$$

$$\left. - (\nabla' \times \bar{U}')^2 - 2(\bar{U}' \cdot \nabla'^2 \bar{U}') \right\}$$

$$+ \frac{\gamma \nabla'^2 T'}{RePr} + \gamma(\gamma-1) M_\infty^2 H_\infty f(x,y) \tag{A7}$$

where the dimensionless ratios are defined as follows:

Reynolds number: $\qquad Re = \rho_\infty U_\infty \ell_1 / \eta_\infty$

Mach number: $\qquad M_\infty = U_\infty / \sqrt{\gamma R T}$

Prandtl number: $\qquad Pr = C_{p_\infty} \eta_\infty / \kappa_\infty$

Heat quantity: $\qquad H_\infty = Q_0 \ell_1 / \rho_\infty U_\infty^3$

Scaling factor: $\qquad L = \ell_1 / \ell_2$

For flows in which conduction and viscosity can be neglected, two flows will be dynamically similar when γ, M_∞ (Mach number in the absence of heat addition) and H_∞ are the same.

Retaining the viscous, conduction, and heat addition terms, the governing equations, Eqs. (A5) through (A7), in two-dimensions become:

$$\rho'\left(\frac{\partial u'}{\partial x'} + L\frac{\partial v'}{\partial y'}\right) + u'\frac{\partial \rho'}{\partial x'} + Lv'\frac{\partial \rho'}{\partial y'} = 0 \qquad (A8)$$

x-direction momentum equation:

$$\rho'\left(u'\frac{\partial u'}{\partial x'} + Lv'\frac{\partial u'}{\partial y'}\right) = -\frac{T'}{M_\infty^2}\frac{\partial \rho'}{\partial x'} - \frac{\rho'T'}{\gamma M_\infty^2}\frac{\partial s'}{\partial x'} + \frac{4}{3Re}\frac{\partial^2 u'}{\partial x'^2}$$

$$+ \frac{L}{3Re}\frac{\partial^2 v'}{\partial x'\partial y'} + \frac{L^2}{Re}\frac{\partial^2 u'}{\partial y'^2} \qquad (A9)$$

y-direction momentum equation:

$$\rho'\left(u'\frac{\partial v'}{\partial x'} + Lv'\frac{\partial v'}{\partial y'}\right) = -\frac{LT'}{M_\infty^2}\frac{\partial \rho'}{\partial y'} - \frac{L\rho'T'}{\gamma M_\infty^2}\frac{\partial s'}{\partial y'} + \frac{4L^2}{3Re}\frac{\partial^2 v'}{\partial y'^2}$$

$$+ \frac{L}{3Re}\frac{\partial^2 u'}{\partial x'\partial y'} + \frac{1}{Re}\frac{\partial^2 v'}{\partial x'^2} \qquad (A10)$$

energy equation:

$$\rho'T'\left(u'\frac{\partial s'}{\partial x'} + Lv'\frac{\partial s'}{\partial y'}\right) = \frac{\gamma(\gamma-1)M_\infty^2}{Re}\left[\frac{4}{3}\left\{\left(\frac{\partial u'}{\partial x'}\right)^2 - L\frac{\partial u'}{\partial x'}\frac{\partial v'}{\partial y'}\right.\right.$$

$$\left.\left. + \frac{\partial^2 v'}{\partial y'^2}\right\} + \left(\frac{\partial v'}{\partial x'} + L\frac{\partial u'}{\partial y'}\right)^2\right] + \frac{\gamma}{RePr}\left(\frac{\partial^2 T'}{\partial x'^2} + L^2\frac{\partial^2 T'}{\partial y'^2}\right)$$

$$\gamma(\gamma-1)M_\infty^2 H_\infty\ f(x,y) \qquad (A11)$$

Since the transonic flow region is of interest, a transonic expansion procedure similar to that used for incompressible flow around an airfoil of thickness ratio τ [Ref. 33] will be used. In the following analysis, the heat addition will cause the perturbations from the free-stream conditions. Introducing the following perturbation quantities:

$$u' = 1 + \varepsilon^{2/3} \, \tilde{u}_1' + \varepsilon^{4/3} \, \tilde{u}_2' \quad ; \qquad v' = \varepsilon \tilde{v}_1'$$

$$\rho' = 1 + \varepsilon^{2/3} \, \tilde{\rho}_1' + \varepsilon^{4/3} \, \tilde{\rho}_2' \quad ; \qquad T' = 1 + \varepsilon^{2/3} \, \tilde{T}_1' + \varepsilon^{4/3} \, \tilde{T}_2'$$

$$s' = 1 + \varepsilon^{4/3} \, \tilde{s}_2' \quad ; \qquad 1/Re \sim 0(\varepsilon) \quad ; \qquad H_\infty \sim 0(\varepsilon^{4/3}) \quad ;$$

$$\ell_1 = 1 \quad ; \qquad \ell_2 = \varepsilon^{-1/3} \quad ; \qquad L = \varepsilon^{1/3}$$

the first and second order equations at $M_\infty = 1.0$ become:

First order equations:

$$\frac{\partial \tilde{u}_1'}{\partial x'} + \frac{\partial \tilde{\rho}_1'}{\partial x'} = 0 \tag{A12}$$

$$\frac{\partial \tilde{v}_1'}{\partial x'} + \frac{\partial \tilde{\rho}_1'}{\partial y'} = 0 \tag{A13}$$

$$\frac{\partial \tilde{T}_1'}{\partial x'} + (\gamma-1) \frac{\partial \tilde{u}_1'}{\partial x'} = 0 \tag{A14}$$

Integrating Eq. (A12) gives $\tilde{u}_1' = -\tilde{\rho}_1'$ which, when substituted into Eq. (A13), illustrates that for first order theory the flow is irrotational.

$$\frac{\partial \tilde{v}_1'}{\partial x'} - \frac{\partial \tilde{u}_1'}{\partial y'} = 0 \tag{A15}$$

Finally, Eq. (A14) gives the temperature distribution as:

$$\tilde{T}_1' = (\gamma-1) \, \tilde{\rho}_1' = -(\gamma-1) \, \tilde{u}_1' \tag{A16}$$

Second order equations:

$$\frac{\partial \tilde{u}_2'}{\partial x'} + \rho_1' \frac{\partial \tilde{u}_1'}{\partial x'} + \frac{\partial \tilde{v}_1'}{\partial y'} + \frac{\partial \tilde{\rho}_2'}{\partial x'} + u_1' \frac{\partial \tilde{\rho}_1'}{\partial x'} = 0 \tag{A17}$$

$$\frac{\partial \tilde{u}_2'}{\partial x'} + u_1' \frac{\partial \tilde{u}_1'}{\partial x'} + \rho_1' \frac{\partial \tilde{u}_1'}{\partial x'} = - \frac{1}{M_\infty^2} \left(\frac{\partial \tilde{\rho}_2'}{\partial x'} + T_1' \frac{\partial \tilde{\rho}_1'}{\partial x'} \right)$$
$$- \frac{1}{\gamma M_\infty^2} \frac{\partial \tilde{s}_2'}{\partial x'} + \frac{4\varepsilon^{1/3}}{3} \frac{\partial^2 \tilde{u}_1'}{\partial x'^2} \tag{A18}$$

$$\rho_1' \frac{\partial \tilde{v}_1'}{\partial x'} + u_1' \frac{\partial \tilde{v}_1'}{\partial x'} = - \frac{1}{M_\infty^2} \left(\tilde{T}_1' \frac{\partial \tilde{\rho}_1'}{\partial y'} + \frac{\partial \tilde{\rho}_2'}{\partial y'} \right)$$
$$- \frac{1}{\gamma M_\infty^2} \frac{\partial \tilde{s}_2'}{\partial y'} + \varepsilon^{1/3} \frac{\partial^2 \tilde{v}_1'}{\partial x'^2} \tag{A19}$$

$$\frac{\partial \tilde{s}_2'}{\partial x'} = \gamma \varepsilon^{1/3} \frac{\partial^2 \tilde{T}_1'}{\partial x'^2} + \gamma(\gamma-1) \, M_\infty^2 \, f(x,y) \tag{A20}$$

Combining Eqs. (A17) through (A19) and using Eqs. (A12) and (A16), the transonic perturbation equation is obtained.

$$-(\gamma+1) \, u_1' \frac{\partial \tilde{u}_1'}{\partial x'} + \frac{\partial \tilde{v}_1'}{\partial y'} = - \frac{4\varepsilon^{1/3}}{3} \frac{\partial^2 \tilde{u}_1'}{\partial x'^2} + \varepsilon^{1/3} \frac{\partial^2 \tilde{T}_1'}{\partial x'^2} + (\gamma-1) f(x,y)$$
$$\tag{A21}$$

58

The first term on the right-hand side of Eq. (A21) represents the effect of viscosity, the second term the conduction, and the last the heat addition. As can be seen, both the viscous and conduction terms contain a $\varepsilon^{1/3}$ term when the Reynolds number is of the order of ε^{-1}, and, hence, are small and can be neglected under most circumstances. If, however, the Reynolds number is of the order of $\varepsilon^{-2/3}$ or smaller, both terms become important and must be retained in the perturbation equation. Since to first order the flow is irrotational, the velocity potentials $\tilde{u}_1' = \partial\phi/\partial x'$ and $\tilde{v}_1' = \partial\phi/\partial y'$ can be introduced into Eq. (A21) giving:

$$-(\gamma+1)\,\phi_{x'}\,\phi_{x'x'} + \phi_{y'y'} = -\frac{(3\gamma+1)\,\varepsilon^{1/3}}{3}\,\phi_{x'x'x'}$$

$$+ (\gamma-1)\,f(x',\varepsilon^{-1/3}y') \qquad (A22)$$

A similar analysis can be carried out for a freestream Mach number close to unity. In this case, the freestream Mach number can be approximated by $M_\infty = 1 + K\varepsilon^{2/3}$ and the transonic expansion gives:

$$(K + (\gamma+1)\,\phi_{x'})\,\phi_{x'x'} - \phi_{y'y'} = \frac{(3\gamma+1)\,\varepsilon^{1/3}}{3}\,\phi_{x'x'x'}$$

$$- (\gamma-1)\,f(x',\varepsilon^{-1/3}y') \quad . \qquad (A23)$$

APPENDIX B

BRIEF DEVELOPMENT OF BROADBENT'S METHOD OF SOLVING NONLINEAR EQUATIONS OF MOTION WITH HEAT ADDITION

Broadbent's method [Ref. 24] is an inverse solution in which the streamlines, normals, and boundary conditions along at least one streamline and normal are specified and the resulting flow field calculated.

The governing equations for this derivation are as follows:

$$\nabla \cdot (\rho \overline{U}) = 0 \tag{B1}$$

$$\rho \overline{U} \cdot \nabla \overline{U} + \nabla p = 0 \tag{B2}$$

$$\rho \overline{U} \cdot \nabla (h + \frac{1}{2} \overline{U} \cdot \overline{U}) = Q = I\alpha \tag{B3}$$

$$p = \rho RT \tag{B4}$$

In natural coordinates [Ref. 26], these equations become:

$$\frac{\partial}{\partial s} (\rho u \Delta n) = 0 \tag{B5}$$

$$\rho u \frac{\partial u}{\partial s} + \frac{\partial p}{\partial s} = 0 \tag{B6}$$

$$\rho \frac{u^2}{R} + \frac{\partial p}{\partial s} = 0 \tag{B7}$$

$$\rho u \frac{\partial}{\partial s} (h + \frac{1}{2} u^2) = I\alpha \tag{B8}$$

60

A mesh is constructed over the flow field using stream-
lines and normals which are chosen in advance as in Fig. 3.
The cells specify the streamtube boundaries and the mesh
lines the streamline slope and curvature throughout the
flow field. With the mesh specified, Eqs. (B5) through (B7)
are nondimensionalized using uniform freestream flow
properties ($u_{1,j}$, $P_{1,j}$, $\rho_{1,j}$, and $T_{1,j}$), a constant uniform
streamtube width upstream of the perturbations ($\Delta n'_{1,j}$) and
constant Cp.

$$\rho'_{i,j} u'_{i,j} \Delta n'_{i,j} = 1 \tag{B9}$$

$$\tilde{u}'_{i+1,j+1} - \tilde{u}'_{i,j+1} = - \frac{\overline{\Delta n'}_{(i,i+1),j}}{\gamma M_\infty^2} (\tilde{p}'_{i+1,j+1} - \tilde{p}'_{i,j+1}) \tag{B10a}$$

$$\tilde{p}'_{i+1,j+1} - \tilde{p}'_{i+1,j} = - \frac{1}{2} \gamma M_\infty^2 (u'_{i+1,j+1} v'_{i+1,j+1}$$
$$+ u'_{i+1,j} v'_{i+1,j}) \tag{B10b}$$

$$\tilde{T}'_{i+1,j+1} - \tilde{T}'_{i,j+1} + \frac{1}{2} M_\infty^2 (\gamma+1)(u'^2_{i+1,j+1} - u'^2_{i,j+1}) =$$
$$= \frac{(\overline{I\alpha \Delta n'})_{(i,i+1),j}}{Q_\infty} \Delta s'_{i,j+1} = Q'_{i,j+1} \tag{B11}$$

$$P'_{i,j} = \rho'_{i,j} RT'_{i,j} \tag{B12}$$

where Q_∞ is a freestream heat quantity defined in Eq. (12);
$Q'_{i,j+1}$ is a dimensionless heating term; and $v'_{i,j}$ is a
dimensionless inverse radius of curvature.

The slope (dy/dx) and the radius of curvature (R) of the streamlines at a point b (i+1,j) are shown geometrically in Figs. 3. Due to the symmetry of the problem, the slope and the curvature of the centerline streamline are zero (i.e. for all stations $i \geq 1$ and $j = 1$). Assuming that $\Delta y_{i,j} \cong \Delta n_{i,j}$ and $\Delta x_{i,j} \cong \Delta s_{i,j}$ (i.e. to first order the mesh is rectangular), and that the streamline shape is known explicitly, the slope in finite difference form is expressed as:

$$\frac{dy}{dx}\bigg|_{i,j} \equiv \delta_{i,j} = \frac{n'_{i+1,j} - 1/2 \Delta n'_{i+1,j} - n'_{i,j} + 1/2 \Delta n'_{i,j}}{\Delta s'_{i,j}}$$

(B13a)

or:

$$\delta_{i,j} = \frac{\frac{1}{2}\Delta \tilde{n}'_{i+1,1} + \sum_{i=1}^{j-1}\Delta \tilde{n}'_{i+1,1} - \frac{1}{2}\Delta \tilde{n}'_{i+1,j} - \frac{1}{2}\Delta \tilde{n}'_{i,1} - \sum_{i=1}^{j-1}\Delta \tilde{n}'_{i,j} + \frac{1}{2}\Delta n'_{i,j}}{\Delta s'_{i,j}}$$

(B13b)

where

$$n'_{i,1} = \frac{1}{2}\Delta n'_{i,1} = \frac{1}{2}(\tilde{\Delta n}'_{i,1} + 1)$$

(B14a)

$$n'_{i,j} = \frac{1}{2}\Delta n'_{i,1} + \sum_{\ell=1}^{j-1}\Delta n'_{i,1+1} = \frac{1}{2}\Delta \tilde{n}'_{i,1} + \sum_{\ell=1}^{j-1}\Delta \tilde{n}'_{i,1+1} + (j - \frac{1}{2}) ; \quad i \geq 1, \quad j \geq 2$$

(B14b)

The inverse of the radius of curvature (ν) is defined in Eq. (B15) as:

$$\nu = \frac{1}{R} = \frac{d^2 y/dx^2}{(1 + (dy/dx)^2)^{3/2}} \qquad (B15)$$

By nondimensionalizing and substituting the slope obtained in Eqs. (B13a) or (B13b) into Eq. (B15), the following finite difference equation is obtained:

$$\nu'_{i,j} = \frac{\Delta n_{1,j}}{R} = \frac{\dfrac{(\delta_{i,j} - \delta_{i-1,j})}{\Delta s'_{i,j}}}{(1 + (\delta_{i,j})^2)^{3/2}} \qquad (B16)$$

Because the magnitude of the slope $\delta_{i,j}$ is never greater than 10^{-6}, it can be neglected in the denominator simplifying the expression for the curvature. Substituting Eq. (B13b) into Eq. (B16) and retaining only terms of first order, the curvature becomes

$$\nu'_{i,j} = \left[\frac{1}{2}\tilde{\Delta n}'_{i+1,1} + \sum_{\ell=1}^{j-1} \tilde{\Delta n}'_{i+1,1} - \frac{1}{2}\tilde{\Delta n}'_{i+1,j} - \tilde{\Delta n}'_{i,1} - 2\sum_{\ell=1}^{j-1} \tilde{\Delta n}'_{i,1} \right. $$
$$\left. + \tilde{\Delta n}'_{i,j} + \frac{1}{2}\tilde{\Delta n}'_{i-1,1} + \sum_{\ell=1}^{j-1} \tilde{\Delta n}'_{i-1,1} - \frac{1}{2}\tilde{\Delta n}'_{i-1,j} \right] / (\Delta s'_{i,j})^2 \qquad (B17)$$

If the mesh is not specified, Eqs. (B9) through (B12) represent five equations in five unknowns and are nonlinear since $\Delta n'$, p' and u' are dependent functions. When the streamtube shapes are specified, $\Delta n'$ and the curvature ν' are known quantities and the equations become _linear_ in p' and u'. Therefore, Eqs. (B10a) and (B10b) represent two algebraic finite difference equations solvable for p' and u'

throughout the flow field, provided suitable boundary conditions are known. For example, if the values of p' and u' are known at points a (i,j), b (i+1,j) and d (i,j+1) in Fig. 3, the pressure and velocity perturbations can be calculated algebraically at point e (i+1,j+1). This procedure is continued ("marched") throughout the mesh until all flow properties have been determined.

The remaining flow properties, density, and temperature are then calculated from Eqs. (B9) and (B12), the continuity equation and equation of state. Once this has been accomplished, the energy equation, Eq. (B11), is checked to see if the properties calculated from the specified streamline shapes agree with the desired heat distribution. If it does not coincide, an iteration procedure is performed in which the streamline shapes are varied until agreement is obtained.

Boundary conditions are needed along at least one streamline (usually a wall) and one normal (usually freestream conditions). In the transonic thermal blooming problem, the boundary values are chosen as the unperturbed freestream properties upstream of the heat release region and the velocity or pressure on a bounding streamtube which is far enough away from the heat release region that it can be considered isentropic, Fig. 2. With the pressure and/or velocity known on two of the boundaries, the solution for all the flow properties can be calculated as mentioned previously. If a coundary condition is known at other points

64

in the flow field, the resulting properties from the
"marching" procedure must agree with it or the specified
streamtube configuration must be altered until coincidence
between the boundary conditions and heat distribution is
obtained throughout the flow field.

APPENDIX C

DERIVATION FOR THE RELATION BETWEEN AREA VARIATION AND HEAT ADDITION AT PRECISELY MACH 1.0 FLOW

1. AREA CHANGE WITH HEAT ADDITION AT THE SONIC POINT

From the influence coefficients for constant specific heat and molecular weight [Ref. 27], the change in Mach number with heat addition and area variation is given by:

$$\frac{dM^2}{dx} = \frac{G(x)}{1-M^2} \tag{C1a}$$

where

$$G(x) = M^2\left(1+\frac{1}{2}(\gamma-1)M^2\right)\left[(1+\gamma M^2)\frac{d(\ln T_o)}{dx} - 2\frac{d(\ln A)}{dx}\right], \tag{C1b}$$

$d(\ln T_o)/dx$ and $d(\ln A)/dx$ are assumed to be functions of x, the streamwise coordinate, and dx is always positive. Based on the relation between streamline shape and total temperature change obtained from the linear subsonic flow and supersonic flow, Figs. 4 through 7, the following relationship between area variation and total temperature change (heat addition) is chosen:

$$\frac{d(\ln A)}{dx} = \frac{1}{2}(\gamma+1)(1+\beta(x))\frac{d(\ln T_o)}{dx} . \tag{C2}$$

66

β is a variable providing an additional degree of freedom in determining the relationship at Mach 1.0. Substituting Eq. (C2) into Eq. (C1b), $G(x)$ simplifies to:

$$G(x) = M^2 (1+\tfrac{1}{2}(\gamma-1)M^2)((M^2-1)\gamma - (\gamma+1)\beta)\,\frac{d(\ln T_o)}{dx}. \qquad (C3)$$

Since the denominator of Eq. (C1a) tends to zero in the limit as the Mach number approaches unity, the numerator must go to zero to permit a continuous passage from subsonic to supersonic speeds (or vice versa). The condition, when $G(x)$ passes through zero simultaneously with the Mach number becoming unity, is designated the critical point $G(x)$ and, from Eq. (C3), is equal to:

$$\lim_{M \to 1} G(x) \equiv G^*(x) = -\tfrac{1}{2}(\gamma+1)^2\beta\frac{d(\ln T_o)}{dx} = 0 \qquad (C4)$$

Hence, for heat addition $-d(\ln T_o)/dx > 0$, β must equal zero or, equivalently, the area change is directly proportional to the heat addition (i.e. change in total temperature) for steady flow from Mach 1.0, Eq. (C5) is:

$$\frac{d(\ln A)}{dx} = \tfrac{1}{2}(\gamma+1)\,\frac{d(\ln T_o)}{dx}. \qquad (C5)$$

At the critical point, dM^2/dx is of the indeterminate form $0/0$. Therefore, the limiting value of dM^2/dx at the critical point is found by applying L'Hospital's Rule to the

right-hand side of Eq. (Cla).

$$\lim_{M \to 1} \frac{dM^2}{dx} \equiv (\frac{dM^2}{dx})* = \frac{(dG/dx)*}{-(dM^2/dx)*} \qquad \text{(C6a)}$$

or, equivalently,

$$(\frac{dM^2}{dx})* = \pm \sqrt{-(\frac{dG}{dx})*} \qquad . \qquad \text{(C6b)}$$

Eq. (C6b) suggests that $(dM^2/dx)*$ can be positive or negative and the flow can become either subsonic or supersonic from the sonic point. The requirements on β follow from Eq. (C6b) where $G(x)$ is given by Eq. (C3).

$$(\frac{dG}{dx})* = \lim_{\substack{M \to 1 \\ \beta=0}} \frac{dG}{dx} = \frac{1}{2}(\gamma+1) \left[-(\gamma+1)(\frac{d\beta}{dx})* + \gamma(\frac{dM^2}{dx})* \right] \frac{d(\ln T_o)}{dx} \qquad . \\ \text{(C7)}$$

Thus, at the critical point, the flow may be continuous through the sonic speed provided $(dG/dx)*$ is negative and is not zero. For heat addition, Eq. (C7) can be solved for the critical value of $(d\beta/dx)*$, Eq. (C8):

$$(\frac{d\beta}{dx})* > \frac{\gamma}{\gamma + 1} (\frac{dM^2}{dx})* \qquad \text{(C8)}$$

and is graphed in Fig. 1C.

68
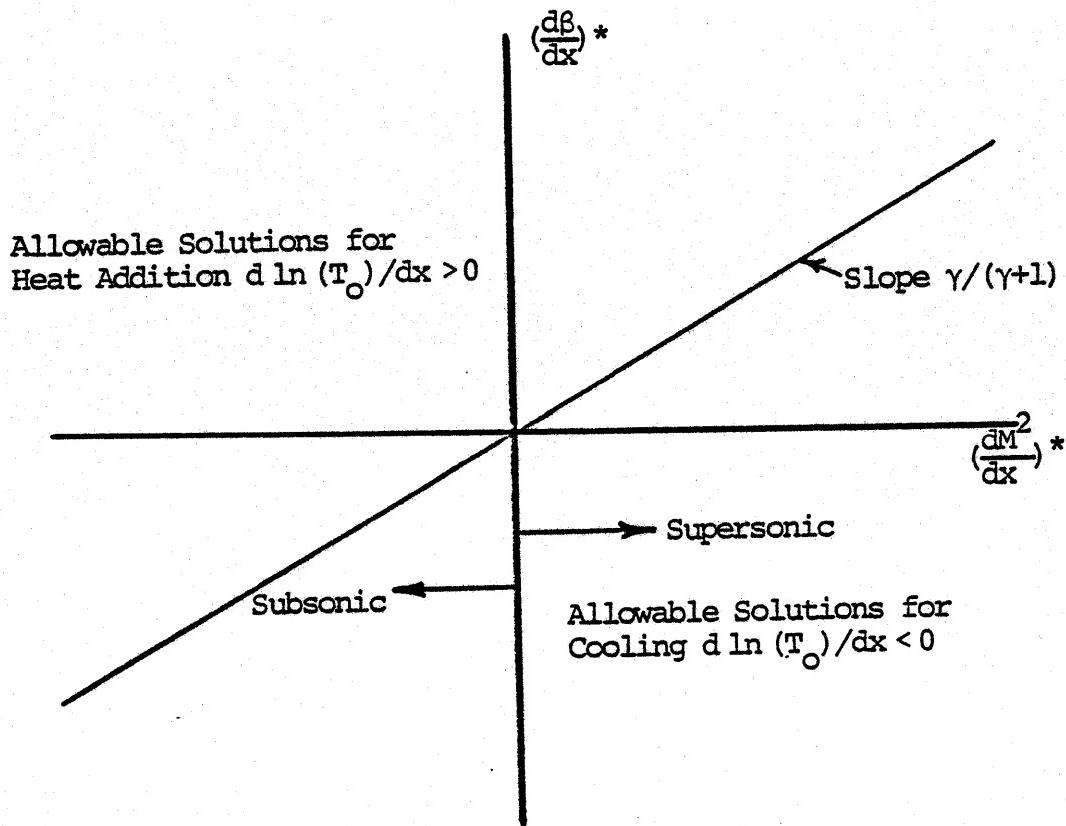
FIGURE 1C. β Variation versus Mach Number Variation
for Sonic Flow

From the sonic flow condition, β must be positive for

supersonic flow and can be either positive or negative

for subsonic flow. The change in β with Mach number squared

must be greater than $\gamma/(\gamma+1)$ for either flow condition,

supersonic or subsonic.

In conclusion, for sonic flow the area variation is

directly proportional to the change in total temperature,

Eq. (C5), where the change of β from the sonic point must

satisfy Eq. (C8).

2. STREAMLINE CONFIGURATION FOR MACH 1.0 FLOW WITH A GAUSSIAN HEAT INPUT DISTRIBUTION

In the first part of this Appendix the streamtube area change was shown to be directly proportional to the change in total temperature at precisely $M_\infty = 1.0$; see Eq. (C5). To derive an expression for the change in total temperature, a slightly different form of the energy equation is used, Eq. (C9),

$$\rho u \frac{\partial}{\partial s} (C_p T_o) = Q = I\alpha \qquad \text{(C9)}$$

in terms of the total temperature T_o. Assuming a constant C_p and a Gaussian heat intensity distribution in the form given in Eq. (2), Eq. (C9) becomes:

$$\frac{dT_{o_{i,j}}}{T_{o_{1,j}}} = \frac{I_o \alpha}{2Q_\infty n'_{1,j}} \int\limits_{-n'_{i,j}}^{n'_{i,j}} \exp{-\frac{y'^2}{2\sigma'^2}} \, dy' \, \exp{-\frac{s_i'^2}{2\sigma'^2}} \, ds'_i \qquad \text{(C10)}$$

where $n'_{i,j}$ represents the total displacement of the jth streamtube from the centerline (j=1), and Q_∞, defined by Eq. (12), is evaluated at $M_\infty = 1.0$.

Equation (C10) is now substituted into Eq. (C9) to give an expression for a change in total streamtube growth over a streamline distance $\Delta s'_i$ at $M_\infty = 1.0$.

$$\frac{dn'_{i,j}}{n'_{i,j}} = \frac{(\gamma+1) I\alpha}{4Q_\infty n'_{1,j}} \int\limits_{-n'_{i,j}}^{n'_{i,j}} \exp{-\frac{y'^2}{2\sigma'^2}} \, dy \, \exp{-\frac{s_i'^2}{2\sigma'^2}} \, ds'_i \qquad \text{(C11)}$$

70

or more conveniently for computational purposes:

$$dn'_{i,1} = \frac{(\gamma+1) I_o \alpha}{4Q_\infty} \left[\int_{-\Delta n'_{i,\frac{1}{2}}}^{\Delta n'_{i,\frac{1}{2}}} \exp-\frac{y'^2}{2\sigma'^2} \, dy' \right] \exp - \frac{s_i'^2}{2\sigma'^2} \, ds_i'$$

$$\cong \frac{1}{4}(\gamma+1) \frac{I_o \alpha}{Q_\infty} \exp - \frac{s_i'^2}{2\sigma'^2} \, ds_i' \quad ; \quad i \geq 1, \; j=1 \qquad \text{(C12a)}$$

and

$$dn'_{i,j} = dn'_{i,1} + \frac{1}{2}(\gamma+1) \frac{I_o \alpha}{Q_\infty}$$

$$\left[\sum_{1}^{j-1} \int_{-(2\ell-1)(\Delta n_{i,\ell}/2)}^{(2\ell+1) \Delta n_{i,\ell}/2} \exp - \frac{y'^2}{2\sigma'^2} \, dy \right] \exp - \frac{s_i'^2}{2\sigma'^2} \, ds_i'$$

$$= dn'_{i,1} + \frac{1}{2}(\gamma+1) \frac{I_o \alpha}{Q_\infty} \sum_{\ell=1}^{j-1} \exp - \frac{(\ell \Delta n'_{i,\ell})^2}{2\sigma'^2} \exp - \frac{s_i'^2}{2\sigma'^2} \, ds_i'$$

$$\text{(C12b)}$$

for streamtubes off of the centerline ($j > 1$). Equations (C12a) and (C12b) can be integrated to give an expression for the total streamtube perturbation from its initial width $n'_{1,j}$ as:

$$n'_{i,1} - n'_{1,1} = \frac{\Delta \tilde{n}'_{i,1}}{2} \cong \frac{1}{2}(\gamma+1) \frac{I_o \alpha \sqrt{2} \; \pi}{Q_\infty} \left\{ 1 + \text{erf} \frac{s_i'}{\sqrt{2} \; \sigma'} \right\} \quad ; \quad i \geq 1$$

$$\text{(C13a)}$$

71

$$n'_{i,j} - n'_{1,j} = \frac{1}{2} \Delta \tilde{n}'_{i,1} + \sum_{\ell=1}^{j-1} \Delta \tilde{n}'_{i,\ell+1}$$

$$\cong \frac{1}{2} \Delta \tilde{n}'_{i,j} + \frac{1}{2}(\gamma+1) \frac{I_o \alpha \sqrt{2} \, \sigma'}{Q_\infty}$$

$$\sum_{\ell=1}^{j-1} \exp - \frac{\ell^2}{2\sigma'^2} (1 + \mathrm{erf} \frac{s'_i}{\sqrt{2} \, \sigma'}) \quad ; \quad i \geq 1, \; j > 1 \; . \tag{C13b}$$

An alternate form of Eqs. (C13a) and (C13b) which can be used in Eqs. (B13a) and (B13b) to simplify the expressions for the slope and the radius of curvature of the streamlines is as follows:

$$\Delta \tilde{n}'_{i,j} = \frac{(\gamma+1) \sqrt{2} \, \sigma' \, I_o \alpha}{2Q_\infty} \exp\left(- \frac{(j-1)^2}{2\sigma'^2}\right) \left\{ 1 + \mathrm{erf} \frac{s'_i}{2\sigma'} \right\} \; ;$$

$$i \geq 1, \; j \geq 1 \tag{C14}$$

where it has been assumed throughout that the initial streamtube widths are uniform; that is, $\Delta n'_{i,j} = 1$ or $\Delta \tilde{n}'_{i,j} = 0$ for all j.

An expression for a streamtube, which is far enough from the heat release region that it can be considered isentropic, is now derived. Carrying out the integration over y' in Eq. (C12a) and assuming that $n'_{i,j} > 4\sigma'$ an expression for the slope of the bounding streamtube is obtained:

$$\frac{dn'_{i,j}*}{ds'_{i,j}*} = \frac{(\gamma+1) I_o \alpha \sqrt{2\pi} \, \sigma'}{4Q_\infty} \exp - \frac{s'^2_i}{2\sigma'^2} \; ; \quad i \geq 1, \; j \geq 1 \tag{C15}$$

Integrating Eq. (C15) with respect to ds_i' gives an explicit equation for the bounding streamtube perturbation from its initial position $n_{1,j*}'$ as:

$$n_{i,j*}' - n_{1,j}' = \frac{1}{2} \Delta\tilde{n}_{i,1}' + \sum_{\ell=1}^{j*-1} \Delta\tilde{n}_{i,\ell+1}'$$

$$= \frac{(\gamma+1)I_0 \alpha \sigma'^2}{4Q_\infty} \left(1 + \text{erf}\, \frac{s_i'}{\sqrt{2}\sigma'}\right) \quad . \qquad (C16)$$

APPENDIX D

INTEGRAL EQUATION DERIVATION FOR TREATING SMALL DISTURBANCE TRANSONIC FLOW WITH SHOCKS FOR AN INFINITE WALL WITH GAUSSIAN SLOPE

1. GENERAL DERIVATION OF INTEGRAL EQUATION

In this appendix, an integral equation is derived for the small disturbance transonic flow with shocks on an infinite wall with Gaussian slope. The small perturbation, steady, two-dimensional transonic equation without heat addition can be written as:

$$(1-M^2)\phi_{x'x'} + \phi_{y'y'} = (1-M_\infty^2-M_\infty^2(\gamma+1)\phi_{x'})\phi_{x'x'} + \phi_{y'y'} = 0$$

$$\text{(D1)}$$

where the local Mach number is approximated by the freestream Mach number plus a perturbation quantity $(M_\infty^2(\gamma+1)\phi_{x'})$. Equation (D1) is valid only in regions where the necessary derivatives exist and are continuous. Therefore, the integral equation derivation includes an equation for the transition through a shock; the equation is the classical relation for the shock polar [Ref. 34], Eq. (D2).

$$v_b'^2 = (u_a' - u_b')^2 \; \frac{u_a'u_b' - a'^2}{\dfrac{2u_a'^2}{\gamma+1} - u_a'u_b' + a'^2}$$

$$\text{(D2)}$$

where subscripts a and b refer to conditions ahead of and behind the shock. If a small perturbation analysis is carried out on Eq. (D2) similar to that performed in obtaining Eq. (D1), the following relation is found for the perturbation velocity components across the shock wave:

$$(1-M^2)(\tilde{u}'_a - \tilde{u}'_b)^2 + (\tilde{v}'_a - \tilde{v}'_b)^2 = M_\infty^2 (\gamma+1)(\tilde{u}'_a + \tilde{u}'_b)(\tilde{u}'_a - \tilde{u}'_b)^2/2$$

(D3)

Equation (D3) corresponds to the shock polar curve for shock waves of small strength that are inclined at any angle between that of normal shock waves and that of the Mach lines.

The applicable boundary conditions for the integral equation analysis are that the perturbation velocity must vanish far upstream of the disturbance, Eq. (D4):

$$\left. \frac{\partial \phi}{\partial x'} \right|_{x=-\infty} = \left. \frac{\partial \phi}{\partial y'} \right|_{x=-\infty} = 0$$

(D4)

and that the flow must be tangent to the wall surface, Eq. (D5):

$$\left. \frac{\partial \phi}{\partial y'} \right|_{y'=0} = \frac{\partial z'}{\partial x'} \simeq \frac{\partial n'_{i,j*}}{\partial s'_{i,j*}} = \tau \exp - \frac{s_i'^2}{2\sigma'^2}$$

(D5)

where $\partial z'/\partial x'$ is the slope of the wall surface in the x' (s') direction which can be approximated by Eq. (C15); and τ is an equivalent thickness ratio for the surface defined as the

75

maximum wall growth t (cm) in the y-direction divided by a characteristic length $\sqrt{2\pi}\ \sigma$ for $M_\infty = 1.0$.

$$\tau = \frac{t}{\sqrt{2\pi}\ \sigma} \quad ; \qquad t = \frac{(\gamma-1)I_o \alpha \pi \sigma^2}{\gamma p_\infty u_\infty} \tag{D6}$$

Also, it is necessary to prescribe that the direct influence of a disturbance in the supersonic region proceeds only in the downstream direction.

Sprieter and Alksne [Ref. 10] derive in detail the integral equation by a Green's function analysis for transonic flow around bodies having subsonic freestream velocities, and a local shock discontinuity. The nonlinear term in the differential equation was maintained. This derivation can by extended to the streamtube configuration of the boundary condition for the internal region. For the sake of brevity, only the important equations and pertinent assumptions will be given in the following analysis.

Since the object of the analysis is to determine the pressure perturbation and/or velocity perturbation on the bounding streamtube, an equivalent equation for the velocity perturbation can be readily obtained by differentiating Eq. (D1) with respect to x'; it is:

$$(1 - M_\infty^2)\tilde{u}'_{x'x'} + \tilde{u}'_{y'y'} = M_\infty^2(\gamma+1)\frac{\partial^2}{\partial x'^2}\left(\frac{\tilde{u}'^2}{2}\right) \tag{D7}$$

76

For the Green's function analysis, it is advantageous to normalize Eq. (D7) with the following linear transformation:

$$\bar{x} \equiv x' \quad ; \quad \bar{y} \equiv \beta y' \quad ;$$

$$\bar{u} \equiv \frac{M_\infty^2 (\gamma+1) \tilde{u}'}{\beta^2} \quad ; \quad \bar{v} \equiv \frac{M_\infty^2 (\gamma+1) \tilde{u}'}{\beta^3} \tag{D8}$$

where $\beta = \sqrt{1 - M^2}$

In this way, Eq. (D7) reduces to the following:

$$\frac{\partial^2 \bar{u}}{\partial \bar{x}^2} + \frac{\partial^2 \bar{u}}{\partial \bar{y}^2} \equiv \nabla^2 \bar{u} = \frac{\partial^2}{\partial \bar{x}^2} \left(\frac{\bar{u}^2}{2}\right) \tag{D9}$$

where $\bar{u}$ can further be defined by the approximation to the local Mach number, Eq. (D1), namely $M^2 \cong M_\infty^2 (1 + (\gamma+1)\tilde{u})$, as:

$$\bar{u} = \frac{M_\infty^2 (\gamma+1) \tilde{u}'}{1 - M_\infty^2} = \frac{M^2 - M_\infty^2}{1 - M_\infty^2} \tag{D10}$$

From Eq. (D10), it is clear that for a subsonic freestream Mach number: $\bar{u} < 1$ when the local flow is subsonic, $\bar{u} = 1$ when it is sonic, and $\bar{u} > 1$ when it is supersonic.

The Green's function analysis is a Neuman problem for finding a function $\bar{u}$ in a bounded region R, bounded by a finite number of closed smooth contours C, such that Eq. (D9) is satisfied in R, $\bar{u}$ and its first partial derivative are continuous in R (shocks are excluded by judicious selection of the bounding contour) and the normal derivative $\partial \bar{u}/\partial \bar{y}$ is prescribed on the boundary of R, Fig. 1D.
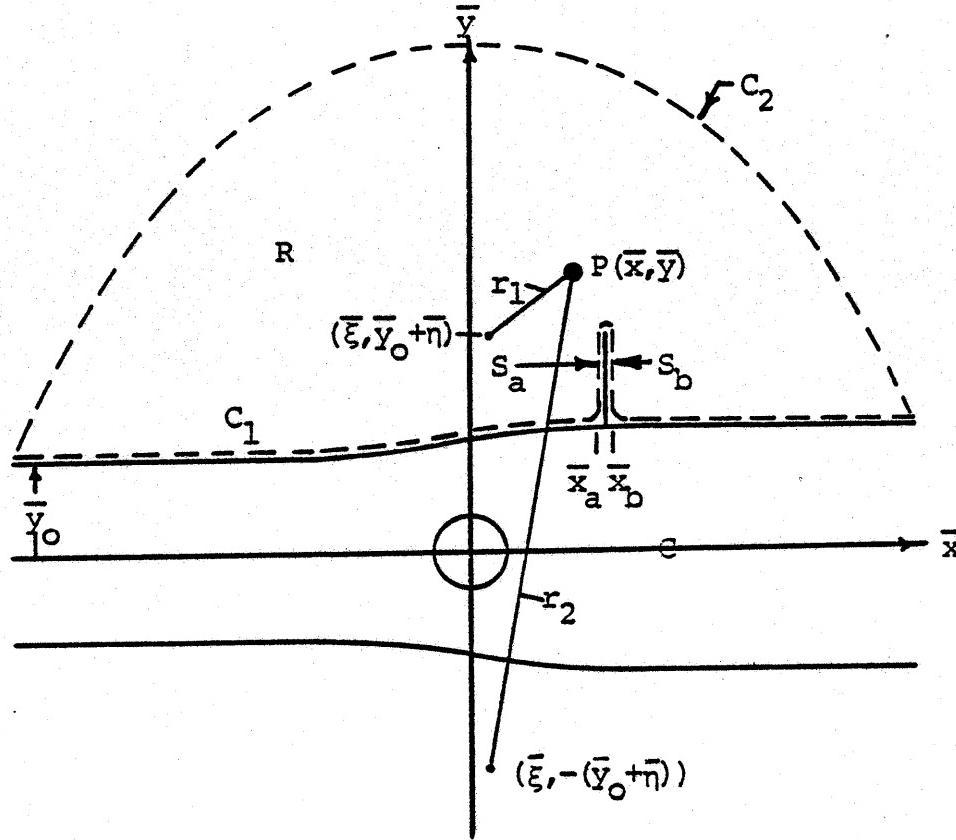
FIGURE 1D. Integration Region for Green's Function Analysis on Flows Past Bounding Streamtubes at Transonic Speeds

Green's theorem states that:

$$\int_C (\bar{u}\nabla G\cdot\bar{n} - G\nabla\bar{u}\cdot\bar{n})\, dC = \iint_R (\bar{u}\nabla^2 G - G\nabla^2\bar{u})\, dR \qquad (D11)$$

where the directional derivative on the left side are taken along the normal, drawn inward, to the curve C.

The Green's function G is constructed so that it satisfies

the Laplace equation $\nabla^2 G = \delta(\bar{\xi}-\bar{x}, \bar{\eta}-\bar{y}+\bar{y}_o)$ with $\partial G/\partial\bar{n} = 0$ on C_1.

$$G(\bar{\xi},\bar{\eta},\bar{x},\bar{y}-\bar{y}_o) = \frac{1}{2\pi} \ln(\frac{r_1}{r_2}) \equiv \frac{1}{2\pi} \ln(R) \qquad (D12)$$

where

$$R = \frac{\sqrt{(\bar{x}-\bar{\xi})^2 + (\bar{y}-\bar{y}_o-\bar{\eta})^2}}{\sqrt{(\bar{x}-\bar{\xi})^2 + (\bar{y}+\bar{y}_o+\bar{\eta})^2}}$$

and $\bar{\xi}$ and $\bar{\eta}$ are the variables of integration while $\bar{x}$ and $\bar{y}$

are the coordinates of a point P. With the Green's function

of Eq. (D12), Eq. (D11) becomes:

$$\bar{u}(\bar{x},\bar{y}) - \int_{-\infty}^{\infty}\int_{0}^{\infty} G \frac{\partial^2}{\partial\xi^2} (\frac{\bar{u}^2}{2})\, d\bar{\eta}d\bar{\xi}$$

$$= \int_{-\infty}^{\infty}(G \frac{\partial\bar{u}}{\partial\bar{n}} - \bar{u} \frac{\partial G}{\partial\bar{n}})\Big|_{\bar{\eta}=0} d\bar{\xi} - \int_{S_a} (G \frac{\partial\bar{u}}{\partial\bar{n}} - \bar{u} \frac{\partial G}{\partial\bar{n}})\Big|_{\bar{x}=\bar{x}_a} d\bar{\eta}$$

$$+ \int_{S_b} (G \frac{\partial\bar{u}}{\partial\bar{n}} - \bar{u} \frac{\partial G}{\partial\bar{n}}\Big|_{\bar{x}=\bar{x}_b} d\bar{\eta} + \int_{C_2} (G \frac{\partial\bar{u}}{\partial\bar{n}} - \bar{u} \frac{\partial G}{\partial\bar{n}})\, dC \qquad (D13)$$

where the respective integration regions and contours are

designated in Fig. 1D. Integrating the remaining surface

integral by parts twice with respect to $\bar{\xi}$, applying the

Green's function boundary condition on C_1 ($\bar{\eta}=0$ or $\bar{y}=\bar{y}_o$),

allowing the radius r of the curve C_2 go to infinity, and

decomposing the line integral over the shock wave into components parallel to the axes of the coordinate system yields Eq. (D14).

$$\bar{u}(\bar{x},\bar{y}) - \frac{1}{2}\bar{u}^2(\bar{x},\bar{y}) = \bar{u}_{Lw} + \frac{1}{2}\int_0^\infty\int_{-\infty}^\infty \bar{u}^2\frac{\partial^2 G}{\partial\bar{\xi}^2}d\bar{\xi}d\bar{\eta}$$

$$-\int_S \left\{ \left[G\frac{\partial}{\partial\bar{\xi}}(\bar{u}-\frac{1}{2}\bar{u}^2) - (\bar{u}-\frac{1}{2}\bar{u}^2)\frac{\partial G}{\partial\bar{\xi}} \right]_a \right.$$

$$-\left[G\frac{\partial}{\partial\bar{\xi}}(\bar{u}-\frac{1}{2}\bar{u}^2) - (\bar{u}-\frac{1}{2}\bar{u}^2)\frac{\partial G}{\partial\bar{\xi}} \right]_b$$

$$\left. +\left[\left[G\frac{\partial\bar{u}}{\partial\bar{\eta}} - \bar{u}\frac{\partial G}{\partial\bar{\eta}} \right]_a - \left[G\frac{\partial\bar{u}}{\partial\bar{\eta}} - \bar{u}\frac{\partial G}{\partial\bar{\eta}} \right]_b \right] \frac{\cos(n,\bar{\eta})}{\cos(n,\bar{\xi})} \right\} d\bar{\eta}$$

$$(D14)$$

where $\bar{u}_{Lw}$ represents the linear wall velocity $\bar{u}$ when the wall shape is specified.

$$\bar{u}_L = \int_{-\infty}^\infty \left. G\frac{\partial\bar{u}}{\partial\bar{\eta}} - \bar{u}\frac{\partial G}{\partial\bar{\eta}} \right|_{\bar{\eta}=0} d\bar{\xi} \qquad (D15)$$

Sprieter and Alksne [Ref.10] in their derivation delineate the advantages for integrating the surface integral over R by parts as was done in arriving at Eq. (D14). The advantages are important enough that they are reiterated here. First, the double integral of Eq. (D13) shows a very strong influence

of the velocities in the region immediately surrounding the point P since they are multiplied by ln(R). This influence is largely nullified in the double integral of Eq. (D14) because part of the region has a negative influence and part has a positive influence. The predominant influence in the latter case is furnished by the term $\frac{1}{2} \bar{u}^2$ standing outside the integral. Next, the contribution of distant regions is diminished in importance in the double integral of Eq. (D14) since their influence varies inversely with the square of the distance, rather than with the logarithm in Eq. (D11). A further advantage is that the value of the double integral of Eq. (D14) is continuous through a shock wave rather than discontinuous as is the case with Eq. (D13). Lastly, a point of great importance in the approximate solution arises from the fact that the integration by parts provides extra terms (those containing $\frac{1}{2} \bar{u}^2$) in the integrals along the shock surface S which combine with those already present in such a manner that the contribution of these integrals becomes very small when the shock wave approaches a normal wave, as is usually the case at high subsonic speeds.

Therefore, $\bar{u}$ must satisfy Eq. (D14) where $\bar{u}_L$ is given by Eq. (D15) and the shock relationship Eq. (D16), which is the normalized form of Eq. (D3).

$$(\bar{u}_a - \bar{u}_b)^2 + (\bar{v}_a - \bar{v}_b)^2 = \frac{1}{2} (\bar{u}_a + \bar{u}_b)(\bar{u}_a - \bar{u}_b)^2 \qquad \text{(D16)}$$

In the case of a specified symmetric wall shape, Eq. (D14) can be considerably simplified as it permits the introduction of the boundary conditions which are specified at the outset of the problem, Eqs. (D17a) and (D17b), into the integral over the wall surface.

$$\bar{u}(\bar{x},0) = \bar{u}_{Lw} = \text{KNOWN} \tag{D17a}$$

and

$$\frac{\partial \bar{u}}{\partial \bar{\eta}} = \frac{\partial \bar{v}}{\partial \bar{\xi}} = \left(\frac{\partial \bar{v}}{\partial \bar{\xi}}\right)_L \equiv \frac{\partial^2 \bar{z}}{\partial \bar{\xi}^2} = \bar{\tau}\, \frac{\partial^2}{\partial \bar{\xi}^2} \exp - \frac{\bar{\xi}^2}{2\bar{\sigma}^2} \quad , \tag{D17b}$$

where $\bar{z}$ represents the reduced ordinate of the surface, and $\bar{\tau}$ the reduced thickness ratio given by:

$$\bar{\tau} = \frac{M_\infty^2 (\gamma+1)\tau}{\beta^3} \tag{D18}$$

Substituting the relationships of Eqs. (D17a) and (D17b) into Eq. (D15) completely determines at the outset of the analysis the linear wall velocity distribution:

$$\bar{u}_{Lw}(\bar{x},0) = \lim_{\bar{y}\to\bar{y}_0} \left(\frac{1}{2\pi} \int_{-\infty}^{\infty} (\ln(\frac{r_1}{r_2})\, \frac{d^2\bar{z}}{d\bar{\xi}^2}) \right|_{\bar{\eta}=0} d\bar{\xi}$$

$$= \frac{1}{\pi} \int_{-\infty}^{\infty} \frac{d\bar{z}}{d\bar{\xi}}\, \frac{d\bar{\xi}}{(\bar{x}-\bar{\xi})} \tag{D19}$$

2. SIMPLIFICATION AND APPROXIMATE SOLUTION OF THE INTEGRAL EQUATION FOR TRANSONIC FLOW

To obtain a solution to Eq. (D14), some further assumptions must be made. They are: (a) all shock waves lie in a plane transverse to the beam, and (b) the shock waves are normal (i.e. normal to the local flow direction). These two assumptions reduce Eq. (D16) to an expression, Eq. (D20), which permits an advantageous introduction into Eq. (D14) to eliminate the integral over the shock S, Eq. (D21).

$$(\bar{u} - \tfrac{1}{2} \bar{u}^2)_a = (\bar{u} - \tfrac{1}{2} \bar{u}^2)_b$$

$$\frac{\partial}{\partial \bar{\xi}} (\bar{u} - \tfrac{1}{2} \bar{u}^2)_a = \frac{\partial}{\partial \bar{\xi}} (\bar{u} - \tfrac{1}{2} \bar{u}^2)_b \tag{D20}$$

$$\bar{u}(\bar{x},\bar{y}) = \bar{u}_L(\bar{x},\bar{y}) + \tfrac{1}{2} \bar{u}^2(\bar{x},\bar{y}) + \frac{1}{2\pi} \int_{-\infty}^{\infty}\int_{0}^{\infty} \frac{\bar{u}^2}{2} \frac{\partial^2}{\partial \bar{\xi}^2} \ln\left(\frac{r_1}{r_2}\right) d\bar{\eta} d\bar{\xi} \tag{D21}$$

Equation (D21) will be used as the basis for obtaining the velocity distribution on the bounding streamtube. Approximate solutions of this equation are obtained numerically by starting with an assumed velocity distribution and iterating until convergence is obtained. If mixed flow exists, the initial velocity distribution must include a proper discontinuity complying with the shock relations of Eq. (D20).

Due to the double integral in Eq. (D21), an iteration process would be cumbersome unless it could be reduced to a single integral by introducing suitable approximations. Oswatitsch [Refs. 35 and 36] has shown that approximate knowledge of the velocity distribution in the vicinity of the surface can be expressed in terms of the local coordinate $\bar{y}$, the ordinates of the wall shape $\bar{Z}(\bar{x})$, and the desired but unknown velocity distribution $\bar{u}_w(\bar{x},0)$ on the surface. This permits the reduction of the double integral to a single integral.

Oswatitsch has considered such an approximate relation in which the velocity $\bar{u}(\bar{x},\bar{y})$ starts from the value $\bar{u}_w(\bar{x},0)$ at the surface with an initial rate of change given by the irrotationality condition, Eq. (D22), and vanishing at large distances as $1/\bar{y}^2$.

$$\frac{\partial \bar{u}}{\partial \bar{y}}\bigg|_w = \frac{\partial \bar{v}}{\partial \bar{x}}\bigg|_w \tag{D22}$$

The resulting relation takes the following form:

$$\bar{u}(\bar{x},\bar{y}) = \frac{\bar{u}_w(\bar{x},0)}{\left(1 + (\bar{y}-\bar{y}_o)/b\right)^2} \tag{D23}$$

where b is a function of $\bar{x}$ satisfying the irrotationality condition at $\bar{y} = \bar{y}_o$. Solving for b using the boundary conditions of Eqs. (D17a) and (D17b) yields:

$$b(\bar{x}) = -\frac{2\bar{u}_w(\bar{x},0)}{d^2\bar{z}/d\bar{x}^2} \quad . \tag{D24}$$

Substituting Eq. (D23) into the double integral of Eq. (D21), integrating with respect to $\bar{\eta}$ and setting $\bar{y} = \bar{y}_o$ results in a simplified integral equation for calculating $\bar{u}_w(\bar{x},0)$. For computational purposes, the integral equation is expressed as:

$$\bar{u}_w(\bar{x},0) = \bar{u}_{Lw}(\bar{x},0) + \tfrac{1}{2}\bar{u}_w^2(\bar{x},0) - \tfrac{1}{2}I \tag{D25}$$

where

$$I = \int_{-\infty}^{\infty} \frac{\bar{u}_w^2(\bar{\xi},0)}{b} \, E\!\left(\frac{\bar{\xi}-\bar{x}}{b}\right) \, d\bar{\xi} \tag{D26}$$

and the function E is:

$$E\!\left(\frac{\bar{\xi}-\bar{x}}{b}\right) = E(X) = \frac{4}{(1+X^2)^5}\left[\tfrac{\pi}{2}|X|\,(5-10X^2+X^4) - \right.$$

$$\left. (1-10X^2+5X^4)\ln|X| - \tfrac{1}{12}(1+X^2)(25-71X^2-X^4-X^6)\right]$$

Although I is a function of $\bar{u}_w$ and is unknown, it is informative to rewrite Eq. (D25) by solving for $\bar{u}_w$ in terms of I and $\bar{u}_L$, thus:

$$\bar{u}_w = 1 \pm \sqrt{I - (2u_{Lw}-1)} = 1 \pm \sqrt{I - L} \quad , \tag{D27}$$

85

where

$$L = 2\overline{u}_{Lw} - 1$$

a known function since $\overline{u}_{Lw}$ is known once the wall shape is specified. It should be noted from Eq. (D27) that the discriminant must always be positive in order to obtain real values for $\overline{u}_w$, thus $I \geq L$. Furthermore, the choice of the plus or minus sign determines whether the local velocities are subsonic or supersonic. A change in sign at a point where the radical is zero corresponds to a smooth transition through the sonic speed. A change in sign at a point where the radical is not zero corresponds to a discontinuous jump in velocity, namely, a normal shock from supersonic to subsonic flow when progressing in the flow direction. A discontinuity in the reverse direction is inadmissable since it corresponds to an expansion shock, an impossible phenomenon which violates the second law of thermodynamics.

3. COMPUTATIONAL TECHNIQUE

In this section, a brief description of the computational technique used to solve Eq. (D25) will be presented. Sprieter and Alksne [Ref. 10] describes in great detail how a judicious selection of the initial velocity distribution, depending upon the surface shape and flow configuration (i.e. entirely subsonic flow or mixed flow with possible shocks), is essential in providing a rapid convergence to the solution. It

will be assumed for the following discussion, therefore, that a judiciously selected velocity distribution is known. The method of solution is as follows:

a.   From the known surface shape in normalized coordinates $\bar{Z}$, calculate its first two derivatives with respect to the normalized flow coordinate $\bar{x}$; that is, $d\bar{Z}/d\bar{x}$ and $d^2\bar{Z}/d\bar{x}^2$. Since the normalization depends upon the freestream Mach number, which is unknown, the value of $\bar{\tau}$, Eq. (D18), will be a parameter in the iteration technique.

b.   Calculate the linear wall velocity $\bar{u}_{Lw}(\bar{x},0)$ from Eq. (D19). As $\bar{\tau}$ does not depend on $\bar{\xi}$, it can be taken outside of the integral of Eq. (D19) giving an expression directly proportional to the parameter $\bar{\tau}$.

$$\bar{u}_{Lw}(\bar{x},0) = \bar{\tau}\, W_{Lw}(\bar{x},0) \tag{D28}$$

where $W_{Lw}(\bar{x},0)$ is a function of only the position $\bar{x}$ and is fixed once the surface shape is specified. The quantity L follows immediately from Eq. (D27).

c.   Assume an initial value of $\bar{\tau}$ consistent with the velocity distribution and calculate $b(\bar{x})$ from Eq. (D24).

d.   Since $b(\bar{x})$ is now known and an initial wall velocity $\bar{u}_w(\bar{x},0)$ has been selected, Eq. (D26) can be integrated numerically to get I.

e.   The I function calculated for the initial value of $\bar{\tau}$ is graphed. $\bar{\tau}$ is then varied in the L function until the two curves are tangent at, at least, one point (i.e.

87

I-L = 0). As was stated earlier, I $\geq$ L at all points $\bar{x}$ along the surface for the velocity to be real.

f. Using the L function that satisfies the tangency requirement, a new approximation to the solution is obtained from Eq. (D27), where the sign chosen for the radical is important.

g. The iteration procedure continues with the new $\bar{u}_w(\bar{x},0)$ and $\bar{\tau}$ until both quantities converge to a solution.

h. Once a solution is obtained, the freestream Mach number for a given flow condition is calculated from Eq. (D18) and the local Mach number distribution from Eq. (D10).

APPENDIX E

HODOGRAPH TECHNIQUES FOR TRANSONIC FLOW

The hodograph plane represents a coordinate transformation in which the velocity components are the independent variables. Spatial coordinates x and y are replaced by velocity components $\tilde{u}$ and $\tilde{v}$; that is, the physical coordinates are represented by $x(\tilde{u},\tilde{v})$ and $y(\tilde{u},\tilde{v})$ [Ref. 26]. This coordinate transformation is convenient because it enables the simple presentation of data or solutions and, more importantly, it linearizes the two-dimensional planar transonic flow equation that is nonlinear in the physical plane. This equation is known as the Tricomi or Tricomi-Euler Equation. Boundary conditions are difficult to satisfy [Ref. 15].

The small perturbation transonic equation without heat addition can be written as:

$$(1-M_\infty^2)\frac{\partial \tilde{u}'}{\partial x'} + \frac{\partial \tilde{v}'}{\partial y'} = M_\infty^2(\gamma+1)u'\frac{\partial \tilde{u}'}{\partial x'} \tag{E1}$$

where for irrotational flow

$$\frac{\partial \tilde{u}'}{\partial y'} - \frac{\partial \tilde{v}'}{\partial x'} = 0 \tag{E2}$$

Using the hodograph transformation, Eqs. (E1) and (E2) become:

$$(1-M_\infty^2)\frac{\partial y'}{\partial \tilde{v}'} + \frac{\partial x'}{\partial \tilde{u}'} = M_\infty^2(\gamma+1)u'\,\frac{\partial y'}{\partial \tilde{v}'} \qquad \text{(E3)}$$

and

$$\frac{\partial x'}{\partial \tilde{v}'} - \frac{\partial y'}{\partial \tilde{u}'} = 0 \qquad \text{(E4)}$$

Eqs. (E3) and (E4) are the linear transonic hodograph equations.

As is mentioned in the introduction, the linearized small perturbation equations for supersonic flow are hyperbolic and those for subsonic flow are elliptic. The transonic hodograph equations change from elliptic to hyperbolic when the coefficient of $\partial y'/\partial v'$ changes sign:

$$(1-M_\infty^2) - M_\infty^2(\gamma+1)u' = 0 \qquad \text{(E5)}$$

The critical velocity, where the change of sign occurs, can be directly solved from Eq. (E5).

$$u'* = \frac{(1-M_\infty^2)}{(\gamma+1)M_\infty^2} \qquad \text{(E6)}$$

Therefore, for $u' < u'*$, Eq. (E3) is elliptic, and when $u' > u'*$, it is hyperbolic. The features of transonic flow are captured by the transonic hodograph equations. Since the flow occuring in the external region and on the bounding streamtube is considered to be isentropic two-dimensional

90

and planar, the hodograph method gives a conceptual idea of what the resulting flow configuration should be over an infinite wedge of prescribed shape.

Guderley and Yoshihara [Ref. 15] use the flow angle θ and η, defined in Eq. (E7), as the independent variables.

$$\eta = (\gamma+1)^{1/3}((w-w^*)/w^*) \tag{E7}$$

where $w = \sqrt{u^2 + v^2}$. With this selection of independent variables, the streamfunction in the hodograph plane is:

$$\psi_{\eta\eta} - \eta\,\psi_{\theta\theta} = 0 \tag{E8}$$

and the velocity potential function is:

$$\phi_{\eta\eta} - \eta\,\phi_{\theta\theta} = 0 \tag{E9}$$

The formulation is for a flow with constant stagnation temperature and, hence, can be applied to the solution for the bounding streamtube. For flow over a wedge, Guderley and Yoshihara found a steady solution for M_∞ precisely unity.

Fig. 1Ea shows the flow over the bounding streamtube in the physical plane. Points A, B, C, D, and E are shown mapped in the hodograph plane, Fig. 1Eb. A limiting Mach line is shown in the physical plane. Any characteristic in the region bounded by the sonic line and the limiting Mach
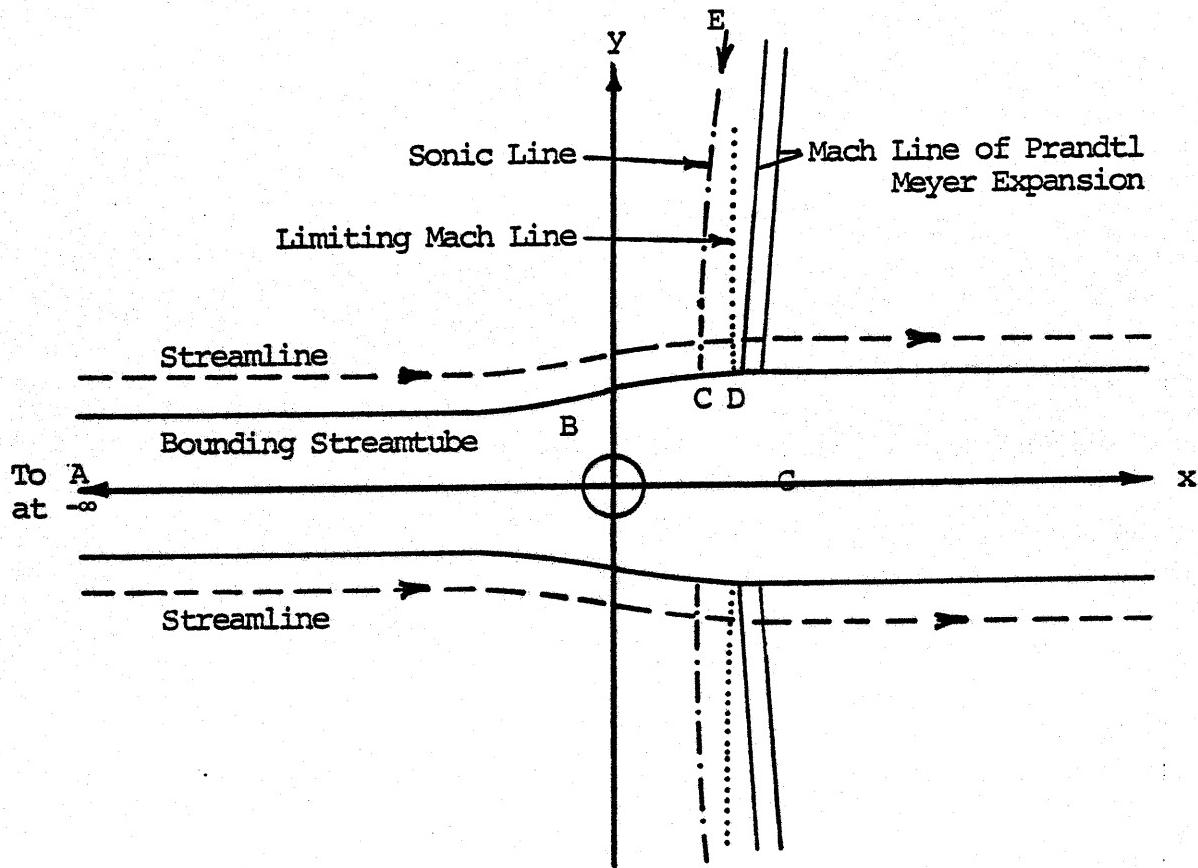
(a) Flow in Physical Plane (Not to scale)
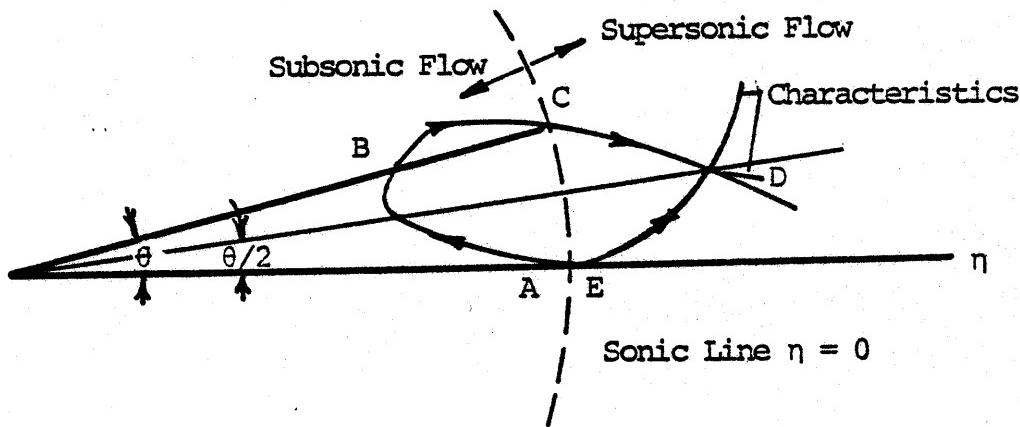
(b) Flow in the Hodograph Plane

FIGURE 1E. Sonic Flow over Bounding Streamtubes
(Physical and Hodograph Plane
Representations)

line can interact with the sonic line. Any characteristic downstream of the limiting Mach line does not interact with the sonic line, and, hence, the flow is not affected by the subsonic flow upstream of the sonic line.

APPENDIX F

DERIVATION OF THE SLUING RATES NECESSARY TO PRECLUDE SIGNIFICANT PHASE DISTORTIONS IN A LASER BEAM AT MACH 1.0

When the phase difference between two points in a laser beam is greater than a quarter of a wavelength, the deviation of the beam from its original direction is sufficient to cause considerable distortion. The range of laser sluing rates necessary to prevent such phase distortions and, hence, to preclude defocusing of the beam at Mach 1.0 is derived.

Consider a laser beam that is slued as shown in Fig. 1. The Mach number of the air relative to the beam varies along the beam as:

$$M = \frac{U}{a} = \frac{\Omega r}{a} \ . \tag{F1}$$

All Mach number regimes occur along the beam. If L represents the radial distance between two stations on the beam where the Mach numbers are M_1 and M_2, it can be determined from Eq. (F1) that L is equal to:

$$L = \frac{(M_2 - M_1) a}{\Omega} \ . \tag{F2}$$

The number of waves (N) of laser radiation in the region of length L is given by:

94

$$N = \frac{L}{\lambda} = \frac{n\nu L}{c} , \qquad \text{(F3)}$$

where λ is the wavelength of the laser beam and is equal to $n\nu/c$. ν (radians $\sec^{-1}$) is the laser frequency equal to approximately 2×10^{13} Hertz for a CO_2 laser, and c (m $\sec^{-1}$) is the speed of light. Therefore, the change in the number of waves in the beam length L, due to a change in the index of refraction, is obtained by differentiating Eq. (F3).

$$dN = \frac{\nu L dn}{c} \qquad \text{(F4)}$$

The change in the refractive index is related to the density perturbations in the beam, a known quantity, through the Gladstone-Dale Law [Ref. 37], a simplified version of the Lorentz-Lorenz Law for gases with $n \cong 1$, Eq. (F5):

$$n = 1 + k\rho , \qquad \text{(F5)}$$

where k is the Gladstone-Dale constant which is approximately equal to 2.25×10^{-4} m^3/kgm for air with wavelengths beyond the near infrared ($\lambda > 1\mu$). Differentiating Eq. (F5) and substituting it and Eq. (F2) into Eq. (F4), the desired expression for the change in the number of waves is obtained as:

$$DN = \left(\frac{k(M_2 - M_1)a\nu\rho_\infty}{\Omega c}\right)\frac{d\rho}{\rho_\infty} . \qquad \text{(F6)}$$

It is of interest to determine the range of sluing rates for which the change in the number of waves is less than a quarter of a wavelength at Mach 1.0 from Eq. (F7):

$$\Omega \geq \frac{4k(M_2-M_1)a\nu\rho_\infty}{c} (\tilde{\rho}'_{Max} - \tilde{\rho}'_{Min}) \ . \qquad \text{(F7)}$$

where $\tilde{\rho}'_{Max}$ is the maximum positive density perturbation and $\tilde{\rho}'_{Min}$ is the minimum (maximum negative) density perturbation in the beam at Mach 1.0, points A and B in Fig. 11, respectively. As an example, using $M_2 = 1.001$, $M_1 = 0.999$, the flow properties in Table I, and the maximum difference in the density perturbations at Mach 1.0 from Fig. 11 of 1.5×10^{-4}, the sluing rate must be greater than 7.5×10^{-3} radians/sec.

APPENDIX G

SUBSONIC AND SUPERSONIC THERMAL BLOOMING
AND COMPUTER PROGRAM (BLOOM)

Tsien and Beilock [Ref. 38] have obtained solutions for the linearized equations of motion with heat addition for subsonic and supersonic flow. The solutions are for a line heat source q in a uniform, two-dimensional planar flow which can be considered to be a perturbation on an initially one-dimensional flow.

In 1971 and 1972 studies were conducted at NPS by Fuhs [Ref. 39] on the applicatin of external heat to the reduction of drag. These studies required thorough analysis of heat addition in both subsonic and supersonic flows. The analysis of the flow with heat addition found two other applications. One application was external burning assisted projectile. This application was studied by CDR. W. J. H. Smithey [Ref. 40]. The other application was recognized by Fuhs [Ref. 4]; this involves the density inhomogeneity arising from quantum inefficiency. Professors Biblarz and Fuhs [Ref. 5] developed the capability and extended the analysis to predict density inhomogeneity in a large gas dynamic laser; see the paper by Fuhs, Biblarz, Cawthra and Campbell [Ref. 6] for details of the experiment. Subsequent to the application of linearized solutions to flow internal to a laser, it became apparent that the analysis could predict flow properties in thermal blooming. In a series of papers and presentations, Fuhs,

Biblarz, Burden and Carey [Refs. 7, 8 and 41-43] developed
the appropriate analysis for linearized thermal blooming.

1.   SUBSONIC FLOW WITH HEAT ADDITION

The perturbations to the flow [Ref. 38] are given by:

$$\tilde{u}' = \frac{(\gamma-1)q}{2\pi\gamma p_\infty \beta u_\infty} \frac{x}{(x^2 + \beta^2 y^2)} \tag{G1}$$

$$\tilde{v}' = \frac{(\gamma-1)\beta q}{2\pi\gamma p_\infty u_\infty} \frac{y}{(x^2 + \beta^2 y^2)} \tag{G2}$$

$$\tilde{p}' = - \frac{(\gamma-1)M_\infty q}{2\pi a_\infty \beta p_\infty} \frac{x}{(x^2 + \beta^2 y^2)} \tag{G3}$$

$$\tilde{\rho}' = - \frac{(\gamma-1)M_\infty q}{2\pi a_\infty^3 \beta \rho_\infty} \frac{x}{(x^2 + \beta^2 y^2)} - \frac{(\gamma-1)q}{M_\infty a_\infty^3 \rho_\infty} \delta(y) I(x) \tag{G4}$$

where the symbols are defined in the list of symbols and
$\beta = \sqrt{1 - M^2}$ for subsonic Mach numbers. The second term in
Eq. (G4) is the wake of the line heat source q. The
temperature perturbation can be obtained from the equation
of state.

Biblarz and Fuhs [Ref. 6] in applying Eqs. (G1) through
(G4) to laser internal aerodynamics have presented the
integral equations used to solve the unbounded heat release
region problem (i.e. subsonic thermal blooming) and are
listed below for completeness. Since the heat source is
volume distributed, instead of a single infinitesimal rod,
an integral representation was used to account for all
contributions to the flow properties over the volume. The
geometry involved in the calculation is shown in Fig. 1G.

98
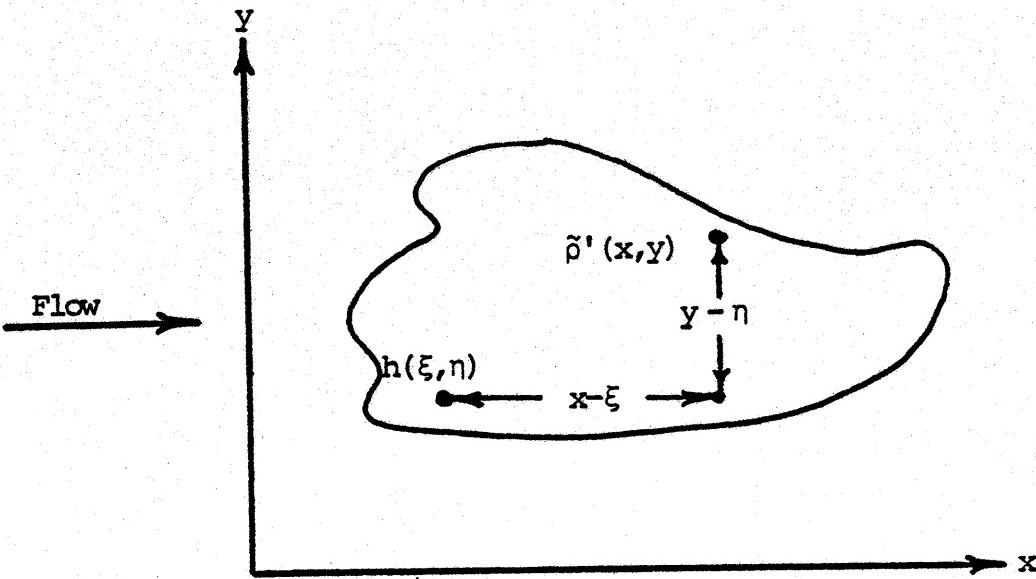
FIGURE 1G.   Geometry of Flow

$$\tilde{u}' = \frac{(\gamma-1)}{2\pi\beta p_\infty u_\infty} \int_\xi \int_\eta \frac{(x-\xi)\ h(\xi,\eta)}{(x-\xi)^2 + \beta^2(y-\eta)^2}\ d\xi d\eta \qquad (G5)$$

$$\tilde{v}' = \frac{(\gamma-1)\beta}{2\pi\gamma p_\infty u_\infty} \int_\xi \int_\eta \frac{(y-\eta)\ h(\xi,\eta)}{(x-\xi)^2 + \beta^2(y-\eta)^2}\ d\xi d\eta \qquad (G6)$$

$$\tilde{p}' = -\frac{(\gamma-1)M_\infty}{2\pi a_\infty p_\infty \beta} \int_\xi \int_\eta \frac{(x-\xi)\ h(\xi,\eta)}{(x-\xi)^2 + \beta^2(y-\eta)^2}\ d\xi d\eta \qquad (G7)$$

$$\tilde{\rho}' = -\frac{(\gamma-1)M_\infty}{2\pi a_\infty^3 \beta\rho_\infty} \int_\xi \int_\eta \frac{(x-\xi)\ h(\xi,\eta)}{(x-\xi)^2 + \beta^2(y-\eta)^2}\ d\xi d\eta$$

$$\qquad -\frac{(\gamma-1)}{a_\infty^2 u_\infty \rho_\infty} \int_\xi \int_\eta h(\xi,\eta)\ \delta(y-n)\ I(x-\xi)\ d\xi d\eta \qquad (G8)$$

99

The heat quantity $h(x,y)$ is related to the laser output intensity through the kinetic lag that may be present. To develop an equation incorporating the lag between laser energy and heating, it is necessary to examine the kinetics of relaxation. An exponential function describes the relaxation with a relaxation time τ [Refs. 44 and 45]. The heat release function is given by:

$$h(x,y) = I_0\alpha \int_{-\infty}^{x} f(x',y) \exp[-\frac{(x-x')}{u_\infty\tau}]\,dx' \qquad \text{(G9)}$$

where $Q = I_0\alpha\, f(x,y)$ is the laser energy per time per volume. The volume can be interpreted as an area times the span of the heat addition zone across the planar flow.

If significant variations of beam intensity in the radial (beam) direction exist, the two-dimensional heat addition function can be approximated from the three-dimensional $h(x,y,r)$ by an average:

$$h(x,y) = \frac{1}{\Delta r} \int_{r_i}^{r_{i+1}} h(x,y,r)\,dr \qquad \text{(G10)}$$

where $\Delta r = r_{i+1} - r_i$. The beam is divided into segments Δr in length and Eqs. (G5) through (G8) are solved for each segment.

If the heat release $h(x,y)$ is constant, the equations can be integrated in closed form. The resulting integrals are:

100

$$\tilde{u}' = \frac{(\gamma-1)I_o\alpha}{2\pi\gamma p_\infty\beta u_\infty} M(x,y;\xi,\eta,\beta) \tag{G11}$$

$$\tilde{v}' = \frac{(\gamma-1)I_o\alpha}{2\pi\gamma p_\infty\beta u_\infty} N(x,y;\xi,\eta,\beta) \tag{G12}$$

$$\tilde{p}' = -\frac{(\gamma-1)M_\infty I_o\alpha}{2\pi a_\infty\beta p_\infty} M(x,y;\xi,\eta,\beta) \tag{G13}$$

$$\tilde{\rho}' = -\frac{(\gamma-1)M_\infty I_o\alpha}{2\pi a_\infty^3\beta \rho_\infty} M(x,y;\xi,\eta,\beta)$$

$$-\frac{(\gamma-1)I_o\alpha}{a_\infty^2 u_\infty\rho_\infty} \int_\xi\int_\eta \delta(y-\eta)\ I(x-\xi)\ d\xi d\eta \tag{G14}$$

where

$$M(x,y;\xi,\eta,\beta) = \left[\left[\frac{(y-\eta)}{2}\ \ln\left[\frac{(x-\xi)^2 + \beta^2(y-\eta)^2}{\beta^2(y-\eta)^2}\right]\right.\right.$$

$$\left.\left.+ \frac{(x-\xi)}{\beta}\ \tan^{-1}\left[\frac{\beta(y-\eta)}{(x-\xi)}\right]\right]_{\eta_1}^{\eta_2}\right]_{\xi_1}^{\xi_2}$$

$$N(x,y;\xi,\eta,\beta) = \left[\left[\frac{(x-\xi)}{2\beta^2}\ \ln\left[\frac{(x-\xi)^2 + \beta^2(y-\eta)^2}{\beta^2}\right]\right.\right.$$

$$\left.\left.- \frac{(x-\xi)}{\beta^2} + \frac{(y-\eta)}{\beta}\ \tan^{-1}\left[\frac{(x-\xi)}{\beta(y-\eta)}\right]\right]_{\eta_1}^{\eta_2}\right]_{\xi_1}^{\xi_2}$$

The first term in Eqs. (G8) and (G14) correspond to the density perturbations in regions outside the wake and the last term represents the contribution of the wake and can be interpreted as the consequence of the heat convected along the streamlines by the flow.

2. SUPERSONIC FLOW WITH HEAT ADDITION

The perturbations to the flow are also formulated by Tsein and Beilock [Ref. 38] as:

$$\tilde{u}' = -\frac{(\gamma-1)q}{2\gamma p_\infty \beta u_\infty} \, \delta(x - \beta y) \tag{G15}$$

$$\tilde{v}' = \frac{(\gamma-1)q}{2\gamma p_\infty u_\infty} \, \delta(x - \beta y) \tag{G16}$$

$$\tilde{p}' = \frac{(\gamma-1)M_\infty q}{2a_\infty \beta p_\infty} \, \delta(x - \beta y) \tag{G17}$$

$$\tilde{\rho}' = -\frac{(\gamma-1)M_\infty q}{2a_\infty^3 \beta \rho_\infty} \, \delta(x - \beta y) - \frac{(\gamma-1)q}{M_\infty a_\infty^3 \rho_\infty} \, \delta(y) \, I(x) \tag{G18}$$

Fuhs [Refs. 4 and 39] has modified these equations into an integral form as:

$$\tilde{u}' = -\frac{(\gamma-1)}{2\gamma p_\infty \beta u_\infty} \int_0^S h(\xi,\eta) \, \sin \mu \, dS \tag{G19}$$

$$\tilde{v}' = \frac{(\gamma-1)}{2\gamma p_\infty u_\infty} \int_0^S h(\xi,\eta) \, \sin \mu \, dS \tag{G20}$$

$$\tilde{p}' = \frac{(\gamma-1)M_\infty}{2a_\infty \beta p_\infty} \int_0^S h(\xi,\eta) \, \sin \mu \, dS \tag{G21}$$

$$\tilde{\rho}' = \frac{(\gamma-1)M_\infty}{2a_\infty^3 \beta \rho_\infty} \int_0^S h(\xi,\eta) \, \sin \mu \, dS$$

$$- \frac{(\gamma-1)}{M_\infty a_\infty^3 \rho_\infty} \int_\xi \int_\eta h(\xi,\eta) \, \delta(y-\eta) \, I(x-\xi) \, d\xi d\eta \tag{G22}$$

where the symbology is the same as that used in the subsonic equations except that $\beta = \sqrt{M^2 - 1}$ for supersonic Mach numbers.

3. COMPUTER PROGRAM

The FORTRAN computer program BLOOM, included at the end of this appendix, was written to compute and/or plot the flow perturbations ($\tilde{u}'$, $\tilde{v}'$, $\tilde{p}'$ and $\tilde{\rho}'$) in the subsonic and supersonic flow with heat addition. Using a modified version of the computer program DIDER [Ref. 5] as a subroutine, the subsonic perturbation equations, Eqs. (G5) through (G9), and the supersonic perturbation equations, Eqs. (G19) through (G22), are numerically integrated to obtain the linear thermal blooming solutions. The program calculates the two-dimensional field at any cross section of the laser beam where the energy release distribution is known. Finite kinetics are incorporated as described by Eq. (G9).

The program (BLOOM) is versatile in that it can calculate the flow quantities for several subsonic and/or supersonic freestream Mach numbers, heat release distributions, relaxation rates, and freestream flow properties in a single computer run. Since the length of time for each individual case depends primarily on the size of the flow region and on the mesh that is superimposed upon it, time requirements must be determined on an individual basis. For the results presented in Figs. 4 through 7 and Figs. 12 and 13 from the program BLOOM, the two-dimensional region of interest was 60 cm. square centered at the origin of the Gaussian heat release distribution and was descretized into a mesh of cells 1 cm. square for subsonic flow ($M_\infty = 0.999$) and into rectangular cells whose size is determined by the Mach angle for supersonic flow

(M_∞ = 1.001). Supersonically, the ratio of cell height Δy to cell length Δx is equal to tan μ. The subsonic results take approximately 25 minutes and 140 K of memory (without plotting subroutine CONTUR) while the supersonic results take approximately 3 minutes and 285 K of memory (without plotting routine CONTUR) to compile and execute using an IBM 360 computer.

The program can also calculate constant heat release distributions for single and multi-pass laser beam configurations with or without wall reflections and kinetics. In its present form, the program can not calculate supercritical (mixed) flows across the beam.

A main feature of the supersonic portion of the program is that it sets up the characteristic lines belonging to each individual cell (i.e. their diagonals) and adds up the contributions for each flow property from the characteristics and, in the case of the density perturbation, from the wake at each cell. The calculations along the characteristics are facilitated by the choice of cell shape and size as described above.

```
C       PROGRAM BLOOM

        COMMON/ONE/IM,JM,BTA,ZMA,XDEL,YDEL,ZIO,SGM
        COMMON/TWO/ACH,AWAK,XLAG,ZH,ZL
        COMMON/THREE/GMA,TA,PA,U,ARHO,TAU
C
C       SPECIFY IN,JN CONSISTENT WITH MATRIX DIMENSIONS.
C
C          A.  SUPERSONIC FLOW (MACH NUMBER > 0)
C              1.  JN SHOULD BE EQUAL TO OR GREATER THAN THE NUMBER OF
C                  ROWS IN THE Y-DIRECTION (JM).
C              2.  FROM THE NUMBER OF CELLS IN THE Y-DIRECTION (JM-1),
C                  CALCULATE THE CELL WIDTH (YDEL) FROM THE KNOWN TOTAL
C                  Y-DIMENSION (ZH); THAT IS: YDEL = ZH/(JM-1).
C              3.  DIVIDE YDEL BY THE TANGENT OF THE MACH ANGLE TO OBTAIN
C                  THE CELL WIDTH IN THE X-DIRECTION (XDEL).
C              4.  DIVIDE XDEL INTO THE TOTAL X-DIMENSION (ZL) TO DETER-
C                  MINE THE NUMBER OF CELLS IN THE X-DIRECTION (IM-1).
C              5.  DIMENSION (IN) SHOULD BE AT LEAST IM+1.
C
C          B.  SUBSONIC FLOW (MACH NUMBER < 0)
C              1.  JN IS EQUAL TO THE NUMBER OF ROWS IN THE Y-DIRECTION
C                  JM.
C              2.  IN EQUALS JN.

        IN=65
        JN=65
C
C       SUBSONIC WITH CONSTANT HEAT INPUT - SET IFLAG=1
C
        IFLAG=0
C
C       DENSITY PERTURBATIONS:            TABULATED ONLY         - SET JFLAG=1
C                                         GRAPHED ONLY           - SET JFLAG=2
C                                         TABULATED AND GRAPHED  - SET JFLAG=3
C
        JFLAG=3
C
C       VELOCITY AND PRESSURE PERTURBATIONS: TABULATED ONLY      - SET KFLAG=1
C                                            GRAPHED ONLY         - SET KFLAG=2
C                                            TABULATED AND GRAPHED - SET KFLAG=3
C
        KFLAG=3
C
C       PHIXX AND PHIYY:                  TABULATED ONLY         - SET LFLAG=1
C                                         GRAPHED ONLY           - SET LFLAG=2
C                                         TABULATED AND GRAPHED  - SET LFLAG=3
```

```
C
         LFLAG=0

C        INPUT PHYSICAL CONSTANTS
C        ALL UNITS MUST BE CONSISTENT TO INSURE DIMENSIONLESS OUTPUTS.
C        THE UNITS USED FOR THESE PARTICULAR RUNS WERE AS FOLLOWS:
C             GMA - DIMENSIONLESS
C             TA (AMBIENT TEMPERATURE) - DEGREES KELVIN
C             PA (AMBIENT PRESSURE) - KGM / MTR-SEC SQR'D
C             ALPHA (ABSORPTION) - 1 / CM

  100 NAMELIST/FIRST/GMA,TA,PA,ALPHA
      IF (IFLAG.EQ.1) ALPHA=1.0
      READ(5,FIRST)
      WRITE (6,900)
      WRITE(6,FIRST)
      RHOA=PA/(287.21*TA)
      VELA=SQRT(GMA*TA*287.21)

C        INPUT - ZMA, JM, ZL, ZH, TAU, ZIO, SGM
C        ALL UNITS MUST BE CONSISTENT TO INSURE DIMENSIONLESS OUTPUTS.
C        THE UNITS USED FOR THESE PARTICULAR RUNS WERE AS FOLLOWS:
C             ZMA (MACH NUMBER) - DIMENSIONLESS
C             JM (NUMBER OF ROWS IN THE Y-DIRECTION) - DIMENSIONLESS
C             ZL (TOTAL LENGTH OF INTEREST IN X-DIRECTION) - CM
C             ZH (TOTAL LENGTH OF INTEREST IN Y-DIRECTION) - CM
C             TAU (KINETICS) - SECONDS
C             ZIO (INTENSITY) - WATTS / MTR SQR'D
C             SGM (STANDARD DEVIATION OF GAUSSIAN BEAM) - CM

      READ (5,910,END=999) ZMA,JM,ZL,ZH,TAU,ZIO,SGM
      IF (IFLAG.EQ.1) ZIO=1.0
      YDEL=ZH/(JM-1)
      IF(ZMA.LT.1.0) XDEL=YDEL
      IF (ZMA.LT.1.0) GO TO 200
      ZMU=ARSIN(1.0/ZMA)
      XDEL=YDEL/TAN(ZMU)
  200 IM=ZL/XDEL + 1
      IF(ZMA.GT.1.0) BTA=SQRT(ZMA**2-1.)
      IF(ZMA.LT.1.0) BTA=SQRT(1.-ZMA**2)
      U=ZMA*VELA
      ACH=(GMA-1.0)*YDEL*ALPHA/2.0
      ARHO=ZMA/(VELA**3*BTA*RHOA)*XDEL*ALPHA
      AWAK=(GMA-1.)/(VELA**2*U*RHOA)*XDEL*ALPHA
```

```
      IF (TAU.LT.1.0E-25) GO TO 210
      XPON=XDEL/(U*TAU*100)
      IF (XPON.GT.35.0) GO TO 210
      XLAG=1/EXP(XPON)
      GO TO 220
  210 XLAG=0.0
  220 CONTINUE
      IMX=IM
C
C     IM WILL BE INCREMENTED BY ONE TO INITIALIZE CALCULATIONS IN DIDER
C
      IM=IM+1
      IF(JM.GT.JN.OR.IM.GT.IN) GO TO 240
      GO TO 250
  240 WRITE (6,920)
  250 CONTINUE
      CALL DIDER (IN,JN,IFLAG)
      CALL WRKR (IN,IMX,JFLAG,KFLAG,LFLAG)
  900 FORMAT('1',T50,'INPUT PARAMETERS',////)
  910 FORMAT (F8.6,I3,2F10.7,2E10.3,F7.5)
  920 FORMAT('1','ALLOWED DIMENSIONS FOR THE ARRAY LESS THAN REQUIRED')
      GO TO 100
  999 STOP
      END
```

107

```
C     SUBROUTINE DIDER

      SUBROUTINE DIDER (IN,JN,IFLAG)
      COMMON/ONE/IM,JM,BTA,ZMA,XDEL,YDEL,ZIO,SGM
      COMMON/TWO/ACH,AWAK,XLAG,ZH,ZL
C
C     DIMENSION ZI(IN,JN), IN AND JN CONSISTENT WITH MATRIX DIMENSIONS,
C     AND XI1(I), XI2(I), ETA1(I), AND ETA2(I), I EQUAL TO THE NUMBER OF
C     CONSTANT HEAT RELEASE DISTRIBUTIONS DESIRED.
C
      DIMENSION ZI(65,65),XI1(8),XI2(8),ETA1(8),ETA2(8),ZIR(8)
C
C     DIMENSION CHR(IN,JN), CHRX(IN,JN), CHRY(IN,JN), WAK(IN,JN), ZIC(IN,JN) -
C     IN AND JN THE SAME AS ZI(IN,JN)
C
      COMMON/FOUR/CHR(65,65),CHRX(65,65),CHRY(65,65),WAK(65,65),ZIC(65,6
     15)
      C1(A,B)=(ACH*XDEL/3.14159)*(A/(A**2+B**2))
      F(A,B,C)=((B/2.0)*ALOG(A**2+B**2)+A*SIGN(1.0,A)*ARSIN(B/SQRT(A**2+
```

```
     1B**2)))*(GMA-1.0)*C/(6.28318*BTA)
      IF (IFLAG.EQ.1) GO TO 15

C
C     FILL IN ENERGY DENSITY (GAUSSIAN HEAT RELEASE DISTRIBUTION)
C
      DO 5 I=1,IM
      DO 5 J=1,JM
      ZI(I,J)=0.0
    5 CONTINUE
      XZIO=1-XLAG
      X1=ZL/2.0
      Y1=ZH/2.0
      DO  10  I=2,IM
      DO  10  J=1,JM
      YY=(J-1)*YDEL
      XX=(I-2)*XDEL
      S=((XX-X1)**2+(YY-Y1)**2)/(2.0*SGM**2)
      IF(S.GT.35.0) GO TO 10
      ZI(I,J)=ZIO*XZIO/EXP(S)
   10 CONTINUE
      GO TO 45

C
C     FILL IN ENERGY DENSITY (CONSTANT HEAT RELEASE DISTRIBUTION)
C
C     INPUT ZIR(I) - WATTS / MTR SQR'D-CM FOR EACH CONSTANT HEAT RELEASE
C     DISTRIBUTION (I).   ALL UNITS MUST BE CONSISTENT TO INSURE DIMEN-
C     SIONLESS OUTPUTS.
C
   15 READ (5,400) (ZIR(I),I=1,8)
      DO 20 I=3,23
      DO 20 J=2,17
      ZI(I,J)=ZIR(1)
   20 CONTINUE
      DO 22 I=11,15
      DO 22 J=9,10
      ZI(I,J)=ZIR(2)
   22 CONTINUE
      DO 24 I=26,46
      DO 24 J=2,17
      ZI(I,J)=ZIR(3)
   24 CONTINUE
      DO 26 I=34,38
      DO 26 J=9,10
      ZI(I,J)=ZIR(4)
   26 CONTINUE
      DO 28 I=3,23
```

```
      DO 28 J=20,35
      ZI(I,J)=ZIR(5)
   28 CONTINUE
      DO 30 I=11,15
      DO 30 J=27,28
      ZI(I,J)=ZIR(6)
   30 CONTINUE
      DO 32 I=26,46
      DO 32 J=20,35
      ZI(I,J)=ZIR(7)
   32 CONTINUE
      DO 34 I=34,38
      DO 34 J=27,28
      ZI(I,J)=ZIR(8)
   34 CONTINUE
C
C     ZEROIZE COMPUTATIONAL MATRICES AND CALCULATE HEAT RELEASE FROM
C     KINETICS.
C
   45 DO 50 J=1,JM
      ZIC(1,J)=0.0
      WAK(1,J)=0.0
      DO 50 I=2,IM
      ZIC(I,J)=0.0
      WAK(I,J)=0.0
      CHR(I,J)=0.0
      CHRX(I,J)=0.0
      CHRY(I,J)=0.0
      ZIC(I,J)=ZIC(I-1,J)*XLAG + ZI(I,J)
      WAK(I,J)=WAK(I-1,J) + (ZIC(I,J)+ZIC(I-1,J))/2
   50 CONTINUE
C
C     COMPUTE WAKE TERM OF DENSITY PERTURBATION.
C
      DO 60 J=1,JM
      DO 60 I=2,IM
   60 WAK(I,J)=AWAK*WAK(I,J)
      IF(IFLAG.EQ.1) GO TO 200
      IF(ZMA.LT.1.0) GO TO 110
C
C     CALCULATE CONTRIBUTIONS FROM CHARACTERISTICS FOR SUPERSONIC FLOW.
C
      DO 100 I=2,IM
      DO 100 J=1,JM
      JL=J
      JR=J
      L=I
      DO 80 N=2,I
```

```
      L=L-1
      JR=JR-1
      IF(JR.LT.1) GO TO 70
      CHRX(I,J)=CHRX(I,J)+ACH*(ZIC(L,JR)+ZIC(L+1,JR+1))/2.0
   70 JL=JL+1
      IF (JL.GT.JM) GO TO 80
      CHRY(I,J)=CHRY(I,J)+ACH*(ZIC(L,JL)+ZIC(L+1,JL-1))/2.0
   80 CONTINUE
      CHR(I,J)=CHRX(I,J)+CHRY(I,J)
      CHRY(I,J)=CHRY(I,J)-CHRX(I,J)
      CHRX(I,J)=-CHR(I,J)
  100 CONTINUE
      RETURN
C
C     CALCULATE CONTRIBUTIONS FROM SOURCE TERMS FOR SUBSONIC FLOW.
C
  110 DO 150 I=2,IM
      DO 150 J=1,JM
      II1=MAXO(2,I-15)
      II2=MINO(IM,I+15)
      DO 150 II=II1,II2
      DO 150 JJ=1,JM
      IF((II.EQ.I).AND.(JJ.EQ.J)) GO TO 150
      UX=(I-II)*XDEL
      UY=(JJ-J)*YDEL*BTA
      CHR(I,J)=CHR(I,J)-C1(UX,UY)*ZIC(II,JJ)
      CHRX(I,J)=-CHR(I,J)
      CHRY(I,J)=CHRY(I,J)+C1(UY,UX)*ZIC(II,JJ)
  150 CONTINUE
      RETURN
  200 CONTINUE


C     CALCULATE CONTRIBUTIONS FROM SOURCE AND WAKE TERMS FOR SUBSONIC
C     FLOW WITH CONSTANT HEAT RELEASE DISTRIBUTION.
C
C     INPUT THE ORDINATES OF EACH CONSTANT HEAT RELEASE DISTRIBUTION:
C          XI1(I) AND XI2(I) IN THE X-DIRECTION - CM.
C          ETA1(I) AND ETA2(I) IN THE Y-DIRECTION - CM.
C
C     NOTE* A.  IN THE X (FLOW) DIRECTION:
C              1.   MINIMUM VALUE OF XI1(I) IS 0.0.
C              2.   MAXIMUM VALUE OF XI2(I) IS ZL.
C           B.  IN THE Y-DIRECTION (HEAT DISTRIBUTION ABOVE CENTERLINE):
C              1.   MINIMUM VALUE OF ETA1(I) IS 0.0.
C              2.   MAXIMUM VALUE OF ETA2(I) IS ZH/2.
C           C.  IN THE Y-DIRECTION (HEAT DISTRIBUTION BELOW CENTERLINE):
C              1.   MINIMUM VALUE OF ETA1(I) IS -ZH/2.
```

```
C       2.   MAXIMUM VALUE OF ETA2(I) IS 0.0.
C    D.   IN THE Y-DIRECTION (HEAT DISTRIBUTION ACROSS CENTERLINE)
C       1.   MINIMUM VALUE OF ETA1(I) IS -ZH/2.
C       2.   MAXIMUM VALUE OF ETA2(I) IS ZH/2.
C
      READ (5,410) (XI1(I),XI2(I),ETA1(I),ETA2(I),I=1,8)
      DO 300 K=1,8
      DO 250 I=2,IM
      DO 250 J=1,JM
      UX=XDEL*(I-2)
      UY=(ZH/2.0-YDEL*(J-1))
      DO 250 IMF=1,5
      IMG=IMF-3
      CHR(I,J)=CHR(I,J)+F((UX-XI2(K)),(UY-(-1)**IMG*ETA1(K)+IMG*ZH)*BTA,
     1ZIR(K))-F((UX-XI2(K)),(UY-(-1)**IMG*ETA2(K)+IMG*ZH)*BTA,ZIR(K))-F
     2((UX-XI1(K)),(UY-(-1)**IMG*ETA1(K)+IMG*ZH)*BTA,ZIR(K))+F((UX-XI1(K
     3)),(UY-(-1)**IMG*ETA2(K)+IMG*ZH)*BTA,ZIR(K))
      CHRY(I,J)=CHRY(I,J)+F((UY-(-1)**IMG*ETA2(K)+IMG*ZH)*BTA,(UX-XI2(K)
     1),ZIR(K))-F((UY-(-1)**IMG*ETA1(K)+IMG*ZH)*BTA,(UX-XI2(K)),ZIR(K))-
     2F((UY-(-1)**IMG*ETA2(K)+IMG*ZH)*BTA,(UX-XI1(K)),ZIR(K))+F((UY-(-1)
     3**IMG*ETA1(K)+IMG*ZH)*BTA,(UX-XI1(K)),ZIR(K))
  250 CONTINUE
  300 CONTINUE
      DO 350 I=2,IM
      DO 350 J=1,JM
      CHRX(I,J)=-CHR(I,J)
  350 CONTINUE
  400 FORMAT (4E12.2)
  410 FORMAT (4F10.6)
      RETURN
      END



C    SUBROUTINE WRKR

      SUBROUTINE WRKR (IN,IMX,JFLAG,KFLAG,LFLAG)
      COMMON/ONE/IM,JM,BTA,ZMA,XDEL,YDEL,ZIO,SGM
      COMMON/THREE/GMA,TA,PA,U,ARHO,TAU
C
C     DIMENSION CHR(IN,JN), CHRX(IN,JN), CHRY(IN,JN), WAK(IN,JN), ZIC(IN,JN) -
C     IN AND JN THE SAME AS ZI(IN,JN) IN THE MAIN PROGRAM
C
      COMMON/FOUR/CHR(65,65),CHRX(65,65),CHRY(65,65),WAK(65,65),ZIC(65,6
     15)
C
```

```
C       SEE LISTING OF SUBROUTINE CONTUR FOR INFORMATION ON TITLE(12), LTG(3),
C       CL(8) AND OTHER PERTINENT PARAMETERS.
C
        IF (IFLAG.EQ.1) GO TO 10
        REAL*8 TITLE(12),TLINE1(6,6)/'                  ',' I','SODENSIT','Y C
       1ONTOU','RS        ',' ',' ','        ',' IS','OPRESSUR','E C
       2ONTOU','RS        ',' ',' ',' ','U PERTUR','BATION V','ELO
       3CITY ','CONTOURS',' ',' ',' ',' ','V PERTUR','BATION V','ELO
       4CITY ','CONTOURS',' ',' ',' ',' ','        ','        ','  P
       5HIXX ',' ',' ',' ',' ',' ','        ','        ','PHIY
       6YY   ',' )        ',' ',' ','/,TLINE2(5)/'    HEAT','  INPUT -','  GAU
       7SSIA','N         ',' ','    MACH '/
        GO TO 20
 10     REAL*8 TITLE(12),TLINE1(6,6)/'                  ',' I','SODENSIT','Y C
       1ONTOU','RS        ',' ',' ','        ',' IS','OPRESSUR','E C
       2ONTOU','RS        ',' ',' ',' ','U PERTUR','BATION V','ELO
       3CITY ','CONTOURS',' ',' ',' ',' ','V PERTUR','BATION V','ELO
       4CITY ','CONTOURS',' ',' ',' ',' ','        ','        ','  P
       5HIXX ',' ',' ',' ',' ',' ','        ','        ','PHIY
       6YY   ',' )        ',' ',' ','/,TLINE2(5)/'    HEAT','  INPUT -','  CON
       7STAN','T         ',' ','    MACH '/
 20     LOGICAL*1 LTG(3)/.TRUE.,.TRUE.,.TRUE./
        REAL*4 CL(16)/-60.0,-55.0,-50.0,-45.0,-40.0,-35.0,-30.0,-25.0,-20.
       10,-15.0,-10.0,-5.0,0.0,5.0,10.0,15.0/
        JL=JM/2
        JL1=(JM+1)/2
        APRES=1.0E+06*ZMA**2/BTA/U/PA
        AYVEL=1.0E+06/GMA/U/PA
        AXVEL=AYVEL/BTA
        DL=YDEL/XDEL
        CP=GMA*159.56/(GMA-1)
        TO=TA*(1+(GMA-1)*ZMA**2/2.)
        IMXX=IM-2
        JMX=JM-1
        DO 50 I=1,5
        J=I+6
 50     TITLE(J)=TLINE2(I)
        CALL REREAD
        READ (5,950) AMA
        READ (99,960) TITLE(12)
C
C       ZIC GIVES DENSITY PERTURBATIONS
C
        DO 100 I=2,IM
        DO 100 J=1,JM
 100    ZIC(I-1,J)=1.0E+06*(ARHO*CHR(I,J)-WAK(I,J))
        IF (IFLAG.EQ.1) JL1=JM
        IF (JFLAG.EQ.0) GO TO 160
```

```
      IF (JFLAG.EQ.2) GO TO 140
      IF(ZMA.LT.1.0) GO TO 110
      WRITE (6,900) ZMA
      GO TO 120
      IF (IFLAG.EQ.1) GO TO 115
110   WRITE (6,901) ZMA
      GO TO 120
115   WRITE (6,902) ZMA
120   WRITE (6,910) TAU
      WRITE (6,920) IMX,JM
      WRITE (6,930)
      DO 130 I=1,IMX
130   WRITE (6,940) (ZIC(I,J),J=1,JL1)
      IF (JFLAG.EQ.1) GO TO 160
140   DO 150 I=1,6
150   TITLE(I)=TLINE1(I,1)
      CALL CONTUR (ZIC,IMX,JM,IN,CL,-8,TITLE,6,6,LTG)
C
C     ZIC GIVES PRESSURE PERTURBATIONS
C     CHR GIVES X-VELOCITY PERTURBATION
C     WAK GIVES Y-VELOCITY PERTURBATION
C
160   DO 200 I=2,IM
      DO 200 J=1,JM
      ZIC(I-1,J)=APRES*CHR(I,J)
      CHR(I-1,J)=CHRX(I,J)*AXVEL
      WAK(I-1,J)=CHRY(I,J)*AYVEL
200   CONTINUE
      IF (KFLAG.EQ.3) GO TO 260
      IF (KFLAG.EQ.2) GO TO 245
      IF (JFLAG.EQ.1.OR.JFLAG.EQ.3) GO TO 222
      IF (ZMA.LT.1.0) GO TO 210
      WRITE (6,900) ZMA
      GO TO 220
      IF (IFLAG.EQ.1) GO TO 215
210   WRITE (6,901) ZMA
      GO TO 220
215   WRITE (6,902) ZMA
220   WRITE (6,910) TAU
      WRITE (6,920) IMX,JM
      WRITE (6,931)
      GO TO 224
222   WRITE (6,932)
224   DO 230 I=1,IMX
230   WRITE (6,940) (ZIC(I,J),J=1,JL1)
      WRITE (6,933)
      DO 235 I=1,IMX
235   WRITE (6,940) (CHR(I,J),J=1,JL1)
```

```
      WRITE (6,934)
      DO 240 I=1,IMX
240   WRITE (6,940) (WAK(I,J),J=1,JL1)
      IF (KFLAG.EQ.1) GO TO 260
245   DO 250 I=1,6
250   TITLE(I)=TLINE1(I,2)
      CALL CONTUR (ZIC,IMX,JM,IN,CL,-8,TITLE,6,6,LTG)
      DO 252 I=1,6
252   TITLE(I)=TLINE1(I,3)
      CALL CONTUR (CHR,IMX,JM,IN,CL,-8,TITLE,6,6,LTG)
      DO 254 I=1,6
254   TITLE(I)=TLINE1(I,4)
      CALL CONTUR (WAK,IMX,JM,IN,CL,-8,TITLE,6,6,LTG)
260   IF (LFLAG.EQ.0) RETURN
      DO 300 J=1,JM
      CHRX(1,J)= CHR(2,J)-CHR(1,J)
      CHRX(IMX,J)= CHR(IMX,J)-CHR(IMXX,J)
      DO 300 I=2,IMXX
      CHRX(I,J)=(CHR(I+1,J)-CHR(I-1,J))/2.0
300   CONTINUE
      DO 400 I=1,IMX
      CHRY(I,1)=(WAK(I,1)-WAK(I,2))/DL
      CHRY(I,JM)=(WAK(I,JMX)-WAK(I,JM))/DL
      DO 400 J=2,JMX
      CHRY(I,J)=(WAK(I,J-1)-WAK(I,J+1))/(2.0*DL)
400   CONTINUE
C
C     CHRX GIVES PHIXX
C     CHRY GIVES PHIYY
C
      IF (LFLAG.EQ.2) GO TO 635
      IF(JFLAG.EQ.1.OR.JFLAG.EQ.3.OR.KFLAG.EQ.1.OR.KFLAG.EQ.3) GO TO 612
      IF (ZMA.LT.1.0) GO TO 600
      WRITE (6,900) ZMA
      GO TO 610
      IF (IFLAG.EQ.1) GO TO 605
600   WRITE (6,901) ZMA
      GO TO 610
605   WRITE (6,902) ZMA
610   WRITE (6,910) TAU
      WRITE (6,920) IMX,JM
      WRITE (6,935)
      GO TO 614
612   WRITE (6,936)
614   DO 620 I=1,IMX
620   WRITE (6,940) (CHRX(I,J),J=1,JL1)
      WRITE (6,937)
      DO 630 I=1,IMX
```

```
630 WRITE (6,940) (CHRY(I,J),J=1,JL1)
    IF (LFLAG.EQ.1) RETURN
635 DO 640 I=1,6
640 TITLE(I)=TLINE1(I,5)
    CALL CONTUR (CHRX,IMX,JM,IN,CL,-8,TITLE,6,6,LTG)
    DO 650 I=1,6
650 TITLE(I)=TLINE1(I,6)
    CALL CONTUR (CHRY,IMX,JM,IN,CL,-8,TITLE,6,6,LTG)
900 FORMAT ('1',//30X,'SUPERSONIC CASE (M=',F7.5,') AND GAUSSIAN HEAT
   1RELEASE DISTRIBUTION',//)
901 FORMAT ('1',//30X,'SUBSONIC CASE (M=',F7.5,') AND GAUSSIAN HEAT RE
   1LEASE DISTRIBUTION',//)
902 FORMAT ('1',//30X,'SUBSONIC CASE (M=',F7.5,') AND CONSTANT HEAT RE
   1LEASE DISTRIBUTION',//)
910 FORMAT (30X,'KINETICS (TAU=',E10.3,') AND NO WALLS',//)
920 FORMAT (30X,'MATRIX: ',I3,' COLUMNS AND ',I3,' ROWS',//)
930 FORMAT (50X,'TOTAL DENSITY CHANGES, TOP HALF OF LASER BEAM',//)
931 FORMAT (46X,'PRESSURE PERTURBATIONS,  TOP HALF OF LASER BEAM',//)
932 FORMAT ('1',45X,'PRESSURE PERTURBATIONS,  TOP HALF OF LASER BEAM',
   1//)
933 FORMAT ('1',45X,'U PERTURBATION VELOCITY, TOP HALF OF LASER BEAM',
   1//)
934 FORMAT ('1',45X,'V PERTURBATION VELOCITY, TOP HALF OF LASER BEAM',
   1//)
935 FORMAT (66X,'PHIXX',//)
936 FORMAT ('1',65X,'PHIXX',//)
937 FORMAT ('1',65X,'PHIYY',//)
940 FORMAT (1X,1P13E10.2)
950 FORMAT (F8.6)
960 FORMAT (A8)
    RETURN
    END
```

LIST OF REFERENCES

1. Lehnigk, S. H., and Steverding, B., "High Intensity Light Propagation and Induced Natural Laminar Flow," U.S. Army Missile Research, Development and Engineering Laboratory; U.S. Army Missile Command, Redstone Arsenal, Alabama. Inc. many refs.

2. Rosenstock, H.B., and Tucker, J.W., "An Upper Limit on the Thermal Defocusing of a Light Beam," NRL Memorandum Report 2109, Apr. 1970.

3. Tucker, J.W., and DeWitt, R.N., "Atmospheric Propagation with Thermal Blooming," NRL Report 7038, 31 Dec. 1969.

4. Fuhs, A.E., "Density Inhomogeneity in a Laser Cavity due to Heat Release," AIAA Journal, 11, pp. 374-375, Mar. 1973.

5. Biblarz, O., and Fuhs, A.E., "Density Changes in a Laser Cavity Including Wall Reflections and Kinetics of Energy Release," AIAA Paper No. 73-141.

6. Biblarz, O., and Fuhs, A.E., "Laser Internal Aerodynamics and Beam Quality," Developments in Laser Technology - II, 41, Society of Photo Optical Instrumentation Engineers, 1973.

7. Fuhs, A. E., Biblarz, O., and Carey, E. F., "Thermal Blooming in Supersonic Slewing," Bulletin of American Physical Society, 18, p. 1485, Nov. 1973. Abstract only.

8. Burden, H. W., Biblarz, O., and Fuhs, A. E., "Thermal Blooming in Subsonic Slewing," Bulletin of American Physical Society, 18, p. 1490, Nov. 1973. Abstract only.

9. Fuhs, A. E., Biblarz, O., Cawthra, J. K., and Campbell, J. L., "Experimental Verification of Density Inhomogeneity due to Lasing in a Gas-Dynamic Laser," Applied Physics Letters, 24, pp. 132-134, Feb. 1974.

10. Sprieter, J. R., and Alksne, A. Y., "Theoretical Prediction of Pressure Distribution on Nonlifting Airfoils at High Subsonic Speeds," NACA Technical Note 3096, Mar. 1954. Inc. many refs.

11. Sprieter, J. R., and Alksne, A. Y., "Thin Airfoil Theory Based on Approximate Solution of the Transonic Flow Equation," NACA Report 1359, 1958. Inc. many refs.

12. Murman, E. M., and Cole, J. D., "Calculation of Plane Steady Transonic Flow," AIAA Journal, pp. 114-121, Jan. 1971.

13. Hosokawa, I., "Transonic Flow Past a Wavy Wall," Jour. of the Physical Society of Japan, 15, No. 11, pp. 2080-2086, Nov. 1960.

14. Guderley, K. G., The Theory of Transonic Flow, Pergamon Press, 1962. Inc. many refs.

15. Guderley, G., and Yoshihara, H., "The Flow over a Wedge Profile at Mach Number 1," J. Aero. Sci., 17, pp. 723-735, Nov. 1950.

16. Oswatitsch, K., and Keune, F., "The Flow Around Bodies of Revolution at Mach Number 1," Proceedings of the Conference on High Speed Aeronautics, Polytechnic Institute of Brooklyn, 1955.

17. Zierep, J., "Schallnahe Stromungen mit Warmezufuhr," Acta Mechanica, 8, pp. 126-132, 1969. Translated as Royal Establishment Library Translation 1452, Feb. 1970 with English title, "Transonic Flow with Heat Input."

18. Munn, M. W., "Laser Heat Induced Density Changes in Gases: Dependence upon Time and Transverse Flow Velocity, I.," Lockheed Missiles and Space Company Report D356026, Nov. 1973 revised Jan. 1974.

19. Ellinwood, J. W., and Mirels, H., "Density Perturbations in Transonic Sluing Laser Beams," Space and Missile Systems Organization (SAMSO), Technical Report 75-98, 5 Mar. 1975.

20. Brown, R. T., Berger, P. J., Gebhardt, F. G., and Smith, D. C., "Influence of Dead Zones and Transonic Slewing on Thermal Blooming," United Aircraft Research Laboratories, Mid-term Technical Report, 12 Nov. 1973.

21. Broadbent, E. G., "An Exact Numerical Method of Calculating Inviscid Heated Flows in Two-Dimensions with an Example of Duct Flow," Ingenieur-Archiv, 40, pp. 14-28, 1971 (Springer-Verlag).

22. Broadbent, E. G., "An Extended Numerical Method of Calculating Two-Dimensional or Axisymmetric Heated Flows Allowing for Dissipation," Ingenieur-Archiv, 40, pp. 81-95, 1971 (Springer-Verlag).

23. Broadbent, E. G., "Axisymmetric Flow with Heat Addition to Simulate Base-burning," Zeitschrift für Flugwissenschaften, 21, pp. 1-15, Jan. 1973.

24. Broadbent, E. G., "Flowfield Calculations for Some Supersonic Sections with Ducted Heat Addition," Ingenieur-Archiv, 42, pp. 89-103, 1973.

25. Broadbent, E. G., "Some Shockless Axisymmetric Flows with Heat Addition," Zeitschrift für Flugwissenschaften, 21, pp. 91-101, Mar. 1973.

26. Liepmann, H. W. and Roshko, A., Elements of Gas Dynamics, John Wiley and Sons, 1957.

27. Shapiro, A. H., Compressible Fluid Flow, Ronald Press Co., New York, Vol. I., 1953, pp. 83-84, 231.

28. Vincenti, W. G., and Wagoner, C. B., "Transonic Flow Past a Wedge Profile with Detached Bow Wave — General Analytical Method and Final Calculated Results," NACA Technician Note 2339, 1951.

29. Liepmann, H. W., and Bryson, A. E., Jr., "Transonic Flow Past Wedge Sections," Jour. Aero. Sci., 17, No. 12, pp. 745-755, Dec. 1950.

30. Bryson, A. E., Jr., "An Experimental Investigation of Transonic Flow Past Two-Dimensional Wedge and Circular-Arc Sections Using a Mach-Zehnder Interferometer," NACA Technical Note 2560, 1951.

31. Huebner, K., Finite Element Method for Engineers, Wiley Interscience, 1975.

32. Sherman, A., and Sutton, G. W., Engineering Magneto-hydrodynamics, McGraw Hill Book Co., 1965, pp. 113-122, 296-299.

33. Ashley, H., and Landahl, M. T., Aerodynamics of Wings and Bodies, Addison-Wesley Publishing Co., Inc., 1965, pp. 230-244.

34. Sauer, R., Introduction to Theoretical Gas Dynamics, J. W. Edwards, Ann Arbor, 1947, p. 108.

35. Oswatitsch, K., "Die Geshwindigkeitverteilung bei lokalen Uberschallgebieten an flachen Profiltes," Zeitschrift fur Angewandte Mathematik und Mechanik, Bd. 20, Hr. 1/2 Jan./Feb. 1950, S. 17-24.

36. Oswatitsch, K., "Die Geschwindigkeitverteilung an Symmetrischen Profilen beim Auftreten lokaler Überschallgebiete," Acta Physica Austriaca, Bd. 4, Nr. 2-3, Dec. 1950, S. 228-271.

37. Wolfe, W. L., Handbook of Military Infrared Technology, Office of Naval Research, Dept. of the Navy, Washington D. C., 1965, p. 839.

38. Tsien, H. S., and Beilock, M., "Heat Source in a Uniform Flow," J. Aero. Sci., 16, p. 756, 1949.

39. Fuhs, A. E., "Quasi Area for Heat Addition in Transonic and Supersonic Flight Regimes," Technical Report AFAPL-TR-72-10, Aug. 1972.

40. Smithey, W. J. H., "Projectile Thrust-Drag Optimization with External Burning," Naval Postgraduate School, Ph.D. Thesis, June 1974.

41. Biblarz, O., Carey, E. F., Fuhs, A. E., and Burden, H., "Numerical Results for Thermal Blooming in Transonic Slewing," Bulletin of American Physical Society, 19, p. 1157, Nov. 1974.

42. Fuhs, A. E., Burden, E., and Carey, E. F., "An Exact Inverse Solution to Thermal Blooming in Transonic Slewing," Bulletin of American Physical Society, 19, p. 1158, Nov. 1974.

43. Fuhs, A. E., "Propagation of Laser Beams which are Rapidly Slewed," Proceedings of The Electro-Optical Systems Design/International Laser Conference, 1975.

44. Read, A. W., "Vibration Relaxation In Gases," Progress in Reaction Kinetics, pp. 203-235, 3, Pergamon Press, New York, 1965.

45. Vincenti, W. G., and Kruger, C. E., Jr., Introduction to Physical Gas Dynamics, Wiley, New York, 1965.

INITIAL DISTRIBUTION LIST

11. Dr. Barry Hogge
    Air Force Weapons Laboratory
    Kirtland Air Force Base
    New Mexico 87147   1

12. Major Keith Gilbert
    Air Force Weapons Laboratory
    Kirtland Air Force Base
    New Mexico 87147   1

13. Mr. Thomas Gregory
    NASA Ames Research Center
    Moffett Field, California 94035   1

14. Captain Raymond Saunders, USAF
    NASA Ames Research Center
    Moffett Field, California 94035   1

15. Mr. Ronald Dettling
    Naval Weapon Center
    China Lake, California 93555   1

16. Dr. George Sutton
    AVCO Everett Research Laboratory
    2385 Revere Beach Parkway
    Everett, Massachusetts 02149   1

17. Dr. Harold Mirels
    Aerodynamics and Propulsion Laboratory
    Aerospace Corporation
    Los Angeles, California 90245   1

18. Professor Julian D. Cole
    Department of Engineering
    University of California at Los Angeles
    Los Angeles, California 90024   1

19. Professor M. D. VanDyke
    Department of Aeronautics and Astronautics
    Stanford University
    Stanford, California 94305   1

20. Professor O. Biblarz
    Department of Aeronautics
    Naval Postgraduate School
    Monterey, California 93940   1

21. Dr. E. G. Broadbent
    Royal Aeronauticsl Establishment
    Farnborough, ENGLAND   1

22. LCDR E. Fenton Carey, Jr.
    VAW-121
    NAS Norfolk, Virginia 23511   3